EUROPEAN ORGANISATION FOR NUCLEAR RESEARCH (CERN)

Submitted to: JHEP

CERN-EP-2025-135
4th July 2025

Measurement of the top-quark pole mass in dileptonic $t\bar{t}$ + 1-jet events at $\sqrt{s}$ = 13 TeV with the ATLAS experiment

The ATLAS Collaboration

A measurement of the top-quark pole mass m_t^{pole} is presented in $t\bar{t}$ events with an additional jet, $t\bar{t}$ + 1-jet, produced in pp collisions at $\sqrt{s}$ = 13 TeV. The data sample, recorded with the ATLAS experiment during Run 2 of the LHC, corresponds to an integrated luminosity of 140 fb^{-1}. Events with one electron and one muon of opposite electric charge in the final state are selected to measure the $t\bar{t}$ + 1-jet differential cross-section as a function of the inverse of the invariant mass of the $t\bar{t}$ + 1-jet system. Iterative Bayesian Unfolding is used to correct the data to enable comparison with fixed-order calculations at next-to-leading-order accuracy in the strong coupling. The process $pp \to t\bar{t}j$ ($2 \to 3$), where top quarks are taken as stable particles, and the process $pp \to b\bar{b}l^+\nu l^-\bar{\nu}j$ ($2 \to 7$), which includes top-quark decays to the dilepton final state and off-shell effects, are considered. The top-quark mass is extracted using a χ^2 fit of the unfolded normalized differential cross-section distribution. The results obtained with the $2 \to 3$ and $2 \to 7$ calculations are compatible within theoretical uncertainties, providing an important consistency check. The more precise determination is obtained for the $2 \to 3$ measurement: m_t^{pole} = 170.7 ± 0.3 (stat.) ± 1.4 (syst.) ± 0.3 (scale) ± 0.2 (PDF ⊕ α_S) GeV, which is in good agreement with other top-quark mass results.

Contents

1 Introduction

The mass of the top quark plays a fundamental role in the Standard Model (SM) of particle physics. The parameters of the SM Lagrangian — the masses of the elementary particles and the strength of their interactions — are not predicted by the SM, but must be measured experimentally. In the SM, the masses of the elementary particles arise from interactions with the Higgs field. The top quark Yukawa coupling is approximately 1 and the top quark mass strongly affects the evolution of the Higgs quartic coupling to high scales [1, 2], which determines the shape of the Higgs potential and the stability of the quantum vacuum. The SM also predicts a relation among the masses of the Higgs boson, the W boson [3], and the top quark. Precise measurements of these masses and other fundamental parameters allow a test of this important relation [4, 5].

Direct measurements of the top-quark mass parameter in Monte Carlo (MC) generators, based on fits to the observed distributions of top-quark decay products, have reached excellent experimental precision [6]. The results of these measurements are generally identified with the top-quark pole mass. The ambiguity in this identification, from limitations of the stable-top-quark picture and non-perturbative effects, is estimated to be a few hundred MeV [7]. Work is ongoing to improve the understanding of the top-quark mass parameter in Monte Carlo generators [8, 9]. The pole mass definition moreover has an intrinsic renormalon ambiguity [10, 11].

The top-quark mass can also be extracted from measurements of the top-quark pair production cross-section, either through inclusive or differential approaches. In this case, the mass scheme is defined by the fixed-order (FO) prediction for the cross-section in quantum chromo dynamics (QCD). This leaves no ambiguity when such measurements are used in other phenomenological studies done in perturbation theory, such as the calculations of the stability of the electroweak (EW) vacuum. The mass extraction procedure yields an estimate of the theory uncertainty, greater flexibility in the choice of the mass scheme, and the possibility to take advantage of future theory progress without redoing the measurement.

In this paper, the top-quark pole mass m_t^{pole} is measured in $t\bar{t}$ events with an additional jet ($t\bar{t}$ + 1-jet) produced in proton–proton (pp) collisions at $\sqrt{s}$ = 13 TeV. Following the method proposed in Ref. [12], the dependence of the normalized cross-section of $t\bar{t}$ + 1-jet production as a function of the invariant mass $\sqrt{s_{t\bar{t}+1\text{-jet}}}$ of the $t\bar{t}$ + 1-jet system on m_t^{pole} is studied. In the differential cross section, the top quark pair production threshold region at $m_{t\bar{t}} \approx 2m_t$ has a pronounced top-quark mass sensitivity which is further enhanced in the $t\bar{t}$ + 1-jet final state, as the additional jet allows events from the threshold region to be experimentally more accessible. At the same time the impact of a bound-state enhancement at threshold [13–19] not included in fixed-order calculations, is diluted by the presence of the additional jet. The observable is defined as:

$$\mathcal{R}(\rho_s; m_t^{\text{pole}}) = \frac{1}{\sigma_{t\bar{t}+1\text{-jet}}} \cdot \frac{\mathrm{d}\sigma_{t\bar{t}+1\text{-jet}}}{\mathrm{d}\rho_s} \quad \text{, with} \quad \rho_s = \frac{2m_0}{\sqrt{s_{t\bar{t}+1\text{-jet}}}}. \tag{1}$$

The constant m_0 is set to m_0 = 170 GeV to ensure that ρ_s is bounded between 0 and 1, as in Ref. [20]. This convention is arbitrary and has no impact on the final top-quark mass measurement.

Previously, the ATLAS collaboration measured the top-quark pole mass in $t\bar{t}$ + 1-jet events using $\sqrt{s}$ = 7 TeV [20] and $\sqrt{s}$ = 8 TeV [21] pp collision data, in the semileptonic $t\bar{t}$ decay channel, resulting in total uncertainties of 2.3 GeV (1.3%) and 1.2 GeV (0.7%) on the top-quark pole mass, respectively. This analysis targets the dilepton decay channel of the $t\bar{t}$ system and uses the complete Run 2 data sample, corresponding to 140 fb^{-1}, allowing the dilepton channel to provide competitive sensitivity. The CMS

collaboration published the first measurement of the top-quark pole mass in $t\bar{t}$ + 1-jet events in the dilepton channel [22] at $\sqrt{s}$ = 13 TeV using 36.3 fb^{-1} resulting in a total uncertainty of 1.36 GeV (0.8%).

The final state targeted by this analysis has two charged leptons, two neutrinos, two b-jets, and an additional jet with high transverse momentum. Events are selected that have an electron and a muon candidate, at least three jets and a significant amount of missing transverse momentum. The four-momentum of the $t\bar{t}$ system is reconstructed using a combination of two methods, as detailed in Section 4.

The ρ_s distribution is corrected to the level of stable top quarks, undoing the impact of top-quark decay, hadronization, and detector response, using Iterative Bayesian Unfolding (IBU) [23]. The top-quark pole mass is obtained from a fit of the normalized differential cross-section $\mathcal{R}(\rho_s; m_t^{\text{pole}})$ to a FO calculation of the $2 \to 3$ process $pp \to t\bar{t}$ + 1-jet at next-to-leading-order (NLO) accuracy in QCD [24].

The data are also corrected to a parton level phase space defined by leptons, neutrinos and jets formed of quarks and gluons just before hadronization. This enables a comparison of the measured observable with a FO NLO QCD calculation for the $2 \to 7$ process $pp \to b\bar{b}l^+\nu l^-\bar{\nu}j$ that includes top-quark decay effects and full non-resonant contributions [25]. In this second approach there is no need to correct the data for the top-quark decay, and hence a smaller reliance on the description of the decay in Monte Carlo generators. Associated single top-quark production with a W boson is included in the $2 \to 7$ calculation.

This paper is structured as follows. A brief description of the ATLAS detector is found in Section 2. The data and MC samples used in this analysis are summarized in Section 3. The object definitions, object selections, and control distributions are shown in Section 4. The parton-level definitions and the FO predictions are described in Section 5. The reconstruction of the $t\bar{t}$ + 1-jet system and the unfolding of the differential cross-section are described in Section 6, and the estimate of the experimental uncertainties affecting the measurement is outlined in Section 7. The extraction of the top-quark mass in the pole mass scheme using a fit to the FO $t\bar{t}$ + 1-jet predictions is discussed in Section 8, together with a description of the theoretical uncertainties associated with the mass measurement. The results are then summarized in Section 9 and conclusions are given in Section 10.

2 ATLAS detector

The ATLAS detector [26] at the LHC covers nearly the entire solid angle around the collision point.[1] It consists of an inner tracking detector surrounded by a thin superconducting solenoid, electromagnetic and hadronic calorimeters, and a muon spectrometer incorporating three large superconducting air-core toroidal magnets.

The inner-detector system (ID) is immersed in a 2 T axial magnetic field and provides charged-particle tracking in the range $|\eta| < 2.5$. The high-granularity silicon pixel detector covers the vertex region and typically provides four measurements per track, the first hit generally being in the insertable B-layer (IBL) installed before Run 2 [27, 28]. It is followed by the SemiConductor Tracker (SCT), which usually provides eight measurements per track. These silicon detectors are complemented by the transition radiation tracker (TRT), which enables radially extended track reconstruction up to $|\eta| = 2.0$. The TRT also provides

[1] ATLAS uses a right-handed coordinate system with its origin at the nominal interaction point (IP) in the center of the detector and the z-axis along the beam pipe. The x-axis points from the IP to the center of the LHC ring, and the y-axis points upwards. Cylindrical coordinates (r, ϕ) are used in the transverse plane, ϕ being the azimuthal angle around the z-axis. The pseudorapidity is defined in terms of the polar angle θ as $\eta = -\ln\tan(\theta/2)$. Angular distance is measured in units of $\Delta R \equiv \sqrt{(\Delta\eta)^2 + (\Delta\phi)^2}$.

electron identification information based on the fraction of hits (typically 30 in total) above a higher energy-deposit threshold corresponding to transition radiation.

The calorimeter system covers the pseudorapidity range $|\eta| < 4.9$. Within the region $|\eta| < 3.2$, electromagnetic calorimetry is provided by barrel and endcap high-granularity lead/liquid-argon (LAr) calorimeters, with an additional thin LAr presampler covering $|\eta| < 1.8$ to correct for energy loss in material upstream of the calorimeters. Hadronic calorimetry is provided by the steel/scintillator-tile calorimeter, segmented into three barrel structures within $|\eta| < 1.7$, and two copper/LAr hadronic endcap calorimeters. The solid angle coverage is completed with forward copper/LAr and tungsten/LAr calorimeter modules optimized for electromagnetic and hadronic energy measurements, respectively.

The muon spectrometer (MS) comprises separate trigger and high-precision tracking chambers measuring the deflection of muons in a magnetic field generated by the superconducting air-core toroidal magnets. The field integral of the toroids ranges between 2.0 and 6.0 T m across most of the detector. Three layers of precision chambers, each consisting of layers of monitored drift tubes, cover the region $|\eta| < 2.7$, complemented by cathode-strip chambers in the forward region, where the background is highest. The muon trigger system covers the range $|\eta| < 2.4$ with resistive-plate chambers in the barrel, and thin-gap chambers in the endcap regions.

The luminosity is measured mainly by the LUCID–2 [29] detector that records Cherenkov light produced in the quartz windows of photomultipliers located close to the beampipe.

Events were selected by the first-level trigger system implemented in custom hardware, followed by selections made by algorithms implemented in software in the high-level trigger [30]. The first-level trigger accepted events from the 40 MHz bunch crossings at a rate close to 100 kHz, which the high-level trigger further reduced in order to record complete events to disk at about 1.25 kHz.

A software suite [31] is used in data simulation, in the reconstruction and analysis of real and simulated data, in detector operations, and in the trigger and data acquisition systems of the experiment.

3 Data and simulated samples

This analysis is performed using the full Run 2 pp data recorded with the ATLAS experiment at $\sqrt{s} = 13$ TeV. Once all quality requirements [32] are applied, the recorded data corresponds to an integrated luminosity of 140.0 ± 1.2 fb^{-1} [33], obtained using the LUCID-2 detector [29] for the primary luminosity measurements, complemented by measurements using the inner detector and calorimeters.

The events in this data sample are required to satisfy the trigger requirements for single electrons or muons [30, 34–36].

Simulated MC events are used to correct the data and estimate background processes. Detector effects are simulated fully using GEANT4 [37]. A few MC samples used for tests and crosschecks employ a faster detector simulation (`AtlFast2`) that makes use of parameterized showers in the calorimeters [38].

The nominal $t\bar{t}$ MC sample is generated using POWHEG-BOX-v2 [39–41] with the heavy-quark production (HVQ) process at NLO accuracy in QCD [42], assuming a top-quark mass of $m_t^{\mathrm{MC}} = 172.5$ GeV and dileptonic top-quark pair decay. The proton structure in the Matrix Element (ME) is modeled using the NNPDF 3.0 NLO parton distribution functions (PDF) set [43]. The POWHEG-BOX-v2 event generator is interfaced with PYTHIA 8.230 [44] which simulates parton shower (PS), fragmentation, hadronization,

and the underlying event (UE). The h_{damp} parameter that controls the emission of the first gluon is set to $1.5 \cdot m_t^{\text{MC}}$, while the factorization scale μ_{r} and renormalization scale μ_{f} are set to $\mu_{\text{r}}^2 = \mu_{\text{f}}^2 = (m_t^2 + p_{\text{T}}^2)$, where the top-quark transverse momentum (p_{T}) is evaluated before radiation [45]. The A14 ATLAS UE tune [46] together with the NNPDF 2.3 leading-order (LO) PDF set [47] is applied for Pythia 8 showering. Finite top-quark width effects are implemented by reweighting the simulated events such that the top-quark mass distribution follows a Breit–Wigner distribution. The inclusive $t\bar{t}$ cross-section in the simulation is normalized to the next-to-next-to-leading-order (NNLO) cross-section including the resummation of soft gluon emissions at next-to-next-to-leading-logarithmic (NNLL) accuracy calculated using the Top++2.0 software [48]. The resulting cross-section for the $t\bar{t}$ process is $\sigma_{t\bar{t}} = 831.8$ pb [49–54]. To estimate the systematic uncertainty associated with the $t\bar{t}$ nominal sample, additional simulations are generated, as detailed in Section 7.2.

The tW production process is simulated using Powheg-Box-v2 interfaced with Pythia 8 with the A14 UE tune and the NNPDF2.3 LO PDF set. Samples are normalized to the cross-section calculation at approximate NNLO accuracy [55]. The overlap between $t\bar{t}$ and tW production is removed using the diagram-removal procedure [56], and an additional tW simulation employing the alternative diagram-subtraction scheme [57] is used to study its associated uncertainty.

Further $t\bar{t}$ and tW samples with varied top-quark mass ranging from $m_t^{\text{MC}} = 169$ GeV to $m_t^{\text{MC}} = 176$ GeV are used for analysis validation. A MC sample based on the $bb4l$ Powheg package [58] interfaced to Pythia 8, currently under development and scrutiny within ATLAS, is used to validate the $2 \rightarrow 7$ result obtained with the MC ensemble of $t\bar{t}$ and tW production.

The Z+jets production with $Z \rightarrow e^+e^-/\mu^+\mu^-/\tau^+\tau^-$ is modeled using Sherpa 2.2.1 [59]. The matrix elements are calculated for up to two additional partons at NLO accuracy in QCD and four partons at LO using the Comix [60] and OpenLoops [61] matrix element generators, merged with the Sherpa parton shower using the ME+PS@NLO prescription [62]. The NNPDF3.0 NNLO PDF set is used together with a dedicated parton shower tuning developed by the Sherpa authors. The samples are normalized to the total Z+jets cross-section at NNLO accuracy [63], obtained with the FEWZ program [64], and a 50% normalization uncertainty is associated to them.

The production of diboson ($WW/WZ/ZZ$) events in association with jets is simulated using Sherpa 2.2.2 with the dedicated UE tune from Sherpa and the NNPDF3.0 NNLO PDF set. In the simulation, matrix elements at NLO accuracy in QCD for up to one additional parton and at LO accuracy for up to three additional parton emissions are employed. A 50% normalization uncertainty is assigned to the diboson MC samples.

The processes $t\bar{t}Z$, $t\bar{t}W$ are simulated using MadGraph5_aMC@NLO interfaced with Pythia 8. The associated Higgs boson and $t\bar{t}$ production ($t\bar{t}H$) is simulated using Powheg+Pythia 8 [65]. For the $t\bar{t}Z$, $t\bar{t}W$, and $t\bar{t}H$ production processes, the NNPDF 3.0 NLO PDF set is used in the ME, while the A14 UE tune is applied with NNPDF2.3 LO in the parton shower. The production processes are normalized to the corresponding NLO QCD+EW theoretical cross-sections [66].

All MC samples are overlaid with additional pp interactions (pileup), generated with Pythia 8.186 [67] using the NNPDF2.3 LO PDF set and the A3 set of tuned parameters [68], and the average number of interactions per bunch crossing is reweighted to match that in data. All simulated samples other than those generated with Sherpa use the `EvtGen` [69] program to simulate the decays of bottom and charm hadrons.

The number of events where at least one of the reconstructed lepton candidates originates from the decay of a hadron or a jet incorrectly identified as a lepton (fake leptons) is estimated by using the truth information associated to the reconstructed lepton in MC simulations. If the reconstructed lepton is found not to originate from a true lepton, the event is marked as a fake-lepton background event. A $t\bar{t}$ sample with the same setting as the nominal one, but also including semileptonic top-quark decays, and the tW MC sample are used for the fake leptons estimation. The fake leptons contribution amounts approximately to 1% of the total event yield in the dilepton selection and a normalization uncertainty of 50% is associated to it. The final estimate is found to be compatible within uncertainties with other data-driven estimates [70].

A summary of the MC generators used to simulate the most important processes can be found in Table 1.

Table 1: A summary of basic MC generator settings used to simulate various SM processes and the cross-section uncertainty used in their normalization.

Sample	Generator	ME PDF	Shower	Normalization	Cross-section [pb]	Norm. unc. [%]
$t\bar{t}$	Powheg	NNPDF3.0	Pythia 8	NNLO+NNLL	831.8 [51–54]	6.1
Single-top (tW)	Powheg	NNPDF3.0	Pythia 8	(Approx)NNLO	71.7 [55, 71]	5.3
Z+jets	Sherpa 2.2.1	NNPDF3.0	Sherpa 2.2.1	NNLO	2107.0 [63, 64]	50
Diboson	Sherpa 2.2.2	NNPDF3.0	Sherpa 2.2.1	NLO	176.0 [72]	50
$t\bar{t}Z$	MG5_aMC@NLO	NNPDF3.0	Pythia 8	NLO(QCD+EW)	0.88 [66]	14
$t\bar{t}W$	MG5_aMC@NLO	NNPDF3.0	Pythia 8	NLO(QCD+EW)	0.60 [66]	13
$t\bar{t}H$	MG5_aMC@NLO	NNPDF3.0	Pythia 8	NLO(QCD+EW)	0.51 [66]	13

4 Object reconstruction and event selection

Electron candidates are identified by matching energy deposits in the electromagnetic calorimeter with a corresponding track in the inner tracking detector. Electrons are required to satisfy the Tight identification criteria [73] and to lie within $|\eta| < 2.47$, with the calorimeter transition region of $1.37 < |\eta| < 1.52$ being excluded. Electron candidates must pass the Tight isolation requirement [73] that removes fake and non-prompt electrons from heavy flavor decays. Muon candidates are reconstructed by combining a track in the inner tracking detector with either a track or hits in the muon spectrometer. Muons fulfilling Medium track requirements [74] with $|\eta| < 2.5$ and satisfying the Tight isolation requirement of Ref. [74] are selected. The performance of lepton reconstruction and identification efficiency is measured in data and used to calibrate the performance in the simulations [73–76].

Both electrons and muons are required to have $p_{\mathrm{T}} > 20$ GeV. The transverse impact parameter divided by its estimated uncertainty is required to be less than five (three) for electron (muon) candidates and the longitudinal impact parameter must be smaller than 0.5 mm for both lepton flavors.

Jets are reconstructed using the anti-k_t algorithm [77] with a radius parameter $R = 0.4$ from particle flow objects [78] that combine information from topological clusters [79] and the track information for the charged component. The jet response is calibrated with MC simulations and in situ measurements [80]. Only jets with $p_{\mathrm{T}} > 25$ GeV and $|\eta| < 2.5$ are considered. To suppress jets from pileup, the jet vertex tagger (JVT) [81] must satisfy JVT > 0.50 for jets with $p_{\mathrm{T}} < 60$ GeV and $|\eta| < 2.4$. Jets containing b-hadrons are identified using the DL1r algorithm [82] at the 85% tagging efficiency working point. Measurements of the efficiency of the b-tagging algorithm in data are used to adjust the simulation to match the performance measured in data [83–85].

An overlap removal procedure is applied to avoid double-counting the same reconstructed objects. Jets within $\Delta R = 0.2$ of an electron or muon are discarded and electrons within $0.2 < \Delta R < 0.4$ of the remaining jets are rejected. Jets with less than three tracks are removed if they overlap with a muon within $\Delta R = 0.4$.

The missing transverse momentum ($E_{\mathrm{T}}^{\mathrm{miss}}$) is computed as the negative vectorial sum of the transverse momenta of all identified and calibrated objects in the detector, including a track-based term to account for the energy from particles not associated with a reconstructed lepton or jet [86, 87].

4.1 Event selection

Events are required to have at least one primary vertex with at least two associated tracks with $p_{\mathrm{T}}^{\mathrm{track}} > 0.5$ GeV. The selection further requires the presence of exactly one electron and one muon of opposite electric charge, separated by $\Delta R > 0.4$. The lepton with the highest p_{T} is required to have $p_{\mathrm{T}} > 28$ GeV to ensure high efficiency of the single-lepton triggers.

A requirement of $E_{\mathrm{T}}^{\mathrm{miss}} > 30$ GeV is imposed, due to the presence of undetected neutrinos. Exactly two b-tagged jets with $p_{\mathrm{T}} > 30$ GeV are required. Among the remaining jets, the p_{T}-leading one is required to have $p_{\mathrm{T}} > 50$ GeV. The relatively high p_{T} requirement on this jet, referred to as the *extra jet* in the following, reduces the uncertainties from the jet energy calibration, the uncertainty due to the choice of parton-shower model, and the probability that the additional jet used in the $t\bar{t}$ + 1-jet system reconstruction originates from pileup. It also reduces the theoretical uncertainties in the FO theory calculations.

Each lepton is associated a b-jet such that the sum of the invariant masses of the two possible lepton and b-jet systems ($m_{(\ell b)_1} + m_{(\ell b)_2}$) is minimized. A requirement of $m_{(\ell b)_i} < 200$ GeV, with $i \in \{1, 2\}$, is imposed on each of the two lepton and b-jet pairs, to avoid a region of phase space which is known to be difficult to model [88].

4.2 Reconstruction of the $t\bar{t}$ system

The reconstruction of the $t\bar{t}$ system requires an estimate of the kinematic properties of the two neutrinos from the W boson decays. The neutrino four-vectors are derived from the observed $E_{\mathrm{T}}^{\mathrm{miss}}$ and the properties of the other objects in the event. In this measurement, a combination of the loose kinematic reconstruction [89] and ϕ-weighting reconstruction [90] methods is employed. No top-quark mass assumption is introduced in these methods, and the combination of the two methods has a high reconstruction efficiency of around 98%.

The loose kinematic reconstruction does not attempt to reconstruct the neutrino and anti-neutrino, but determines the kinematic properties of the $\nu\bar{\nu}$ system. The transverse momentum of the $\nu\bar{\nu}$ system is obtained directly from the $E_{\mathrm{T}}^{\mathrm{miss}}$. The di-neutrino longitudinal momentum and energy are set equal to the longitudinal momentum and energy of the charged-lepton pair. The $t\bar{t}$ system is then reconstructed from the two charged leptons, the two selected b-tagged jets, and the neutrino system in the selected events.

Around 25% of the events reconstructed with the loose method have the reconstructed invariant mass of the W boson pair and neutrino pair not satisfying $m(W^+W^-) \geq 2m_W^{\mathrm{PDG}}$ and $m(\nu\bar{\nu}) \geq 0$, and are hence not considered as physical solutions. For those events, the $t\bar{t}$ system is reconstructed with an alternative approach based on the ϕ-weighting method [90]. For each event, each of the neutrino azimuthal angle is set to a random value, hence fixing the p_{T} of each individual neutrino. Then, neutrino longitudinal

momenta are inferred assuming that each neutrino four-momentum and its pairing with a lepton reconstructs a W boson with mass m_W^{PDG}. A b-jet is assigned to each lepton–neutrino pair to compute the quantity $\chi^2_\phi = (m_{\nu\ell b} - m_{\bar{\nu}\ell\bar{b}})/(m_{\nu\ell b} + m_{\bar{\nu}\ell\bar{b}})$, where $m_{\nu\ell b}$ and $m_{\bar{\nu}\ell\bar{b}}$ are the masses of the two reconstructed top-quark candidates in the event, each obtained summing the four-momenta of one neutrino, one charged lepton and one b-jet. The azimuthal angle phase space (ϕ_1, ϕ_2) of the neutrinos is scanned with 100 random values from a uniform distribution and all the combinations of neutrinos, charged leptons and b-jets are used in the calculation of χ^2_ϕ, hence providing 1600 possible values for it[2]. The solution which minimizes the difference between the reconstructed mass of top and anti-top quark, as quantified by χ^2_ϕ, is taken for the $t\bar{t}$ system definition.

To form the $t\bar{t}$ + 1-jet system the extra jet is selected as the highest in p_{T} among the untagged jets with $|\eta| < 2.5$, and it is added to the $t\bar{t}$ system. The p_{T} requirement on the extra jet is raised to 60 GeV for the $2 \to 7$ measurement, to match the value chosen for the FO calculation.

Figure 1 illustrates the resolution of ρ_{s} achieved by the reconstruction algorithm, estimated using the nominal $t\bar{t}$ MC simulation based on Powheg+Pythia 8, where the resolution is taken as the root mean square of the $(\rho_{\text{s}}^{\text{reco}} - \rho_{\text{s}}^{\text{true}})/\rho_{\text{s}}^{\text{true}}$ distribution and ρ_{s} is defined in Eq. (1). The resolution of the combined loose kinematic and ϕ-weighting reconstruction is compared with that of the individual loose kinematic and ϕ-weighting methods alone, and to the resolution obtained with perfect neutrino reconstruction, based on MC truth information. The gain in statistical power from combining the loose and ϕ methods outweighs the slight reduction in resolution. Although the presence of undetected neutrinos affects the resolution of the reconstructed observable, the employed $t\bar{t}$ system reconstruction technique ensures the ρ_{s} distribution can be measured accurately, maintaining the observable resolution within the 0.05–0.1 range.

The event yields in the simulation and data after all selection requirements are given in Table 2. The $t\bar{t}$ signal purity is greater than 95%. The largest background contributions originate from single-top-quark production, fake leptons from $t\bar{t}$ and single-top-quark events and associated production of $t\bar{t}$ with a heavy boson. Smaller contributions are expected from diboson and Z+jets processes. The observed number of events agrees with the expected yield within 4%, a difference which is covered by the uncertainty in the SM prediction, as reported in Table 1.

Table 2: Event yields after the final selection for the values of minimum $p_{\text{T}}^{\text{extrajet}}$ considered in the analysis. The uncertainties only contain the cross-section normalization components, while for the $t\bar{t}$ sample also statistical and systematic uncertainties, as defined in Section 7.2, are considered.

	$p_{\text{T}}^{\text{extrajet}} > 50$ GeV	$p_{\text{T}}^{\text{extrajet}} > 60$ GeV
$t\bar{t}$	103000 ± 7000	86000 ± 6000
Single top	1840 ± 100	1470 ± 80
Diboson	53 ± 27	48 ± 23
Z+jets	55 ± 28	48 ± 24
$t\bar{t}V + t\bar{t}H$	590 ± 80	530 ± 70
Fake leptons	750 ± 380	640 ± 320
Total MC	106000 ± 7000	89000 ± 6000
Data	102215	85366
Data/MC	0.96	0.96

[2] The number of possible neutrino–lepton pairings is 8 due to the two-fold ambiguity in longitudinal momentum for each neutrino and the two lepton-neutrino combinations. An additional factor two in the possible solutions comes from the pairing with jets.

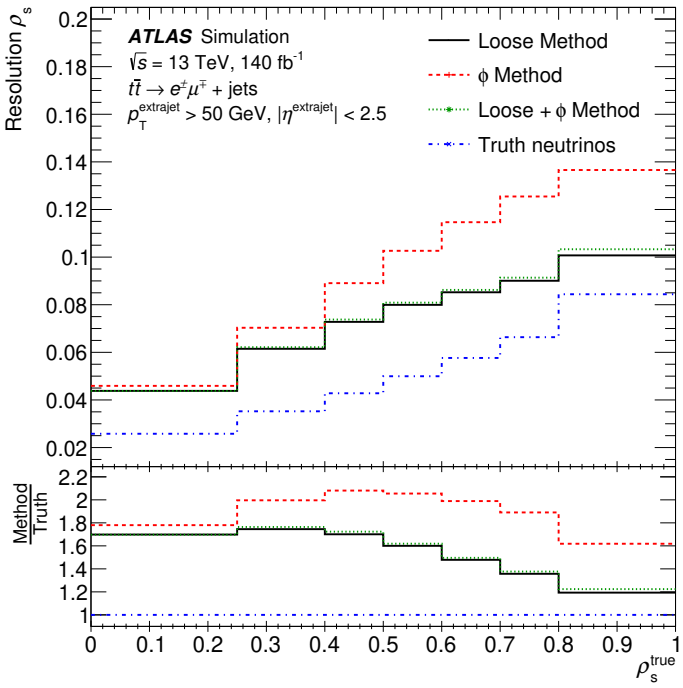

Figure 1: Resolution of the ρ_s observable for events reconstructed with the combined loose kinematic and ϕ-weighting reconstruction methods, in the $e^{\pm}\mu^{\mp}$decay channel of the $t\bar{t}$ + 1-jet system, simulated using POWHEG+PYTHIA 8. The resolution obtained from each individual reconstruction method is also shown together with the best possible scenario, where the neutrino momenta are known from truth information in the MC (blue). Only events satisfying the respective reconstruction method requirements are considered.

The observed ρ_s distributions for the full Run 2 data set are shown in Figure 2. Overall, reasonable agreement is observed between the reconstructed distribution in the data and the SM expectation generated with MC simulations of the signal and background processes.

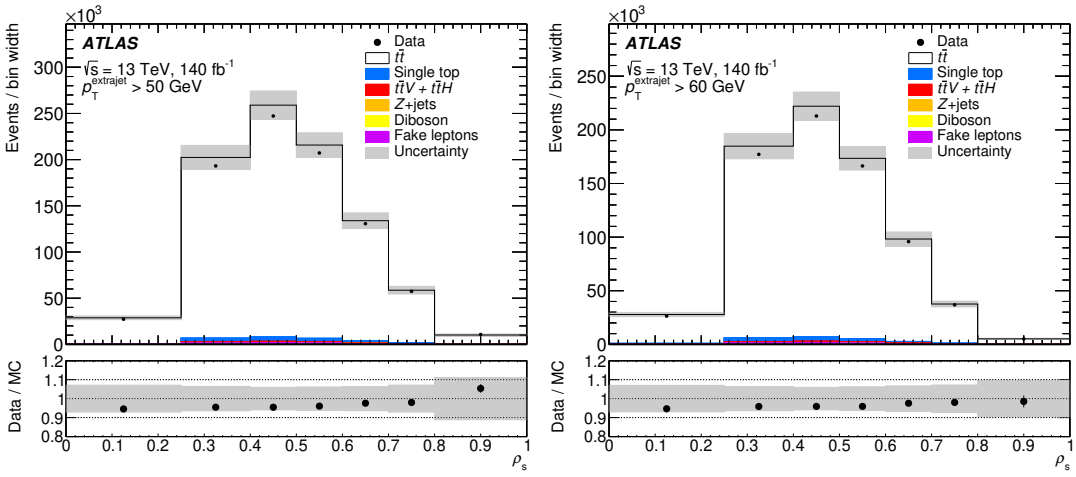

(a) (b)

Figure 2: Detector level distributions of the ρ_s variable in the $t\bar{t}$ + 1-jet system after the final selection in the $e^{\pm}\mu^{\mp}$ decay channel, for a cut on the extra jet p_T corresponding to (a) 50 GeV and (b) 60 GeV. Data (filled markers) are compared with the SM expectation with $m_t^{MC} = 172.5$ GeV (histogram). The uncertainty band represents the total uncertainty on the MC prediction, including all statistical and systematic components.

5 Parton-level definitions and fixed-order calculations

To compare the measured observable to FO theoretical predictions, the data is corrected to parton level. Two FO calculations are considered. The first FO prediction for $\mathcal{R}(\rho_s; m_t^{pole})$ is computed at NLO accuracy in the strong coupling for stable top quarks. Results are obtained using the TTBARJ process in POWHEG-BOX-V2 [24], with the on-shell top quarks in the pole-mass scheme. This calculation is referred to as $2 \to 3$ in the following, as three objects are considered in the final state. The extra jet is defined from gluons and non-top quarks with the anti-k_t algorithm [91] implemented in FastJet [92], with radius parameter $R = 0.4$, and is required to have $p_T > 50$ GeV and $|\eta| < 2.5$. In a previous mass measurement in $t\bar{t}$ + 1-jet events [21], a similar calculation was used where the renormalization and factorization scales where fixed to the top-quark mass. In the current measurement, dynamic scales are used in the calculation, which was observed to lead to reduced changes in the observable when scales were varied by factors of 0.5 and 2. The factorization and renormalization scales are set to $\mu_f, \mu_r = \mu_0 = E_T/2$ according to the recommendations in Ref. [93], with $E_T = \sum_{i\in[t,\bar{t},j]} \sqrt{p_T^{i\,2} + m_i^2}$, where m_i is the invariant mass of the corresponding object.

The second prediction is a FO NLO QCD of the $pp \to b\bar{b}l^+\nu l^-\bar{\nu} + j$ process and is referred to as $2 \to 7$ in the following. This calculation includes contributions from single-resonant and non-resonant diagrams, as well as the doubly resonant top-quark pair production process hence considering top-quark decay and full off-shell effects. The predictions for $\mathcal{R}(\rho_s; m_t^{pole})$ in the $2 \to 7$ approach were provided by the authors of Ref. [25]. Only electrons and muons are considered as leptons. Asymmetric p_T requirements are imposed on the p_T-leading and p_T-subleading leptons, with both selections matching the detector level selection. All the objects in the seven-particle final state, excluding neutrinos, are separated by $\Delta R > 0.4$ and satisfy $|\eta| < 2.5$. A cut on the sum of neutrinos transverse momenta is set to be $(\sum_\nu p^\nu)_T > 30$ GeV. Jets containing a b-quark parton are required to satisfy $p_T^b > 30$ GeV, while the additional jet must satisfy $p_T^j > 60$ GeV. The renormalization and factorization scale are set to

$\mu_r, \mu_f = \mu_0 = H_T/2 = \frac{1}{2}\sum_{i\in[\ell^+,\ell^-,b,\bar{b},\nu,\bar{\nu},j]} p_T^i$ as suggested in Ref. [25].

The nominal calculations are performed with the PDF4LHC21 PDF set [94]. For comparisons of PDF sets, the calculations are also repeated with the CT18 NLO PDF set with $\alpha_s = 0.118$ [95], NNPDF3.0 NLO [43], ABMP16 [96], and the MSHT20 NLO PDF sets [97]. All considered PDF sets describe the proton content with massless b-quarks (five-flavor scheme). The impact of missing higher-order corrections in the calculations is estimated with scale variations of $\mu_r, \mu_f = \{\frac{1}{2}\cdot\mu_0, 2\cdot\mu_0\}$, avoiding combinations where the ratios of $\mu_r/\mu_f = \{1/4, 4\}$. The running of the strong coupling constant α_s is calculated in the five-flavor scheme. These variations are assessed for $m_t^{\text{pole}} = 172.5$ GeV. Additional theory predictions are calculated for values of m_t^{pole} ranging from 169 GeV to 176 GeV and are interpolated with second order polynomials to produce continuous predictions for $\mathcal{R}(\rho_s; m_t^{\text{pole}})$.

To correct the data to parton level, equivalent definitions are defined in the MC for the $2 \to 3$ and $2 \to 7$ calculations. In the $t\bar{t}$ MC simulation the $2 \to 3$ parton level is defined as follows: the last stable top (anti-)quark after initial state (ISR) and final state (FSR) radiation, and before decay is identified with the on-shell stable top (anti-) quark. The additional parton-level jet is built from all partons after the parton shower and before the hadronization stage which do not originate from top (anti-)quark decays. The anti-k_t algorithm with radius parameter $R = 0.4$ is used for the jet clustering. This parton-level definition is consistently applied to both the Pythia 8 and the Herwig 7 parton showers considered in the measurement. A $t\bar{t}$ + 1-jet event is selected for the $2 \to 3$ parton-level phase space if at least one additional resolved parton-level jet in $|\eta| < 2.5$ and with $p_T > 50$ GeV is found that does not originate from the decay products of the top (anti-) quarks.

For the definition at parton level in the $2 \to 7$ approach an ensemble of MC samples is used, as $t\bar{t}$ production, single-top production, and di-boson production processes all contribute to the $pp \to b\bar{b}l^+\nu_l l^-\bar{\nu}_l + j$ process. Only electrons and muons coming from a W-boson decay are considered as leptons in the final state. The jets are clustered with the anti-k_t algorithm on the partons after the parton shower simulation and before the hadronization step. The b-jets are identified by requiring that the direction of the momentum of the b-quark, from which the jet stems from, lies within $\Delta R = 0.4$ of the jet. Selection cuts on the objects are imposed such that kinematic requirements are synchronized across the FO theory prediction [25], the MC parton-level definition and the event selection at the detector level. The ρ_s variable in the $2 \to 7$ parton-level is obtained by adding the four-vectors corresponding to the charged leptons and neutrinos from the W boson decays, the two p_T-leading b-jets and the p_T-leading additional jet.

6 Differential cross-section measurement

The differential cross-section $\mathrm{d}\sigma_{t\bar{t}+1\text{-jet}}/\mathrm{d}\rho_s$ is obtained by subtracting the background contributions and unfolding to the $2 \to 3$ and $2 \to 7$ parton levels using the IBU algorithm [23]. The background subtraction removes all the expected non-$t\bar{t}$ processes in the $2 \to 3$ measurement. In the $2 \to 7$ case instead, tW production is considered as signal and is not subtracted, since tW and $t\bar{t}$ can produce the same final state once the W bosons and the top quarks decay[3]. The correction to parton level is split into three terms derived from the nominal Powheg+Pythia 8 simulation.

- An acceptance correction considers the events that satisfy the detector-level selection, but do not fulfill the parton-level definition. This correction is implemented as a bin-by-bin factor, defined as

[3] This is also valid for W^+W^- boson production, but its contribution is negligible in this analysis.

the ratio of events selected at the detector level that satisfy the parton-level requirements, divided by the total number of events selected at the detector level.

- A matrix describes the migration of events that satisfy both detector and parton level selections, from bins at the detector level to the bins at the parton level.
- An efficiency correction accounts for parton-level events that fail to meet the detector-level selection. This correction is also implemented as a bin-by-bin factor, computed as the ratio of parton level events which fulfill both parton and detector level selections over parton level events which only need to satisfy the parton level requirements.

The binning of the differential cross-section is optimized such that the high-ρ_s region, that has the highest sensitivity to m_t^{pole} is isolated. At the same time, this region should have a large enough population to ensure less than 5% statistical uncertainty in the high-sensitivity bins of the detector-level distribution. Finally, migrations from bins at detector level to parton level are limited, keeping the diagonal elements of the migration matrix above 40%. The migration matrix, the efficiency, and the acceptance for the $2 \to 3$ parton level unfolding are shown in Figure 3. The low values of the efficiency term reflects the fact that the parton level definition extrapolates for non-dileptonic top-quark pair decays and covers a much more inclusive phase space than the detector level one.

The IBU procedure starts from the parton-level distribution of the nominal signal simulation. It iteratively applies a correction to the parton-level based on the unfolding matrix and the measured spectrum at detector level. These iterations progressively reduce the bias. The number of iterations, and hence the level of regularization, is chosen such that the unfolding procedure does not depend on the value of the top-quark mass. To test this, MC samples with the top-quark mass parameter set to values between $m_t^{\text{MC}} = 169$ GeV and $m_t^{\text{MC}} = 176$ GeV are unfolded. Good convergence with minimal bias is found for all test distributions with 70 (40) iterations for the correction to the $2 \to 3$ ($2 \to 7$) parton level. These settings are used for all the results presented in the following.

The covariance matrix V^{stat} encodes the statistical uncertainty associated with the unfolded differential cross-section. It is built from 50000 pseudo-data distributions generated by varying background-subtracted $\mathrm{d}\sigma_{t\bar{t}+1\text{-jet}}/\mathrm{d}\rho_{\mathrm{s}}$ distribution within its statistical uncertainty, which are unfolded with the nominal unfolding procedure. Experimental systematic effects are added to the statistical covariance matrix to build a full covariance matrix, as explained in detail in Section 7.

The unfolded $\mathrm{d}\sigma_{t\bar{t}+1\text{-jet}}/\mathrm{d}\rho_{\mathrm{s}}$ distribution is normalized to unity to obtain the $\mathcal{R}(\rho_{\mathrm{s}}; m_t^{\text{pole}})$ observable at parton level which is used to extract the top-quark pole mass. The covariance matrix of the normalized differential cross-section is obtained using a Cholesky decomposition [98, 99] with 50000 toys, as described in Ref. [100].

The results for the normalized differential cross-sections at parton level are presented in Figure 4. In the unfolding to the $2 \to 3$ parton-level, the measurement reaches a precision of 8% in the ρ_s bin from 0.7 to 0.8 and 30% in the last bin from 0.8 to 1. The $2 \to 7$ phase space definition is closer to the detector level one and the measurement reaches a slightly better precision of 7% and 24% in the next-to-last and last bins. The predictions for two values of the top-quark pole mass are overlaid on the corrected data, showing the pronounced sensitivity to the top-quark pole mass in these two bins.

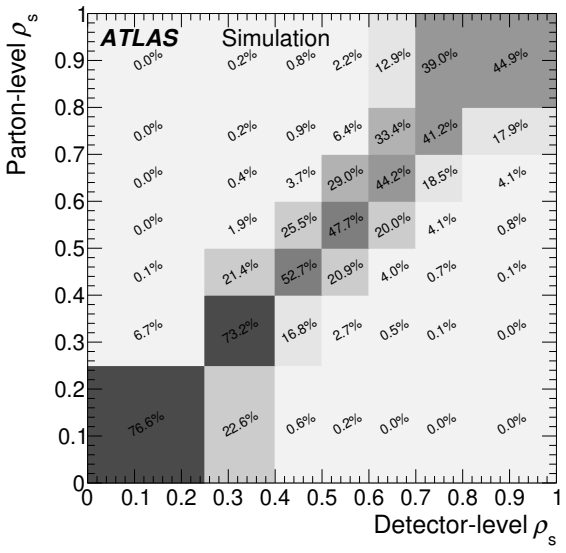

(a)

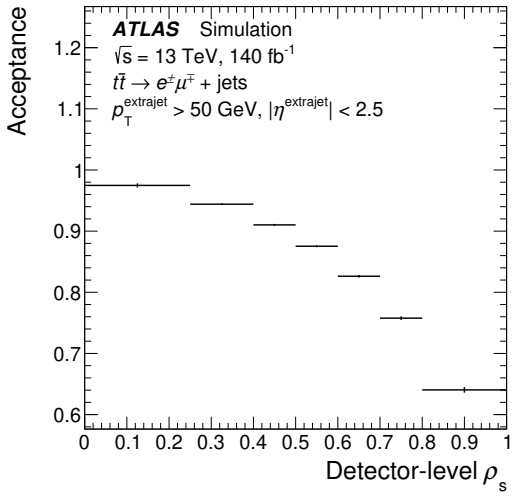

(b)

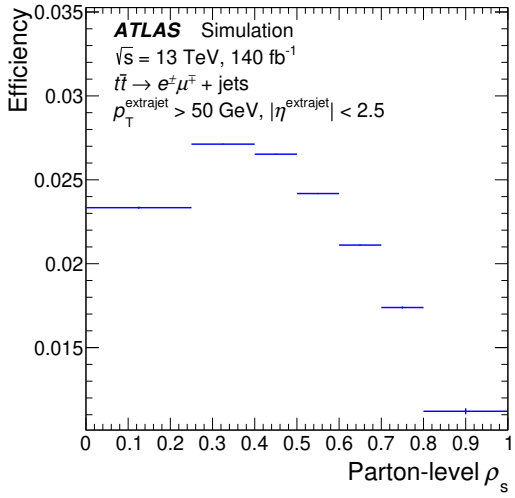

(c)

Figure 3: The (a) migration matrix and (b) the acceptance and (c) efficiency factors for events considered in the unfolding to the $2 \to 3$ parton level. The matrix and correction factors are built from the nominal simulation of $t\bar{t}$ + 1-jet events using the POWHEG+PYTHIA 8 generator. Vertical bars represent MC statistical uncertainties.

7 Systematic uncertainties

To evaluate the systematic uncertainties in the differential cross-section measurement, the nominal unfolding procedure is repeated on alternative pseudo-data distributions, corresponding to each systematic variation. The impact of each systematic uncertainty in the bin i of the unfolded distribution, Δ_i^{syst}, is used to build a covariance matrix associated with that systematic effect, $V_{i,j}^{\text{syst}} = \Delta_i^{\text{syst}} \Delta_j^{\text{syst}}$. If the uncertainty source is obtained by comparing two simulations, the full difference to the nominal result is defined as the uncertainty,

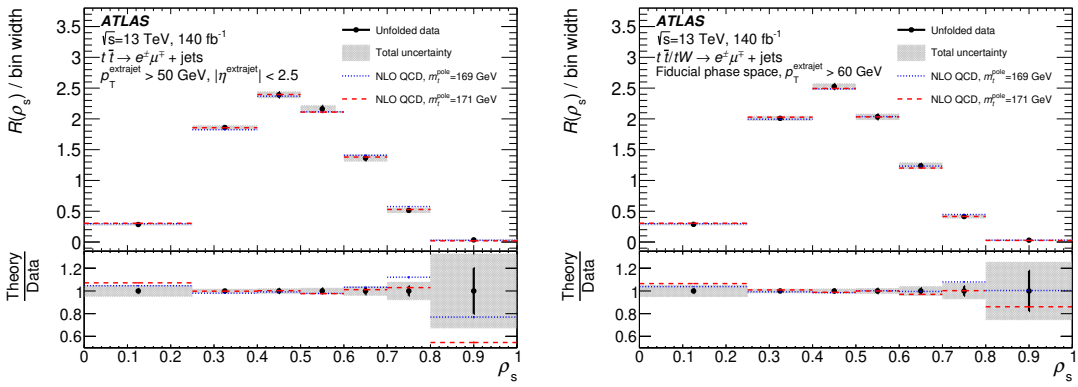

(a) (b)

Figure 4: The measured normalized differential cross-section $\mathcal{R}(\rho_s; m_t^{\text{pole}})$ unfolded to (a) the $2 \to 3$ parton level and (b) the $2 \to 7$ parton level. The error bars on the marker indicate the statistical uncertainty, the gray band the total experimental uncertainty. Theoretical predictions at fixed-order NLO QCD for $m_t^{\text{pole}} = 169$ GeV (dotted line) and $m_t^{\text{pole}} = 171$ GeV (dashed line) are also shown, without their associated uncertainties.

and the opposite-sign variation is assumed to be of identical size. For systematic uncertainty sources that consist of two-sided variations, a symmetric uncertainty is estimated as half of the difference between the up and down variations. If both variations point in the same direction compared with the central result, the maximum is taken as the resulting uncertainty and the opposite-sign variation is assumed to be of identical size.

A separate covariance matrix is constructed for each of the systematic variations and for the statistical uncertainty. The total covariance matrix is obtained adding up all covariance matrices. In this approach all the systematic components are independent of the other components and every individual systematic uncertainty is fully correlated across all bins of the unfolded distribution.

7.1 Experimental uncertainties

Uncertainties originating from the calibration of the objects used in the analysis are evaluated by unfolding the detector-level distribution obtained from MC simulations where the calibrations are varied within their uncertainties. The signal $t\bar{t}$ + 1-jet and background contributions are varied simultaneously for each experimental uncertainty sources.

The following sources of uncertainties are considered:

- The uncertainty in the integrated luminosity of the Run 2 pp collision data at $\sqrt{s} = 13$ TeV is 0.8% [33]. The expected yields of all signal and background processes are varied simultaneously. The uncertainty arising from the imperfect modeling of pileup in the data is estimated by reweighting the pileup profile in all simulated signal and background processes simultaneously [101].
- To estimate the impact of uncertainties in the lepton reconstruction, identification and isolation efficiencies, the MC simulation is varied as a function of lepton p_{T} and η, in a range allowed by measurements performed in $Z \to e^+e^-/\mu^+\mu^-$ and $J/\psi \to e^+e^-/\mu^+\mu^-$ events [74, 75]. Similarly, the trigger efficiencies are varied to account for uncertainties in the measurements of the efficiencies of the

lepton triggers [34, 35]. The effects of the uncertainties in the electron (muon) energy (momentum) scale and resolution are taken into account by varying these within their uncertainties [73, 76].

- Uncertainties in the energy scale of the jets (JES) are taken into account by varying the JES in the simulation. The JES uncertainty is split into 35 components, originating from the in situ calibration, the pileup correction, the dependence on the jet particle content, the punch-through modeling, and the high-p_{T} jet response [102, 103]. The uncertainty due to the jet energy resolution (JER) is evaluated by varying the resolution within its uncertainties as a function of p_{T} and η. The total JER response uncertainty is split into thirteen one-sided sources which are symmetrized to estimate the effect on the measurement. The efficiency of the JVT tagger is corrected in simulation, following a measurement which determines the JVT efficiency with a total uncertainty of $1-2\%$ using the tag-and-probe method in $Z \to \mu^+\mu^-$ events with additional jets [81].
- Uncertainties originating from b-tagging are obtained from in situ efficiency measurements [83–85] and are propagated through the analysis. The b-tagging uncertainties include different sources, split among b-tagging efficiency, and the c- and light-flavor mis-tagging rates.
- The effects of systematic uncertainties in the jets and leptons are propagated to the $E_{\mathrm{T}}^{\mathrm{miss}}$. Additional uncertainties for the scale and resolution of the track-based term [86, 87] are also included.

7.2 Modeling uncertainties

To evaluate the uncertainties in modeling of the simulated events, the internal parameters of the nominal MC simulation are varied and alternative MC generators are employed. To account only for changes in the response at the detector level and avoid convolution of those effects with any parton-level difference, the parton-level spectrum of the alternative MC simulations is reweighted to the one of the nominal Powheg+Pythia 8 simulation.

Many variations are considered to evaluate the uncertainty in the modeling of the $t\bar{t}$ process.

- The uncertainty due to the choice of the matching procedure between matrix element and the parton shower is evaluated by varying the hardness criterion (pThard) in the Powheg+Pythia 8 $t\bar{t}$ simulation from the event scale (pThard = 0) to the lowest p_{T}-value between the Powheg emission, and the inital- and final-state partons (pThard = 1).
- The impact of the choice of the damping parameter value in the Powheg simulation is estimated by setting $h_{\mathrm{damp}} = 3 \cdot m_t^{\mathrm{MC}}$ and comparing the results to the ones obtained with the nominal choice of $h_{\mathrm{damp}} = 1.5 \cdot m_t^{\mathrm{MC}}$.
- To evaluate the impact of missing higher orders in the QCD perturbative calculation of the matrix element, the μ_{r} and μ_{f} scales in the hard-process MC generator are varied by a factor of 0.5 and 2 in the Powheg+Pythia 8 $t\bar{t}$ simulation, independently.
- The dependence of the measurements on the choice of the PS and hadronization models in the simulation is estimated by interfacing the Powheg $t\bar{t}$ simulation with Herwig 7.1.3 [104] using the NNPDF 3.0 NLO PDF set in the ME, and MMHT 2014 LO [105] in the parton shower and the multi-parton interaction model.

- The uncertainty of the α_s value in the multi-parton interactions and the color-reconnection of the beam remnants in Pythia 8 is propagated by varying the Var1 set of parameters of the A14 eigentunes [46].
- The uncertainty associated with the modeling of ISR is evaluated by varying the α_s value in the Pythia 8 parton shower Var3c set of parameters, as per the A14 UE tune variations. To estimate the FSR uncertainty, renormalization and factorization scales in the PS are varied by a factor of 0.5 and 2.
- The uncertainty in the modeling of the radiation in top-quark decays is evaluated by comparing the results of the *recoil-to-top* scheme to one implemented from the nominal simulation, where the second and subsequent gluon emissions recoil against the b-quark (*recoil-to-colored*) [106].
- The uncertainty associated with the color-reconnection modeling is estimated from two alternative models [107], by taking as the alternative sample the one producing the largest difference on the extracted top-quark mass relative to the nominal simulation.
- The uncertainty related to the modeling of top-quark decay is evaluated by comparing the nominal sample to a MC simulation with the same simulation settings, but where the decay of the top-quark is performed with MadSpin [108, 109]. This uncertainty is referred to as *line shape* uncertainty, as it impacts the shape of the top-quark mass distribution.
- The uncertainty of the PDFs are computed using the thirty variations and the nominal version of the PDF4LHC15 PDF set at NLO accuracy [110].
- An additional uncertainty is considered to cover for the effect of $t\bar{t}$ NNLO corrections, which are known to be not fully covered by the scale uncertainties of the $t\bar{t}$ NLO+PS prediction [52–54]. An iterative reweighting procedure is implemented to simulate NNLO+NLL QCD effects in the parton-level p_{T}^{t}, $p_{\mathrm{T}}^{t\bar{t}}$, and $m_{t\bar{t}}$ distributions. The difference between results obtained with the reweighted and the nominal distributions is taken as an uncertainty.

Single top-quark production is the largest non-$t\bar{t}$ process contributing to the selected events. A systematic uncertainty in the sample normalization is assigned from tW cross-section uncertainty. In addition, a dedicated systematic uncertainty is assigned to estimate the impact of the $t\bar{t}$ and tW overlap removal: the diagram-subtraction [57] and diagram-removal [111] schemes are compared with each other and the difference between results is taken as the uncertainty.

As prefaced in Section 3, samples corresponding to other backgrounds are assigned a cross-section normalization uncertainty, indicated in Table 1, while the fake-lepton background is assigned a rate uncertainty of 50%. These uncertainties are propagated by generating pseudo-data with varied normalizations of the background processes. The nominal correction procedure is applied and the shift in the corrected differential cross-section is taken as the uncertainty.

The residual dependence of the unfolding on the top-quark mass parameter in the MC is accounted for by comparing two MC simulations generated with $m_t^{\mathrm{MC}} = 171$ GeV and $m_t^{\mathrm{MC}} = 174$ GeV. The bin-by-bin difference between the unfolded distributions is subtracted by the expected difference from the parton level and the result is used to define an additional systematic uncertainty which covers the residual m_t^{MC} dependence of the unfolding.

To evaluate the uncertainty due to the limited size of the $t\bar{t}$ MC samples used in the data correction procedure, 5000 pseudo-experiments are performed where the unfolding matrix is varied within its statistical uncertainty.

8 Top-quark pole mass extraction

To extract the value of the top-quark pole mass, a fit of $\mathcal{R}(\rho_s; m_t^{\text{pole}})$ as given by the $t\bar{t}$ + 1-jet calculation at NLO QCD accuracy to the unfolded normalized differential cross-section $\mathcal{R}_{\text{data}}^{t\bar{t}+1\text{-jet}}$ is performed. The fit uses the least-squares method, where the best-fit value of m_t^{pole} is the one that minimizes:

$$\chi^2 = \sum_{i,j} \left[\mathcal{R}_{\text{data}}^{t\bar{t}+1\text{-jet}} - \mathcal{R}_{\text{theo}}^{t\bar{t}+1\text{-jet}}(m_t^{\text{pole}})\right]_i \left[\tilde{V}^{-1}\right]_{ij} \left[\mathcal{R}_{\text{data}}^{t\bar{t}+1\text{-jet}} - \mathcal{R}_{\text{theo}}^{t\bar{t}+1\text{-jet}}(m_t^{\text{pole}})\right]_j, \tag{2}$$

where indices i and j refer to the bin number, and $\tilde{V}$ is the covariance matrix of the normalized unfolded spectrum, which includes experimental and modeling uncertainties. For the nominal fit, the PDF4LHC21 PDF set [94] is used, which combines information from the CT18 [95], NNPDF3.1 [112] and MSHT20 [97] PDF sets.

Since the $\mathcal{R}(\rho_s; m_t^{\text{pole}})$ observable is normalized, the entries in the bins are not independent of each other and the normalized covariance matrices cannot be inverted. To calculate the χ^2, the matrix is reduced by removing one column and the corresponding row, as the relative element of the residual vector. As a nominal choice, the first bin is excluded in the sum of Eq. 2, but the result does not depend on the choice of the excluded bin.

8.1 Linearity of the unfolding

To ensure that the measurement of the cross-section does not depend on the top-quark mass in the simulation used to correct the data, Powheg+Pythia 8 simulations are used to generate detector-level ρ_s distributions corresponding to m_t^{MC} values ranging from 169 GeV to 176 GeV. Each of the mass-varied samples is then unfolded to parton level with the nominal m_t^{MC} = 172.5 GeV simulation. A MC–based parton-level template is defined, with a continuous parameterization as a function of m_t^{MC}, constructed similarly to the FO theoretical template. This template is then used in a fit to the unfolded mass-varied distributions to extract a value of the top-quark mass, m_t^{fit}, for each distribution.

In Figure 5, the results of this test are shown. To quantify the bias introduced by the unfolding procedure, a linear fit to the values of $m_t^{\text{fit}} - m_t^{\text{MC}}$ is performed, considering only MC statistical uncertainties. This linear fit has a slope covering a ±170 MeV (±300 MeV) range in the $2 \to 3$ ($2 \to 7$) measurement, at the extreme mass points considered. Such variations are covered by the residual m_t^{MC} dependence systematic uncertainties.

8.2 Theoretical uncertainties

Since m_t^{pole} is extracted from a χ^2 fit to fixed-order theory calculations at NLO accuracy, additional uncertainties due to missing higher-order corrections and the proton PDFs and the strong coupling α_s are included. The uncertainties in the theory calculations due to the missing higher order corrections are estimated with the seven-point variation of the μ_r, μ_f scales: μ_r and μ_f in the theory calculation are varied by factors of 0.5 and 2, avoiding ratios of where $\mu_r/\mu_f = 4$ or $\mu_r/\mu_f = 1/4$. The m_t^{pole} result obtained with the nominal scale choice is compared with all seven variations and the largest upward and downward variations of the mass are taken as the uncertainty.

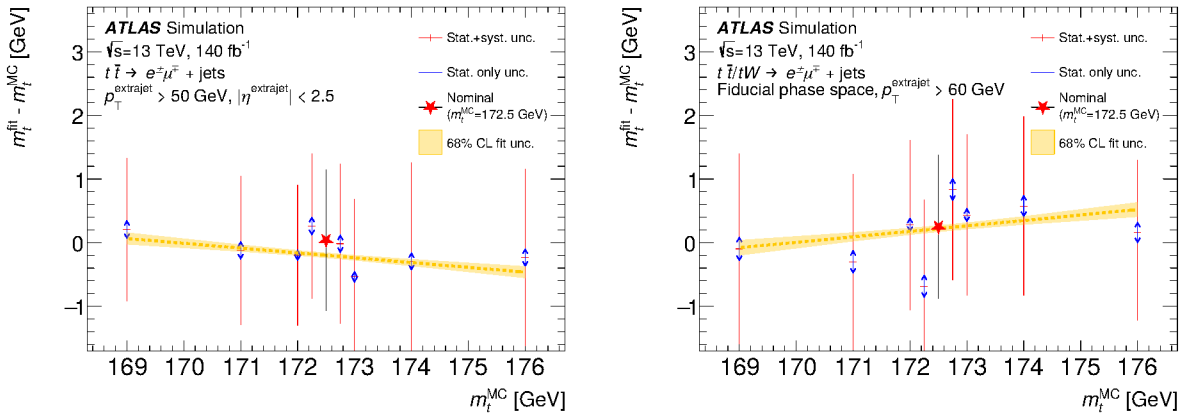

(a) (b)

Figure 5: Difference between the extracted m_t^{fit} value in the χ^2 fit and the mass value m_t^{MC} in the POWHEG+PYTHIA 8 $t\bar{t}$ simulations, (a) for the $2 \rightarrow 3$ and (b) $2 \rightarrow 7$ measurements. Each point corresponds to a mass value extracted using the parameterized mass dependence of the parton-level distributions obtained from the simulated MC samples, with the inner uncertainty bars representing the statistical uncertainties due to the limited size of the simulated samples and the outer bars representing the total experimental uncertainty associated with that measurement. A linear fit is performed across the various mass points, considering only their fully uncorrelated statistical uncertainties. Another uncorrelated effect, which originates from the interplay of statistical and systematic effects in the covariance matrices, further scatters the fitted mass values and is not considered in the linear fit. The 68% confidence level (CL) associated with the fit is shown with a filled area. The 172.5 GeV mass point is not included among the fitted points.

To evaluate the uncertainty due to imperfect knowledge of the proton PDFs used in the fixed-order calculations, predictions are obtained using all the variations of the corresponding PDF set. The PDF uncertainties are presented at the 68% confidence level and are taken in addition to the ones affecting the unfolding and described in Section 7. The value of the QCD coupling α_s in the nominal FO calculation is chosen to be $\alpha_s(M_Z) = 0.118$. To estimate the uncertainty in the choice of α_s, the value is varied between $\alpha_s(M_Z) = 0.117$ and $\alpha_s(M_Z) = 0.119$. The difference to the nominal result is added in quadrature to the PDF uncertainty to form the total PDF$\oplus\alpha_s$ uncertainty.

9 Results

The top-quark pole mass is extracted from the normalized differential cross-section with a least-square fit to FO predictions at NLO accuracy, as discussed in Section 8. The fit yields a χ^2 per degree of freedom χ^2/ndf of 0.88, indicating good agreement between the data and the prediction. The result obtained for the top-quark pole mass in the $2 \rightarrow 3$ approach is:

$$m_t^{\text{pole}} = 170.73 \pm 0.33\ (\text{stat.}) \pm 1.36\ (\text{syst.})\ ^{+0.34}_{-0.28}\ (\text{scale})\ \pm 0.24\ (\text{PDF} \oplus \alpha_s)\ \text{GeV}. \quad (3)$$

This is the main result of this study. The first uncertainty represents the statistical component, originating from the limited size of the recorded Run 2 data sample. Systematic uncertainties in the modeling of the detector response and signal and background processes are included in the second uncertainty contribution, which also includes the statistical uncertainty due to the finite size of the simulated samples. The third and

fourth uncertainty components of Eq. (3) cover the impact of missing higher-order corrections, the choice of the proton PDF set and the QCD coupling constant value in the NLO FO calculation.

A detailed breakdown of the uncertainties in the m_t^{pole} measurement is presented in Table 3. The dominant experimental uncertainties are those related to the b-tagging and jet-response calibration, which amount to approximately 440 MeV and 650 MeV, respectively. Several aspects of $t\bar{t}$ modeling lead to significant uncertainties, in particular the difference between the recoil-to-top and recoil-to-colored schemes in the parton shower and the parton shower generator choice. The theoretical uncertainties from variations of the dynamical renormalization and factorization scales amount to 350–450 MeV. The PDF uncertainties in the calculation, evaluated using the error sets of the PDF4LHC21 combination of PDF sets, add a similar uncertainty.

Table 3: Summary table of the uncertainties on the measurement of m_t^{pole} from a least square fit to the $2 \rightarrow 3$ calculation of Ref. [93]. The detector uncertainties grouped under *Others* correspond to the sum in quadrature of missing transverse energy, pileup re-weighting, and luminosity uncertainties. The factorization scale is responsible for the largest changes in the theoretical prediction and its high variations ($\mu_F \times 2$), yield a smaller value of the top-quark pole mass. The b-tagging and jet-energy response uncertainties are made up of multiple contributions, with the leading jet-energy systematic uncertainties coming from the dependence of the jet energy response on MC modeling and pileup. The MC statistical uncertainty associated with the systematic shift is given in the third column.

Uncertainty source	Δm_t^{pole} [GeV]	MC stat. unc. [GeV]
Data statistics	0.33	-
Detector unc.		
b-tagging and mistag	0.44	0.06
Jets	0.65	0.06
Leptons	0.25	0.06
Others	0.18	0.06
Modeling unc.		
MC statistical uncertainty	0.08	-
Backgrounds normalization	0.02	-
Single-top modeling	0.03	0.06
m_t^{MC} dependence	0.10	0.09
PS Recoil model	0.68	0.06
Parton shower	0.43	0.14
Underlying event	0.39	0.12
Color reconnection	0.13	0.08
ME+PS matching: $p_{\text{T}}^{\text{hard}}$	0.09	0.06
ME+PS matching: h_{damp}	0.26	0.06
ME+PS matching: line shape	0.38	0.12
3D NNLO reweight	0.21	0.06
PDF	0.26	0.06
Initial-state radiation	0.24	0.06
Final-state radiation	0.04	0.16
Factorization scales	0.09	0.06
Renormalization scales	0.03	0.06
Theory unc.		
Scale variations	+0.34 -0.28	+0.05 -0.06
PDF $\oplus$ α_{S}	0.24	+0.06 -0.06
Total	+1.47 -1.44	-

The value of the mass is also reported separately for several PDF sets, as recommended by the PDF4LHC

group [94]:

$$
\begin{aligned}
m_t^{\text{pole}}(\text{CT18 [95]}) &= 170.94 \pm 0.33\ (\text{stat.}) \pm 1.36\ (\text{syst.})\ ^{+0.37}_{-0.28}\ (\text{scale})\ \pm 0.28\ (\text{PDF} \oplus \alpha_s)\ \text{GeV},\\
m_t^{\text{pole}}(\text{MSHT20 [97]}) &= 171.03 \pm 0.33\ (\text{stat.}) \pm 1.36\ (\text{syst.})\ ^{+0.33}_{-0.31}\ (\text{scale})\ ^{+0.26}_{-0.13}\ (\text{PDF} \oplus \alpha_s)\ \text{GeV},\\
m_t^{\text{pole}}(\text{NNPDF30 [43]}) &= 170.70 \pm 0.33\ (\text{stat.}) \pm 1.36\ (\text{syst.})\ ^{+0.34}_{-0.28}\ (\text{scale})\ \pm 0.22\ (\text{PDF} \oplus \alpha_s)\ \text{GeV},\\
m_t^{\text{pole}}(\text{ABMP16 [96]}) &= 172.76 + 0.33\ (\text{stat.}) \pm 1.36\ (\text{syst.})\ ^{+0.33}_{-0.28}\ (\text{scale})\ \pm 0.24\ (\text{PDF} \oplus \alpha_s)\ \text{GeV}.
\end{aligned}
\tag{4}
$$

The central values of the results obtained with CT18 and NNPDF30 agree within approximately 200 MeV with each other and with the PDF4LHC21 result of Eq. (3).

Several crosschecks are performed to verify the consistency of the results. The m_t^{pole} mass is extracted from the $2 \to 7$ measurement with the calculation of Ref. [25]. Despite the $2 \to 7$ cross-section measurement being slightly more precise than the $2 \to 3$ one, the smaller sensitivity close to the $t\bar{t}$ threshold leads to an increase of all uncertainty components on the top-quark mass, yielding:

$$
m_t^{\text{pole}} = 171.69 \pm 0.41\ (\text{stat.}) \pm 1.68(\text{syst.})\ ^{+0.66}_{-1.34}\ (\text{scale})\ ^{+0.49}_{-0.46}\ (\text{PDF} \oplus \alpha_s)\ \text{GeV}\ . \tag{5}
$$

The central value of the $2 \to 7$ result is approximately 1 GeV higher than the $2 \to 3$ one. The difference between the two is covered by the scale uncertainty of the theoretical prediction, which grows from 0.3 – 0.4 GeV in the $2 \to 3$ measurement to approximately 1 GeV in the $2 \to 7$ one. The result for the central value was cross-checked by repeating the $2 \to 7$ analysis with correction factors derived from the $bb4l$ MC simulation instead of the nominal correction factors, and obtaining the same value within 100 MeV.

The differential cross-section measurement and mass extraction are moreover repeated on sub-sets of the data, splitting the data by data-taking period. In each case, the data is corrected using the Monte Carlo simulation corresponding to the sub-set in question. Good agreement is found for the measured m_t^{pole} values in different data-taking periods, with differences covered by single-period statistical uncertainties.

Finally, the top-quark mass measurement based on the $2 \to 3$ parton level prediction is repeated with different choices for the p_{T} cuts on the additional jet, at 30 GeV and 60 GeV. The p_{T} cut variation is synchronized at parton and detector level and the unfolding correction is re-derived for each value. Results for m_t^{pole} are found to be stable against the choice of the p_{T} cut, with changes in the extracted mass value of ±250 MeV.

The results of this analysis are compared with other top-quark mass determinations in Figure 6. The values of the top-quark pole mass in Eq. (3) and Eq. (4) are in agreement with the determination by CMS using the same approach [22] and with earlier ATLAS results on Run 1 data [20, 21]. The uncertainty of the result presented in this paper are slightly larger, mainly due to the more extensive set of modeling uncertainties considered.

These results agree within uncertainties with determinations of the top-quark pole mass from the inclusive cross-section [113]. The central value of the latter tends to be somewhat higher: the ATLAS+CMS Run 1 combination [113] yields $m_t^{\text{pole}} = 173.4\ ^{+1.8}_{-2.0}$ GeV with a prediction based on a version of the NNPDF3.1 PDF without considering top-quark measurements as inputs to the PDF fit. The values obtained in this analysis agree moreover with the precise determination of the top-quark mass obtained from the combination of ATLAS and CMS Run 1 direct measurements [114], i.e. $m_t = 172.52 \pm 0.33$ GeV.

The indirect estimate of the top-quark mass from a recent global electroweak fit [4] is also shown. The indirect determination of the top quark mass from electro-weak precision observables yields $m_t^{\text{pole}} = 176.4 \pm 2.1$ GeV; a difference of about 5 GeV from the nominal result of this analysis.

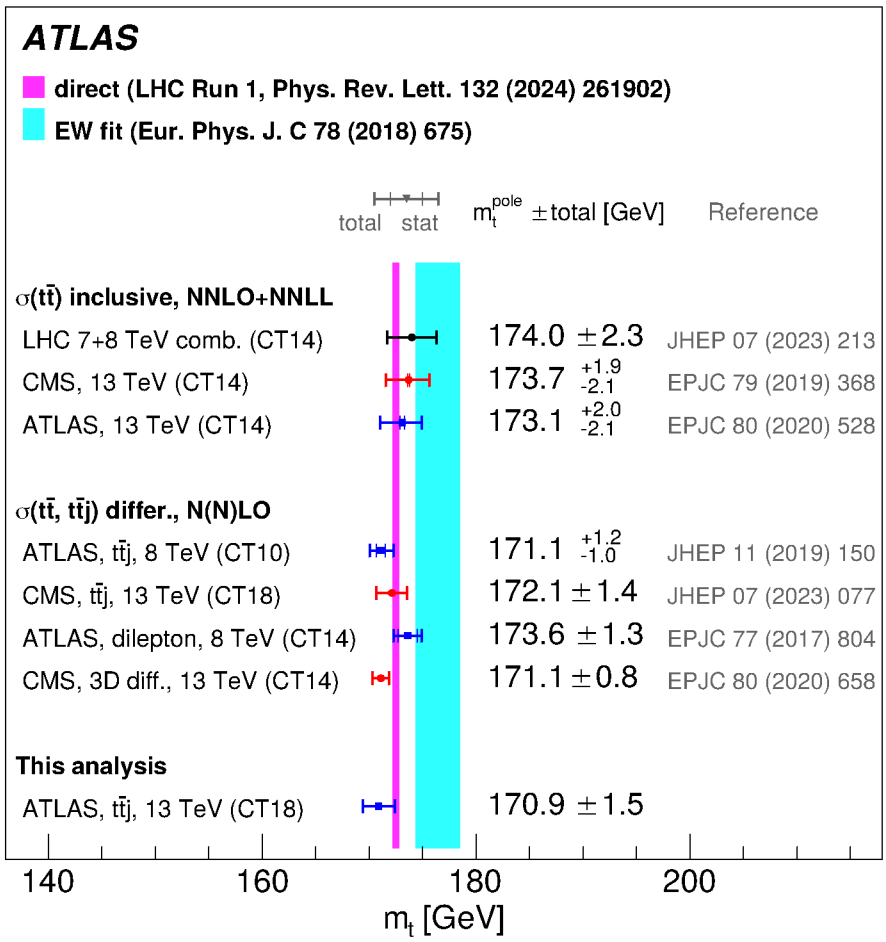

Figure 6: Summary of top-quark mass results at the LHC, obtained from inclusive and differential top-quark-pair production cross-section measurements. For a more uniform comparison, results are chosen that were obtained with the most recent CTEQ PDFs at the time of the publication, as indicated in parentheses. The values shown here do not correspond to the nominal result of the paper in all cases. The value reported for this analysis is obtained from the $2 \rightarrow 3$ prediction.

10 Conclusion

A measurement is presented of the normalized differential cross-section of top-quark-antiquark pair production with an additional high-p_{T} jet as a function of $\rho_{\mathrm{s}} = 2m_0/\sqrt{s_{t\bar{t}+1\text{-jet}}}$, where $m_0 = 170$ GeV. The pp collision data set at $\sqrt{s} = 13$ TeV collected by the ATLAS experiment during Run 2 of the LHC is used, corresponding to an integrated luminosity of 140 fb^{-1}. The measurement is performed in the $e^{\pm}\mu^{\mp}$ decay channel of the $t\bar{t}$ system, where the neutrinos from the W-boson decays are reconstructed using a combination of the loose kinematic reconstruction and ϕ-weighting method. The ρ_{s} distribution is corrected to parton level using the Iterative Bayesian Unfolding technique. Two parton level definitions are employed, considering the top quarks as stable or not. The normalized differential cross-section $\mathcal{R}(\rho_{\mathrm{s}}; m_t^{\mathrm{pole}})$ is presented in seven bins with a relative uncertainty ranging from a few % to approximately 25 % in the ρ_{s} region with the largest mass sensitivity.

The top-quark pole mass m_t^{pole} is extracted from the measured $\mathcal{R}(\rho_{\mathrm{s}}; m_t^{\mathrm{pole}})$ distribution with a least-squares

fit to fixed-order calculations at NLO accuracy in the strong coupling. The top-quark pole mass obtained with the PDF4LHC21 PDF set, in the stable top-quark approximation, is

$$m_t^{\text{pole}} = 170.7 \pm 0.3\ (\text{stat.}) \pm 1.4\ (\text{syst.})\ \pm 0.3\ (\text{scale})\ \pm 0.2\ (\text{PDF} \oplus \alpha_{\text{S}})\ \text{GeV} \quad ,$$

where the uncertainties represent the statistical uncertainty of the data, the experimental and modeling uncertainties from the differential cross-section measurement, the theoretical uncertainty estimated from the choice of renormalization and factorization scales, and the impact of PDF and α_s variations on the theoretical prediction, respectively. The top-quark pole mass is also determined based on cross-section calculations made with different PDF sets.

Several important cross-checks are performed to verify the stability of the result. The result is found to be robust within ± 250 MeV against variations of the p_{T} cut on the additional jet in the interval between 30 and 60 GeV. The result obtained with the $2 \rightarrow 3$ calculation assuming stable top quarks is compared with a result obtained from a fit of the corrected data to a $2 \rightarrow 7$ prediction where finite top-quark width and full off-shell effects are considered, hence testing the agreement in the description of top-quark decay modeling between the perturbative calculation and the Monte Carlo generator. The two results are found to agree within the theoretical uncertainties of the calculations. The measured values of the top quark pole mass agrees, moreover, with the result of precise direct mass measurements, where the LHC Run 1 average $m_t = 172.52 \pm 0.33$ GeV is taken as a reference. Hence, this result provides a confirmation of the interpretation of direct mass measurements in terms of the pole mass scheme, within the uncertainty of the result. The top quark pole mass constitutes an important input to assess the stability of the electroweak vacuum and to fits testing the compatibility of electroweak precision measurements. The differential cross section data are publicly available and can be used in the future to repeat the mass extraction with improved calculations.

Acknowledgements

We thank CERN for the very successful operation of the LHC and its injectors, as well as the support staff at CERN and at our institutions worldwide without whom ATLAS could not be operated efficiently.

The crucial computing support from all WLCG partners is acknowledged gratefully, in particular from CERN, the ATLAS Tier-1 facilities at TRIUMF/SFU (Canada), NDGF (Denmark, Norway, Sweden), CC-IN2P3 (France), KIT/GridKA (Germany), INFN-CNAF (Italy), NL-T1 (Netherlands), PIC (Spain), RAL (UK) and BNL (USA), the Tier-2 facilities worldwide and large non-WLCG resource providers. Major contributors of computing resources are listed in Ref. [115].

We gratefully acknowledge the support of ANPCyT, Argentina; YerPhI, Armenia; ARC, Australia; BMWFW and FWF, Austria; ANAS, Azerbaijan; CNPq and FAPESP, Brazil; NSERC, NRC and CFI, Canada; CERN; ANID, Chile; CAS, MOST and NSFC, China; Minciencias, Colombia; MEYS CR, Czech Republic; DNRF and DNSRC, Denmark; IN2P3-CNRS and CEA-DRF/IRFU, France; SRNSFG, Georgia; BMFTR, HGF and MPG, Germany; GSRI, Greece; RGC and Hong Kong SAR, China; ICHEP and Academy of Sciences and Humanities, Israel; INFN, Italy; MEXT and JSPS, Japan; CNRST, Morocco; NWO, Netherlands; RCN, Norway; MNiSW, Poland; FCT, Portugal; MNE/IFA, Romania; MSTDI, Serbia; MSSR, Slovakia; ARIS and MVZI, Slovenia; DSI/NRF, South Africa; MICIU/AEI, Spain; SRC and Wallenberg Foundation, Sweden; SERI, SNSF and Cantons of Bern and Geneva, Switzerland; NSTC, Taipei; TENMAK, Türkiye; STFC/UKRI, United Kingdom; DOE and NSF, United States of America.

Individual groups and members have received support from BCKDF, CANARIE, CRC and DRAC, Canada; CERN-CZ, FORTE and PRIMUS, Czech Republic; COST, ERC, ERDF, Horizon 2020, ICSC-NextGenerationEU and Marie Skłodowska-Curie Actions, European Union; Investissements d'Avenir Labex, Investissements d'Avenir Idex and ANR, France; DFG and AvH Foundation, Germany; Herakleitos, Thales and Aristeia programmes co-financed by EU-ESF and the Greek NSRF, Greece; BSF-NSF and MINERVA, Israel; NCN and NAWA, Poland; La Caixa Banking Foundation, CERCA Programme Generalitat de Catalunya and PROMETEO and GenT Programmes Generalitat Valenciana, Spain; Göran Gustafssons Stiftelse, Sweden; The Royal Society and Leverhulme Trust, United Kingdom.

In addition, individual members wish to acknowledge support from CERN: European Organization for Nuclear Research (CERN DOCT); Chile: Agencia Nacional de Investigación y Desarrollo (FONDECYT 1230812, FONDECYT 1240864); China: Chinese Ministry of Science and Technology (MOST-2023YFA1605700, MOST-2023YFA1609300), National Natural Science Foundation of China (NSFC - 12175119, NSFC 12275265); Czech Republic: Czech Science Foundation (GACR - 24-11373S), Ministry of Education Youth and Sports (ERC-CZ-LL2327, FORTE CZ.02.01.01/00/22_008/0004632), PRIMUS Research Programme (PRIMUS/21/SCI/017); EU: H2020 European Research Council (ERC - 101002463); European Union: European Research Council (BARD No. 101116429, ERC - 948254, ERC 101089007), European Regional Development Fund (SMASH COFUND 101081355, SLO ERDF), Horizon 2020 Framework Programme (MUCCA - CHIST-ERA-19-XAI-00), European Union, Future Artificial Intelligence Research (FAIR-NextGenerationEU PE00000013), Italian Center for High Performance Computing, Big Data and Quantum Computing (ICSC, NextGenerationEU); France: Agence Nationale de la Recherche (ANR-21-CE31-0022, ANR-22-EDIR-0002); Germany: Baden-Württemberg Stiftung (BW Stiftung-Postdoc Eliteprogramme), Bundesministerium für Bildung und Forschung (BMBF), Deutsche Forschungsgemeinschaft (DFG - 469666862, DFG - CR 312/5-2, DFG - 396021762 - TRR 257); China: Research Grants Council (GRF); Italy: Istituto Nazionale di Fisica Nucleare (ICSC, NextGenerationEU), Ministero dell'Università e della Ricerca (NextGenEU I53D23000820006 M4C2.1.1,

SOE2024_0000023); Japan: Japan Society for the Promotion of Science (JSPS KAKENHI JP22H01227, JSPS KAKENHI JP22H04944, JSPS KAKENHI JP22KK0227, JSPS KAKENHI JP24K23939, JSPS KAKENHI JP25H00650, JSPS KAKENHI JP25H01291, JSPS KAKENHI JP25K01023); México: Universidad Nacional Autónoma de México (DGAPA-PAPIIT IA102224); Norway: Research Council of Norway (RCN-314472); Poland: Ministry of Science and Higher Education (IDUB AGH, POB8, D4 no 9722), Polish National Science Centre (NCN 2021/42/E/ST2/00350, NCN OPUS 2023/51/B/ST2/02507, NCN OPUS nr 2022/47/B/ST2/03059, NCN UMO-2019/34/E/ST2/00393, UMO-2022/47/O/ST2/00148, UMO-2023/49/B/ST2/04085, UMO-2023/51/B/ST2/00920, UMO-2024/53/N/ST2/00869); Portugal: Foundation for Science and Technology (FCT); Spain: Ministry of Science and Innovation (MCIN & NextGenEU PCI2022-135018-2, MICIN & FEDER PID2021-125273NB, RYC2019-028510-I, RYC2020-030254-I, RYC2021-031273-I, RYC2022-038164-I); Sweden: Carl Trygger Foundation (Carl Trygger Foundation CTS 22:2312), Swedish Research Council (Swedish Research Council 2023-04654, VR 2021-03651, VR 2022-03845, VR 2022-04683, VR 2023-03403, VR 2024-05451), Knut and Alice Wallenberg Foundation (KAW 2018.0458, KAW 2022.0358, KAW 2023.0366); Switzerland: Swiss National Science Foundation (SNSF - PCEFP2_194658); United Kingdom: Leverhulme Trust (Leverhulme Trust RPG-2020-004), Royal Society (NIF-R1-231091); United States of America: U.S. Department of Energy (ECA DE-AC02-76SF00515), Neubauer Family Foundation.

References

[1] S. Alekhin, A. Djouadi and S. Moch,
The top quark and Higgs boson masses and the stability of the electroweak vacuum,
Phys. Lett. B **716** (2012) 214, arXiv: 1207.0980 [hep-ph].

[2] G. Degrassi et al., *Higgs mass and vacuum stability in the Standard Model at NNLO*,
JHEP **08** (2012) 098, arXiv: 1205.6497 [hep-ph].

[3] S. Amoroso et al., *Compatibility and combination of world W-boson mass measurements*,
Eur. Phys. J. C **84** (2024) 451, arXiv: 2308.09417 [hep-ex].

[4] Gfitter Group, *Update of the global electroweak fit and constraints on two-Higgs-doublet models*,
Eur. Phys. J. C **78** (2018) 675, arXiv: 1803.01853 [hep-ph].

[5] J. de Blas, M. Pierini, L. Reina and L. Silvestrini, *Impact of the Recent Measurements of the Top-Quark and W-Boson Masses on Electroweak Precision Fits*,
Phys. Rev. Lett. **129** (2022) 271801, arXiv: 2204.04204 [hep-ph].

[6] The ATLAS and CMS collaborations, *Combination of Measurements of the Top Quark Mass from Data Collected by the ATLAS and CMS Experiments at $\sqrt{s}$ = 7 and 8 TeV*,
Phys. Rev. Lett. **132** (2024) 261902, arXiv: 2402.08713 [hep-ex].

[7] P. Azzi et al.,
Report from Working Group 1: Standard Model Physics at the HL-LHC and HE-LHC,
CERN Yellow Rep. Monogr. **7** (2019) 1, arXiv: 1902.04070 [hep-ph].

[8] A. H. Hoang, *What Is the Top Quark Mass?*, Annu. Rev. Nucl. Part. Sci. **70** (2020) 225,
arXiv: 2004.12915 [hep-ph].

[9] S. Ferrario Ravasio, T. Ježo, P. Nason and C. Oleari, *A theoretical study of top-mass measurements at the LHC using NLO+PS generators of increasing accuracy*,
Eur. Phys. J. C **78** (2018) 458, Addendum: Eur. Phys. J. C 79, 859 (2019),
arXiv: 1906.09166 [hep-ph].

[10] M. Beneke, *Pole mass renormalon and its ramifications*, Eur. Phys. J. Spec. Top. **230** (2021) 2565, arXiv: 2108.04861 [hep-ph].

[11] M. Beneke, P. Marquard, P. Nason and M. Steinhauser, *On the ultimate uncertainty of the top quark pole mass*, Phys. Lett. B **775** (2017) 63, arXiv: 1605.03609 [hep-ph].

[12] S. Alioli et al., *A new observable to measure the top-quark mass at hadron colliders*, Eur. Phys. J. C **73** (2013) 2438, arXiv: 1303.6415 [hep-ph].

[13] W.-L. Ju et al., *Top quark pair production near threshold: single/double distributions and mass determination*, JHEP **06** (2020) 158, arXiv: 2004.03088 [hep-ph].

[14] M. V. Garzelli, G. Limatola, S.-O. Moch, M. Steinhauser and O. Zenaiev, *Updated predictions for toponium production at the LHC*, Phys. Lett. B **866** (2025) 139532, arXiv: 2412.16685 [hep-ph].

[15] Y. Kiyo, J. H. Kühn, S. Moch, M. Steinhauser and P. Uwer, *Top-quark pair production near threshold at LHC*, Eur. Phys. J. C **60** (2009) 375, arXiv: 0812.0919 [hep-ph].

[16] Y. Sumino and H. Yokoya, *Bound-state effects on kinematical distributions of top quarks at hadron colliders*, JHEP **09** (2010) 34, arXiv: 1007.0075 [hep-ph].

[17] K. Hagiwara, Y. Sumino and H. Yokoya, *Bound-state effects on top quark production at hadron colliders*, Phys. Lett. B **666** (2008) 71, arXiv: 0804.1014 [hep-ph].

[18] P. Nason, E. Re and L. Rottoli, *Spin Correlations in $t\bar{t}$ Production and Decay at the LHC in QCD Perturbation Theory*, (2025), arXiv: 2505.00096 [hep-ph].

[19] CMS Collaboration, *Observation of a pseudoscalar excess at the top quark pair production threshold*, (2025), arXiv: 2503.22382 [hep-ex].

[20] ATLAS Collaboration, *Determination of the top-quark pole mass using $t\bar{t}$ + 1-jet events collected with the ATLAS experiment in 7 TeV pp collisions*, JHEP **10** (2015) 121, arXiv: 1507.01769 [hep-ex].

[21] ATLAS Collaboration, *Measurement of the top-quark mass in $t\bar{t}$ + 1-jet events collected with the ATLAS detector in pp collisions at $\sqrt{s}$ = 8 TeV*, JHEP **11** (2019) 150, arXiv: 1905.02302 [hep-ex].

[22] CMS Collaboration, *Measurement of the top quark pole mass using $t\bar{t}$+jet events in the dilepton final state in proton–proton collisions at $\sqrt{s}$ = 13 TeV*, JHEP **07** (2023) 077, arXiv: 2207.02270 [hep-ex].

[23] G. D'Agostini, *A multidimensional unfolding method based on Bayes' theorem*, Nucl. Instrum. Meth. A **362** (1995) 487.

[24] S. Alioli, S.-O. Moch and P. Uwer, *Hadronic top-quark pair-production with one jet and parton showering*, JHEP **01** (2012) 137, arXiv: 1110.5251 [hep-ph].

[25] G. Bevilacqua, H. B. Hartanto, M. Kraus and M. Worek,
Off-shell top quarks with one jet at the LHC: a comprehensive analysis at NLO QCD,
JHEP **11** (2016) 098, arXiv: 1609.01659 [hep-ph].

[26] ATLAS Collaboration, *The ATLAS Experiment at the CERN Large Hadron Collider*,
JINST **3** (2008) S08003.

[27] ATLAS Collaboration, *ATLAS Insertable B-Layer: Technical Design Report*,
ATLAS-TDR-19; CERN-LHCC-2010-013, 2010,
URL: https://cds.cern.ch/record/1291633, Addendum: ATLAS-TDR-19-ADD-1;
CERN-LHCC-2012-009, 2012, URL: https://cds.cern.ch/record/1451888.

[28] B. Abbott et al., *Production and integration of the ATLAS Insertable B-Layer*,
JINST **13** (2018) T05008, arXiv: 1803.00844 [physics.ins-det].

[29] G. Avoni et al., *The new LUCID-2 detector for luminosity measurement and monitoring in ATLAS*,
JINST **13** (2018) P07017.

[30] ATLAS Collaboration, *Performance of the ATLAS trigger system in 2015*,
Eur. Phys. J. C **77** (2017) 317, arXiv: 1611.09661 [hep-ex].

[31] ATLAS Collaboration, *Software and computing for Run 3 of the ATLAS experiment at the LHC*,
Eur. Phys. J. C **85** (2025) 234, arXiv: 2404.06335 [hep-ex].

[32] ATLAS Collaboration,
ATLAS data quality operations and performance for 2015–2018 data-taking,
JINST **15** (2020) P04003, arXiv: 1911.04632 [physics.ins-det].

[33] ATLAS Collaboration,
Luminosity determination in pp collisions at $\sqrt{s} = 13$ TeV using the ATLAS detector at the LHC,
Eur. Phys. J. C **83** (2023) 982, arXiv: 2212.09379 [hep-ex].

[34] ATLAS Collaboration, *Performance of the ATLAS muon triggers in Run 2*,
JINST **15** (2020) P09015, arXiv: 2004.13447 [physics.ins-det].

[35] ATLAS Collaboration, *Performance of electron and photon triggers in ATLAS during LHC Run 2*,
Eur. Phys. J. C **80** (2020) 47, arXiv: 1909.00761 [hep-ex].

[36] ATLAS Collaboration,
The ATLAS inner detector trigger performance in pp collisions at 13 TeV during LHC Run 2,
Eur. Phys. J. C **82** (2022) 206, arXiv: 2107.02485 [hep-ex].

[37] S. Agostinelli et al., *Geant4-a simulation toolkit*, Nucl. Instrum. Meth. A **506** (2003) 250.

[38] ATLAS Collaboration, *The ATLAS Simulation Infrastructure*, Eur. Phys. J. C **70** (2010) 823,
arXiv: 1005.4568 [physics.ins-det].

[39] P. Nason, *A new method for combining NLO QCD with shower Monte Carlo algorithms*,
JHEP **11** (2004) 040, arXiv: hep-ph/0409146.

[40] S. Frixione, P. Nason and C. Oleari,
Matching NLO QCD computations with parton shower simulations: the POWHEG method,
JHEP **11** (2007) 070, arXiv: 0709.2092 [hep-ph].

[41] S. Alioli, P. Nason, C. Oleari and E. Re, *A general framework for implementing NLO calculations in shower Monte Carlo programs: the POWHEG BOX*, JHEP **06** (2010) 043,
arXiv: 1002.2581 [hep-ph].

[42] S. Frixione, G. Ridolfi and P. Nason,
A positive-weight next-to-leading-order Monte Carlo for heavy flavour hadroproduction,
JHEP **09** (2007) 126, arXiv: 0707.3088 [hep-ph].

[43] NNPDF Collaboration, R. D. Ball et al., *Parton distributions for the LHC run II*,
JHEP **04** (2015) 040, arXiv: 1410.8849 [hep-ph].

[44] T. Sjöstrand et al., *An introduction to PYTHIA 8.2*, Comput. Phys. Commun. **191** (2015) 159,
arXiv: 1410.3012 [hep-ph].

[45] ATLAS Collaboration, *Studies on top-quark Monte Carlo modelling for Top2016*,
ATL-PHYS-PUB-2016-020, 2016, URL: https://cds.cern.ch/record/2216168.

[46] ATLAS Collaboration, *ATLAS Pythia 8 tunes to 7 TeV data*, ATL-PHYS-PUB-2014-021, 2014,
URL: https://cds.cern.ch/record/1966419.

[47] NNPDF Collaboration, *Parton distributions with LHC data*, Nucl. Phys. B **867** (2013) 244,
arXiv: 1207.1303 [hep-ph].

[48] M. Czakon and A. Mitov,
Top++: A program for the calculation of the top-pair cross-section at hadron colliders,
Computer Physics Communications **185** (2014) 2930, arXiv: 1112.5675 [[hep-ph]].

[49] M. Beneke, P. Falgari, S. Klein and C. Schwinn,
Hadronic top-quark pair production with NNLL threshold resummation,
Nucl. Phys. B **855** (2012) 695, arXiv: 1109.1536 [hep-ph].

[50] M. Cacciari, M. Czakon, M. Mangano, A. Mitov and P. Nason, *Top-pair production at hadron colliders with next-to-next-to-leading logarithmic soft-gluon resummation*,
Phys. Lett. B **710** (2012) 612, arXiv: 1111.5869 [hep-ph].

[51] P. Bärnreuther, M. Czakon and A. Mitov, *Percent-Level-Precision Physics at the Tevatron: Next-to-Next-to-Leading Order QCD Corrections to $q\bar{q} \to t\bar{t}+X$*,
Phys. Rev. Lett. **109** (13 2012) 132001, arXiv: 1204.5201 [hep-ph].

[52] M. Czakon and A. Mitov, *NNLO corrections to top-pair production at hadron colliders: the all-fermionic scattering channels*, JHEP **12** (2012) 054, arXiv: 1207.0236 [hep-ph].

[53] M. Czakon and A. Mitov,
NNLO corrections to top pair production at hadron colliders: the quark-gluon reaction,
JHEP **01** (2013) 080, arXiv: 1210.6832 [hep-ph].

[54] M. Czakon, P. Fiedler and A. Mitov,
Total Top-Quark Pair-Production Cross Section at Hadron Colliders Through $O(\alpha_S^4)$,
Phys. Rev. Lett. **110** (2013) 252004, arXiv: 1303.6254 [hep-ph].

[55] N. Kidonakis and N. Yamanaka,
Higher-order corrections for tW production at high-energy hadron colliders, JHEP **05** (2021) 278,
arXiv: 2102.11300 [hep-ph].

[56] N. Kidonakis, *NNLL resummation for s-channel single top quark production*,
Phys. Rev. D **81** (2010) 054028, arXiv: 1001.5034 [hep-ph].

[57] C. D. White, S. Frixione, E. Laenen and F. Maltoni, *Isolating Wt production at the LHC*,
JHEP **11** (2009) 074, arXiv: 0908.0631 [hep-ph].

[58] T. Ježo, J. M. Lindert, P. Nason, C. Oleari and S. Pozzorini, *An NLO+PS generator for $t\bar{t}$ and Wt production and decay including non-resonant and interference effects*, Eur. Phys. J. C **76** (2016) 691, arXiv: 1607.04538 [hep-ph].

[59] T. Gleisberg et al., *Event generation with SHERPA 1.1*, JHEP **02** (2008) 007, arXiv: 0811.4622 [hep-ph].

[60] T. Gleisberg and S. Höche, *Comix, a new matrix element generator*, JHEP **12** (2008) 039, arXiv: 0808.3674 [hep-ph].

[61] F. Cascioli, P. Maierhöfer, and S. Pozzorini, *Scattering Amplitudes with Open Loops*, Phys. Rev. Lett. **108** (2012) 111601, arXiv: 1111.5206 [hep-ph].

[62] S. Höche, F. Krauss, M. Schönherr and F. Siegert, *QCD matrix elements + parton showers. The NLO case*, JHEP **04** (2013) 027, arXiv: 1207.5030 [hep-ph].

[63] C. Anastasiou, L. Dixon, K. Melnikov and F. Petriello, *High-precision QCD at hadron colliders: Electroweak gauge boson rapidity distributions at next-to-next-to leading order*, Phys. Rev. D **69** (2004) 094008, arXiv: hep-ph/0312266.

[64] R. Gavin, Y. Li, F. Petriello and S. Quackenbush, *FEWZ 2.0: A code for hadronic Z production at next-to-next-to-leading order*, Comput. Phys. Commun. **182** (2011) 2388, arXiv: 1011.3540 [hep-ph].

[65] H. B. Hartanto, B. Jäger, L. Reina and D. Wackeroth, *Higgs boson production in association with top quarks in the POWHEG BOX*, Phys. Rev. D **91** (2015) 094003, arXiv: 1501.04498 [hep-ph].

[66] D. de Florian et al., *Handbook of LHC Higgs Cross Sections: 4. Deciphering the Nature of the Higgs Sector*, CERN Yellow Rep. Monogr. **2** (2017) 1, arXiv: 1610.07922 [hep-ph].

[67] T. Sjöstrand, S. Mrenna and P. Skands, *A brief introduction to PYTHIA 8.1*, Computer Physics Communications **178** (2008) 852, arXiv: 0710.3820 [hep-ph].

[68] ATLAS Collaboration, *The Pythia 8 A3 tune description of ATLAS minimum bias and inelastic measurements incorporating the Donnachie–Landshoff diffractive model*, ATL-PHYS-PUB-2016-017, 2016, URL: https://cds.cern.ch/record/2206965.

[69] D. J. Lange, *The EvtGen particle decay simulation package*, Nucl. Instrum. Meth. A **462** (2001) 152.

[70] ATLAS Collaboration, *Inclusive and differential cross-sections for dilepton $t\bar{t}$ production measured in $\sqrt{s} = 13$ TeV pp collisions with the ATLAS detector*, JHEP **07** (2023) 141, arXiv: 2303.15340 [hep-ex].

[71] ATLAS Collaboration, *Measurement of $W^{\pm}$ and Z Boson Production Cross Sections in pp Collisions at $\sqrt{s} = 13$ TeV with the ATLAS Detector*, ATLAS-CONF-2015-039, 2015, URL: https://cds.cern.ch/record/2045487.

[72] J. M. Campbell and R. K. Ellis, *An update on vector boson pair production at hadron colliders*, Phys. Rev. D **60** (1999) 113006, arXiv: hep-ph/9905386 [hep-ph].

[73] ATLAS Collaboration, *Electron and photon performance measurements with the ATLAS detector using the 2015–2017 LHC proton–proton collision data*, JINST **14** (2019) P12006, arXiv: 1908.00005 [hep-ex].

[74] ATLAS Collaboration, *Muon reconstruction and identification efficiency in ATLAS using the full Run 2 pp collision data set at* $\sqrt{s} = 13$ *TeV*, Eur. Phys. J. C **81** (2021) 578, arXiv: 2012.00578 [hep-ex].

[75] ATLAS Collaboration, *Electron and photon efficiencies in LHC Run 2 with the ATLAS experiment*, JHEP **05** (2024) 162, arXiv: 2308.13362 [hep-ex].

[76] ATLAS Collaboration, *Studies of the muon momentum calibration and performance of the ATLAS detector with pp collisions at* $\sqrt{s} = 13$ *TeV*, Eur. Phys. J. C **83** (2023) 686, arXiv: 2212.07338 [hep-ex].

[77] M. Cacciari, G. P. Salam and G. Soyez, *The anti-k_t jet clustering algorithm*, JHEP **46** (2008) 063, arXiv: 0802.1189 [hep-ph].

[78] ATLAS Collaboration, *Jet reconstruction and performance using particle flow with the ATLAS Detector*, Eur. Phys. J. C **77** (2017) 466, arXiv: 1703.10485 [hep-ex].

[79] W. Lampl et al., *Calorimeter Clustering Algorithms: Description and Performance*, ATL-LARG-PUB-2008-002, 2008, URL: https://cds.cern.ch/record/1099735.

[80] ATLAS Collaboration, *Jet energy scale and resolution measured in proton–proton collisions at* $\sqrt{s} = 13$ *TeV with the ATLAS detector*, Eur. Phys. J. C **81** (2021) 689, arXiv: 2007.02645 [hep-ex].

[81] ATLAS Collaboration, *Tagging and suppression of pileup jets with the ATLAS detector*, ATLAS-CONF-2014-018, 2014, URL: https://cds.cern.ch/record/1700870.

[82] ATLAS Collaboration, *ATLAS flavour-tagging algorithms for the LHC Run 2 pp collision dataset*, Eur. Phys. J. C **83** (2023) 681, arXiv: 2211.16345 [physics.data-an].

[83] ATLAS Collaboration, *ATLAS b-jet identification performance and efficiency measurement with* $t\bar{t}$ *events in pp collisions at* $\sqrt{s} = 13$ *TeV*, Eur. Phys. J. C **79** (2019) 970, arXiv: 1907.05120 [hep-ex].

[84] ATLAS Collaboration, *Calibration of the light-flavour jet mistagging efficiency of the b-tagging algorithms with Z+jets events using* $139\,fb^{-1}$ *of ATLAS proton–proton collision data at* $\sqrt{s} = 13$ *TeV*, Eur. Phys. J. C **83** (2023) 728, arXiv: 2301.06319 [hep-ex].

[85] ATLAS Collaboration, *Measurement of the c-jet mistagging efficiency in* $t\bar{t}$ *events using pp collision data at* $\sqrt{s} = 13$ *TeV collected with the ATLAS detector*, Eur. Phys. J. C **82** (2022) 95, arXiv: 2109.10627 [hep-ex].

[86] ATLAS Collaboration, *E_T^{miss} performance in the ATLAS detector using 2015–2016 LHC pp collisions*, ATLAS-CONF-2018-023, 2018, URL: https://cds.cern.ch/record/2625233.

[87] ATLAS Collaboration, *Performance of missing transverse momentum reconstruction with the ATLAS detector using proton–proton collisions at* $\sqrt{s} = 13$ *TeV*, Eur. Phys. J. C **78** (2018) 903, arXiv: 1802.08168 [hep-ex].

[88] ATLAS Collaboration, *Probing the Quantum Interference between Singly and Doubly Resonant Top-Quark Production in pp Collisions at* $\sqrt{s} = 13$ *TeV with the ATLAS Detector*, Phys. Rev. Lett. **121** (2018) 152002, arXiv: 1806.04667 [hep-ex].

[89] CMS Collaboration, *Measurement of $t\bar{t}$ normalised multi-differential cross sections in pp collisions at $\sqrt{s} = 13$ TeV, and simultaneous determination of the strong coupling strength, top quark pole mass, and parton distribution functions*, Eur. Phys. J. C **80** (2020) 658, arXiv: 1904.05237 [hep-ex].

[90] CDF Collaboration and T. Aaltonen and J. Adelman, *Measurement of the top quark mass at CDF using the "neutrino ϕ weighting" template method on a lepton plus isolated track sample*, Phys. Rev. D **79** (2009) 072005, arXiv: 0901.3773 [hep-ex].

[91] M. Cacciari, G. P. Salam and G. Soyez, *The anti-k_t jet clustering algorithm*, JHEP **04** (2008) 063, arXiv: 0802.1189 [hep-ph].

[92] M. Cacciari, G. P. Salam and G. Soyez, *FastJet user manual*, Eur. Phys. J. C **72** (2012) 1896, arXiv: 1111.6097 [hep-ph].

[93] S. Alioli et al., *Phenomenology of $t\bar{t}j + X$ production at the LHC*, JHEP **05** (2022) 146, arXiv: 2202.07975 [hep-ph].

[94] R. D. Ball et al., *The PDF4LHC21 combination of global PDF fits for the LHC Run III*, J. Phys. G **49** (2022) 080501, arXiv: 2203.05506 [hep-ph].

[95] T.-J. Hou et al., *New CTEQ global analysis of quantum chromodynamics with high-precision data from the LHC*, Phys. Rev. D **103** (2021) 014013, arXiv: 1912.10053 [hep-ph].

[96] S. Alekhin, J. Blümlein, S. Moch and R. Plačakytė, *Parton distribution functions, α_s, and heavy-quark masses for LHC Run II*, Phys. Rev. D **96** (2017) 014011, arXiv: 1701.05838 [hep-ph].

[97] S. Bailey, T. Cridge, L. A. Harland-Lang, A. D. Martin and R. S. Thorne, *Parton distributions from LHC, HERA, Tevatron and fixed target data: MSHT20 PDFs*, Eur. Phys. J. C **81** (2021) 341, arXiv: 2012.04684 [hep-ph].

[98] J. Gentle, *Cholesky Factorization*, Numerical Linear Algebra for Applications in Statistics, p. 101, Springer New York, 1998.

[99] J. Nash, *The Choleski Decomposition*, Compact Numerical Methods for Computers: Linear Algebra and Function Minimisation, 2nd ed, p. 101, Bristol, England: Adam Hilger, 1990.

[100] ATLAS Collaboration, *Measurements of differential cross-sections in top-quark pair events with a high transverse momentum top quark and limits on beyond the Standard Model contributions to top-quark pair production with the ATLAS detector at $\sqrt{s} = 13$ TeV*, JHEP **06** (2022) 063, arXiv: 2202.12134 [hep-ex].

[101] ATLAS Collaboration, *Measurement of the Inelastic Proton–Proton Cross Section at $\sqrt{s} = 13$ TeV with the ATLAS Detector at the LHC*, Phys. Rev. Lett. **117** (2016) 182002, arXiv: 1606.02625 [hep-ex].

[102] ATLAS Collaboration, *Dependence of the Jet Energy Scale on the Particle Content of Hadronic Jets in the ATLAS Detector Simulation*, ATL-PHYS-PUB-2022-021, 2022, URL: https://cds.cern.ch/record/2808016.

[103] ATLAS Collaboration, *Measurements of jet cross-section ratios in 13 TeV proton–proton collisions with ATLAS*, Phys. Rev. D **110** (2024) 072019, arXiv: 2405.20206 [hep-ex].

[104] J. Bellm et al., *Herwig 7.0/Herwig++ 3.0 release note*, Eur. Phys. J. C **76** (2016) 196, arXiv: 1512.01178 [hep-ph].

[105] L. A. Harland-Lang, A. D. Martin, P. Motylinski and R. S. Thorne, *Parton distributions in the LHC era: MMHT 2014 PDFs*, Eur. Phys. J. C **75** (2015) 204, arXiv: 1412.3989 [hep-ph].

[106] ATLAS Collaboration, *Measurement of the top-quark mass using a leptonic invariant mass in pp collisions at $\sqrt{s} = 13$ TeV with the ATLAS detector*, JHEP **06** (2023) 019, arXiv: 2209.00583 [hep-ex].

[107] ATLAS Collaboration, *A study of different colour reconnection settings for Pythia8 generator using underlying event observables*, ATL-PHYS-PUB-2017-008, 2017, URL: https://cds.cern.ch/record/2262253.

[108] S. Frixione, E. Laenen, P. Motylinski and B. R. Webber, *Angular correlations of lepton pairs from vector boson and top quark decays in Monte Carlo simulations*, JHEP **04** (2007) 081, arXiv: hep-ph/0702198 [hep-ph].

[109] P. Artoisenet, R. Frederix, O. Mattelaer and R. Rietkerk, *Automatic spin-entangled decays of heavy resonances in Monte Carlo simulations*, JHEP **03** (2013) 15, arXiv: 1212.3460 [hep-ph].

[110] J. Butterworth et al., *PDF4LHC recommendations for LHC Run II*, J. Phys. G **43** (2015) 023001, arXiv: 1510.03865 [hep-ph].

[111] E. Re, *Single-top Wt-channel production matched with parton showers using the POWHEG method*, Eur. Phys. J. C **71** (2011) 1547, arXiv: 1009.2450 [hep-ex].

[112] R. D. Ball et al., *Parton distributions from high-precision collider data*, Eur. Phys. J. C **77** (2017) 663, arXiv: 1706.00428 [hep-ph].

[113] ATLAS and CMS Collaborations, *Combination of inclusive top-quark pair production cross-section measurements using ATLAS and CMS data at $\sqrt{s} = 7$ and 8 TeV*, JHEP **07** (2023) 213, arXiv: 2205.13830 [hep-ex].

[114] ATLAS and CMS Collaborations, *Combination of Measurements of the Top Quark Mass from Data Collected by the ATLAS and CMS Experiments at $\sqrt{s} = 7$ and 8 TeV*, Phys. Rev. Lett. **132** (2024) 261902, arXiv: 2402.08713 [hep-ex].

[115] ATLAS Collaboration, *ATLAS Computing Acknowledgements*, ATL-SOFT-PUB-2025-001, 2025, URL: https://cds.cern.ch/record/2922210.

The ATLAS Collaboration

G. Aad [104], E. Aakvaag [17], B. Abbott [123], S. Abdelhameed [119a], K. Abeling [55], N.J. Abicht [49], S.H. Abidi [30], M. Aboelela [45], A. Aboulhorma [36e], H. Abramowicz [157], Y. Abulaiti [120], B.S. Acharya [69a,69b,m], A. Ackermann [63a], C. Adam Bourdarios [4], L. Adamczyk [86a], S.V. Addepalli [149], M.J. Addison [103], J. Adelman [118], A. Adiguzel [22c], T. Adye [137], A.A. Affolder [139], Y. Afik [40], M.N. Agaras [13], A. Aggarwal [102], C. Agheorghiesei [28c], F. Ahmadov [39,ad], S. Ahuja [97], X. Ai [143b], G. Aielli [76a,76b], A. Aikot [169], M. Ait Tamlihat [36e], B. Aitbenchikh [36a], M. Akbiyik [102], T.P.A. Åkesson [100], A.V. Akimov [151], D. Akiyama [174], N.N. Akolkar [25], S. Aktas [172], G.L. Alberghi [24b], J. Albert [171], U. Alberti [20], P. Albicocco [53], G.L. Albouy [60], S. Alderweireldt [52], Z.L. Alegria [124], M. Aleksa [37], I.N. Aleksandrov [39], C. Alexa [28b], T. Alexopoulos [10], F. Alfonsi [24b], M. Algren [56], M. Alhroob [173], B. Ali [135], H.M.J. Ali [93,w], S. Ali [32], S.W. Alibocus [94], M. Aliev [34c], G. Alimonti [71a], W. Alkakhi [55], C. Allaire [66], B.M.M. Allbrooke [152], J.S. Allen [103], J.F. Allen [52], P.P. Allport [21], A. Aloisio [72a,72b], F. Alonso [92], C. Alpigiani [142], Z.M.K. Alsolami [93], A. Alvarez Fernandez [102], M. Alves Cardoso [56], M.G. Alviggi [72a,72b], M. Aly [103], Y. Amaral Coutinho [83b], A. Ambler [106], C. Amelung[37], M. Amerl [103], C.G. Ames [111], T. Amezza [130], D. Amidei [108], B. Amini [54], K. Amirie [161], A. Amirkhanov [39], S.P. Amor Dos Santos [133a], K.R. Amos [169], D. Amperiadou [158], S. An[84], C. Anastopoulos [145], T. Andeen [11], J.K. Anders [94], A.C. Anderson [59], A. Andreazza [71a,71b], S. Angelidakis [9], A. Angerami [42], A.V. Anisenkov [39], A. Annovi [74a], C. Antel [37], E. Antipov [151], M. Antonelli [53], F. Anulli [75a], M. Aoki [84], T. Aoki [159], M.A. Aparo [152], L. Aperio Bella [48], M. Apicella[31], C. Appelt [157], A. Apyan [27], M. Arampatzi [10], S.J. Arbiol Val [87], C. Arcangeletti [53], A.T.H. Arce [51], J-F. Arguin [110], S. Argyropoulos [158], J.-H. Arling [48], O. Arnaez [4], H. Arnold [151], G. Artoni [75a,75b], H. Asada [113], K. Asai [121], S. Asatryan [179], N.A. Asbah [37], R.A. Ashby Pickering [173], A.M. Aslam [97], K. Assamagan [30], R. Astalos [29a], K.S.V. Astrand [100], S. Atashi [165], R.J. Atkin [34a], H. Atmani[36f], P.A. Atmasiddha [131], K. Augsten [135], A.D. Auriol [41], V.A. Austrup [103], G. Avolio [37], K. Axiotis [56], A. Azzam [13], D. Babal [29b], H. Bachacou [138], K. Bachas [158,q], A. Bachiu [35], E. Bachmann [50], M.J. Backes [63a], A. Badea [40], T.M. Baer [108], P. Bagnaia [75a,75b], M. Bahmani [19], D. Bahner [54], K. Bai [126], J.T. Baines [137], L. Baines [96], O.K. Baker [178], E. Bakos [16], D. Bakshi Gupta [8], L.E. Balabram Filho [83b], V. Balakrishnan [123], R. Balasubramanian [4], E.M. Baldin [38], P. Balek [86a], E. Ballabene [24b,24a], F. Balli [138], L.M. Baltes [63a], W.K. Balunas [33], J. Balz [102], I. Bamwidhi [119b], E. Banas [87], M. Bandieramonte [132], A. Bandyopadhyay [25], S. Bansal [25], L. Barak [157], M. Barakat [48], E.L. Barberio [107], D. Barberis [18b], M. Barbero [104], M.Z. Barel [117], T. Barillari [112], M-S. Barisits [37], T. Barklow [149], P. Baron [136], D.A. Baron Moreno [103], A. Baroncelli [62], A.J. Barr [129], J.D. Barr [98], F. Barreiro [101], J. Barreiro Guimarães da Costa [14], M.G. Barros Teixeira [133a], S. Barsov [38], F. Bartels [63a], R. Bartoldus [149], A.E. Barton [93], P. Bartos [29a], A. Basan [102], M. Baselga [49], S. Bashiri[87], A. Bassalat [66,b], M.J. Basso [162a], S. Bataju [45], R. Bate [170], R.L. Bates [59], S. Batlamous[101], M. Battaglia [139], D. Battulga [19], M. Bauce [75a,75b], M. Bauer [79], P. Bauer [25], L.T. Bayer [48], L.T. Bazzano Hurrell [31], J.B. Beacham [112], T. Beau [130], J.Y. Beaucamp [92], P.H. Beauchemin [164], P. Bechtle [25], H.P. Beck [20,p], K. Becker [173], A.J. Beddall [82], V.A. Bednyakov [39], C.P. Bee [151], L.J. Beemster [16], M. Begalli [83d], M. Begel [30], J.K. Behr [48], J.F. Beirer [37], F. Beisiegel [25], M. Belfkir [119b], G. Bella [157], L. Bellagamba [24b], A. Bellerive [35], C.D. Bellgraph [68], P. Bellos [21], K. Beloborodov [38], I. Benaoumeur[21], D. Benchekroun [36a], F. Bendebba [36a], Y. Benhammou [157],

K.C. Benkendorfer[61], L. Beresford[48], M. Beretta[53], E. Bergeaas Kuutmann[167], N. Berger[4], B. Bergmann[135], J. Beringer[18a], G. Bernardi[5], C. Bernius[149], F.U. Bernlochner[25], F. Bernon[37], A. Berrocal Guardia[13], T. Berry[97], P. Berta[136], A. Berthold[50], A. Berti[133a], R. Bertrand[104], S. Bethke[112], A. Betti[75a,75b], A.J. Bevan[96], L. Bezio[56], N.K. Bhalla[54], S. Bharthuar[112], S. Bhatta[151], P. Bhattarai[149], Z.M. Bhatti[120], K.D. Bhide[54], V.S. Bhopatkar[124], R.M. Bianchi[132], G. Bianco[24b,24a], O. Biebel[111], M. Biglietti[77a], C.S. Billingsley[45], Y. Bimgdi[36f], M. Bindi[55], A. Bingham[177], A. Bingul[22b], C. Bini[75a,75b], G.A. Bird[33], M. Birman[175], M. Biros[136], S. Biryukov[152], T. Bisanz[49], E. Bisceglie[24b,24a], J.P. Biswal[137], D. Biswas[147], I. Bloch[48], A. Blue[59], U. Blumenschein[96], V.S. Bobrovnikov[39], L. Boccardo[57b,57a], M. Boehler[54], B. Boehm[172], D. Bogavac[13], A.G. Bogdanchikov[38], L.S. Boggia[130], V. Boisvert[97], P. Bokan[37], T. Bold[86a], M. Bomben[5], M. Bona[96], M. Boonekamp[138], A.G. Borbély[59], I.S. Bordulev[38], G. Borissov[93], D. Bortoletto[129], D. Boscherini[24b], M. Bosman[13], K. Bouaouda[36a], N. Bouchhar[169], L. Boudet[4], J. Boudreau[132], E.V. Bouhova-Thacker[93], D. Boumediene[41], R. Bouquet[57b,57a], A. Boveia[122], J. Boyd[37], D. Boye[30], I.R. Boyko[39], L. Bozianu[56], J. Bracinik[21], N. Brahimi[4], G. Brandt[177], O. Brandt[33], B. Brau[105], J.E. Brau[126], R. Brener[175], L. Brenner[117], R. Brenner[167], S. Bressler[175], G. Brianti[78a,78b], D. Britton[59], D. Britzger[112], I. Brock[25], R. Brock[109], G. Brooijmans[42], A.J. Brooks[68], E.M. Brooks[162b], E. Brost[30], L.M. Brown[171,162a], L.E. Bruce[61], T.L. Bruckler[129], P.A. Bruckman de Renstrom[87], B. Brüers[48], A. Bruni[24b], G. Bruni[24b], D. Brunner[47a,47b], M. Bruschi[24b], N. Bruscino[75a,75b], T. Buanes[17], Q. Buat[142], D. Buchin[112], A.G. Buckley[59], O. Bulekov[82], B.A. Bullard[149], S. Burdin[94], C.D. Burgard[49], A.M. Burger[91], B. Burghgrave[8], O. Burlayenko[54], J. Burleson[168], J.C. Burzynski[148], E.L. Busch[42], V. Büscher[102], P.J. Bussey[59], J.M. Butler[26], C.M. Buttar[59], J.M. Butterworth[98], W. Buttinger[137], C.J. Buxo Vazquez[109], A.R. Buzykaev[39], S. Cabrera Urbán[169], L. Cadamuro[66], H. Cai[37], Y. Cai[24b,114c,24a], Y. Cai[114a], V.M.M. Cairo[37], O. Cakir[3a], N. Calace[37], P. Calafiura[18a], G. Calderini[130], P. Calfayan[35], L. Calic[100], G. Callea[59], L.P. Caloba[83b], D. Calvet[41], S. Calvet[41], R. Camacho Toro[130], S. Camarda[37], D. Camarero Munoz[27], P. Camarri[76a,76b], C. Camincher[171], M. Campanelli[98], A. Camplani[43], V. Canale[72a,72b], A.C. Canbay[3a], E. Canonero[97], J. Cantero[169], Y. Cao[168], F. Capocasa[27], M. Capua[44b,44a], A. Carbone[71a,71b], R. Cardarelli[76a], J.C.J. Cardenas[8], M.P. Cardiff[27], G. Carducci[44b,44a], T. Carli[37], G. Carlino[72a], J.I. Carlotto[13], B.T. Carlson[132,r], E.M. Carlson[171], J. Carmignani[94], L. Carminati[71a,71b], A. Carnelli[4], M. Carnesale[37], S. Caron[116], E. Carquin[140g], I.B. Carr[107], S. Carrá[73a,73b], G. Carratta[24b,24a], C. Carrion Martinez[169], A.M. Carroll[126], M.P. Casado[13,h], P. Casolaro[72a,72b], M. Caspar[48], F.L. Castillo[4], L. Castillo Garcia[13], V. Castillo Gimenez[169], N.F. Castro[133a,133e], A. Catinaccio[37], J.R. Catmore[128], T. Cavaliere[4], V. Cavaliere[30], L.J. Caviedes Betancourt[23b], E. Celebi[82], S. Cella[37], V. Cepaitis[56], K. Cerny[125], A.S. Cerqueira[83a], A. Cerri[74a,74b,am], L. Cerrito[76a,76b], F. Cerutti[18a], B. Cervato[71a,71b], A. Cervelli[24b], G. Cesarini[53], S.A. Cetin[82], P.M. Chabrillat[130], R. Chakkappai[66], S. Chakraborty[173], J. Chan[18a], W.Y. Chan[159], J.D. Chapman[33], E. Chapon[138], B. Chargeishvili[155b], D.G. Charlton[21], C. Chauhan[136], Y. Che[114a], S. Chekanov[6], S.V. Chekulaev[162a], G.A. Chelkov[39,a], B. Chen[157], B. Chen[171], H. Chen[114a], H. Chen[30], J. Chen[144a], J. Chen[148], M. Chen[129], S. Chen[89], S.J. Chen[114a], X. Chen[144a], X. Chen[15,ah], Z. Chen[62], C.L. Cheng[176], H.C. Cheng[64a], S. Cheong[149], A. Cheplakov[39], E. Cherepanova[117], R. Cherkaoui El Moursli[36e], E. Cheu[7], K. Cheung[65], L. Chevalier[138], V. Chiarella[53], G. Chiarelli[74a], G. Chiodini[70a], A.S. Chisholm[21], A. Chitan[28b], M. Chitishvili[169], M.V. Chizhov[39,s], K. Choi[11], Y. Chou[142], E.Y.S. Chow[116], K.L. Chu[175],

M.C. Chu [64a], X. Chu [14,114c], Z. Chubinidze [53], J. Chudoba [134], J.J. Chwastowski [87], D. Cieri [112], K.M. Ciesla [86a], V. Cindro [95], A. Ciocio [18a], F. Cirotto [72a,72b], Z.H. Citron [175], M. Citterio [71a], D.A. Ciubotaru[28b], A. Clark [56], P.J. Clark [52], N. Clarke Hall [98], C. Clarry [161], S.E. Clawson [48], C. Clement [47a,47b], Y. Coadou [104], M. Cobal [69a,69c], A. Coccaro [57b], R.F. Coelho Barrue [133a], R. Coelho Lopes De Sa [105], S. Coelli [71a], L.S. Colangeli [161], B. Cole [42], P. Collado Soto [101], J. Collot [60], R. Coluccia[70a,70b], P. Conde Muiño [133a,133g], M.P. Connell [34c], S.H. Connell [34c], E.I. Conroy [129], M. Contreras Cossio[11], F. Conventi [72a,aj], A.M. Cooper-Sarkar [129], L. Corazzina [75a,75b], F.A. Corchia [24b,24a], A. Cordeiro Oudot Choi [142], L.D. Corpe [41], M. Corradi [75a,75b], F. Corriveau [106,ab], A. Cortes-Gonzalez [159], M.J. Costa [169], F. Costanza [4], D. Costanzo [145], B.M. Cote [122], J. Couthures [4], G. Cowan [97], K. Cranmer [176], L. Cremer [49], D. Cremonini [24b,24a], S. Crépé-Renaudin [60], F. Crescioli [130], T. Cresta [73a,73b], M. Cristinziani [147], M. Cristoforetti [78a,78b], V. Croft [117], G. Crosetti [44b,44a], A. Cueto [101], H. Cui [98], Z. Cui [7], B.M. Cunnett [152], W.R. Cunningham [59], F. Curcio [169], J.R. Curran [52], M.J. Da Cunha Sargedas De Sousa [57b,57a], J.V. Da Fonseca Pinto [83b], C. Da Via [103], W. Dabrowski [86a], T. Dado [37], S. Dahbi [154], T. Dai [108], D. Dal Santo [20], C. Dallapiccola [105], M. Dam [43], G. D'amen [30], V. D'Amico [111], J. Damp [102], J.R. Dandoy [35], M. D'andrea [57b,57a], D. Dannheim [37], G. D'anniballe [74a,74b], M. Danninger [148], V. Dao [151], G. Darbo [57b], S.J. Das [30], F. Dattola [48], S. D'Auria [71a,71b], A. D'Avanzo [72a,72b], T. Davidek [136], J. Davidson [173], I. Dawson [96], K. De [8], C. De Almeida Rossi [161], R. De Asmundis [72a], N. De Biase [48], S. De Castro [24b,24a], N. De Groot [116], P. de Jong [117], H. De la Torre [118], A. De Maria [114a], A. De Salvo [75a], U. De Sanctis [76a,76b], F. De Santis [70a,70b], A. De Santo [152], J.B. De Vivie De Regie [60], J. Debevc [95], D.V. Dedovich[39], J. Degens [94], A.M. Deiana [45], J. Del Peso [101], L. Delagrange [130], F. Deliot [138], C.M. Delitzsch [49], M. Della Pietra [72a,72b], D. Della Volpe [56], A. Dell'Acqua [37], L. Dell'Asta [71a,71b], M. Delmastro [4], C.C. Delogu [102], P.A. Delsart [60], S. Demers [178], M. Demichev [39], S.P. Denisov [38], H. Denizli [22a,l], L. D'Eramo [41], D. Derendarz [87], F. Derue [130], P. Dervan [94], A.M. Desai [1], K. Desch [25], F.A. Di Bello [57b,57a], A. Di Ciaccio [76a,76b], L. Di Ciaccio [4], A. Di Domenico [75a,75b], C. Di Donato [72a,72b], A. Di Girolamo [37], G. Di Gregorio [37], A. Di Luca [78a,78b], B. Di Micco [77a,77b], R. Di Nardo [77a,77b], K.F. Di Petrillo [40], M. Diamantopoulou [35], F.A. Dias [117], M.A. Diaz [140a,140b], A.R. Didenko [39], M. Didenko [169], S.D. Diefenbacher [18a], E.B. Diehl [108], S. Díez Cornell [48], C. Diez Pardos [147], C. Dimitriadi [150], A. Dimitrievska [21], A. Dimri [151], Y. Ding[62], J. Dingfelder [25], T. Dingley [129], I-M. Dinu [28b], S.J. Dittmeier [63b], F. Dittus [37], M. Divisek [136], B. Dixit [94], F. Djama [104], T. Djobava [155b], C. Doglioni [103,100], A. Dohnalova [29a], Z. Dolezal [136], K. Domijan [86a], K.M. Dona [40], M. Donadelli [83d], B. Dong [109], J. Donini [41], A. D'Onofrio [72a,72b], M. D'Onofrio [94], J. Dopke [137], A. Doria [72a], N. Dos Santos Fernandes [133a], I.A. Dos Santos Luz [83e], P. Dougan [103], M.T. Dova [92], A.T. Doyle [59], M.P. Drescher [55], E. Dreyer [175], I. Drivas-koulouris [10], M. Drnevich [120], D. Du [62], T.A. du Pree [117], Z. Duan[114a], M. Dubau [4], F. Dubinin [39], M. Dubovsky [29a], E. Duchovni [175], G. Duckeck [111], P.K. Duckett[98], O.A. Ducu [28b], D. Duda [52], A. Dudarev [37], M.M. Dudek [87], E.R. Duden [27], M. D'uffizi [103], L. Duflot [66], M. Dührssen [37], I. Duminica [28g], A.E. Dumitriu [28b], M. Dunford [63a], K. Dunne [47a,47b], A. Duperrin [104], H. Duran Yildiz [3a], A. Durglishvili [155b], G.I. Dyckes [18a], M. Dyndal [86a], B.S. Dziedzic [37], Z.O. Earnshaw [152], G.H. Eberwein [129], B. Eckerova [29a], S. Eggebrecht [55], E. Egidio Purcino De Souza [83e], G. Eigen [17], K. Einsweiler [18a], T. Ekelof [167], P.A. Ekman [100], S. El Farkh [36b], Y. El Ghazali [62], H. El Jarrari [37], A. El Moussaouy [36a], D. Elitez [37], M. Ellert [167], F. Ellinghaus [177], T.A. Elliot [97], N. Ellis [37], J. Elmsheuser [30], M. Elsawy [119a], M. Elsing [37], D. Emeliyanov [137], Y. Enari [84], I. Ene [18a], S. Epari [110], D. Ernani Martins Neto [87], F. Ernst[37], M. Errenst [177],

M. Escalier[66], C. Escobar[169], E. Etzion[157], G. Evans[133a,133b], H. Evans[68], L.S. Evans[48], A. Ezhilov[38], S. Ezzarqtouni[36a], F. Fabbri[24b,24a], L. Fabbri[24b,24a], G. Facini[98], V. Fadeyev[139], R.M. Fakhrutdinov[38], D. Fakoudis[102], S. Falciano[75a], L.F. Falda Ulhoa Coelho[133a], F. Fallavollita[112], G. Falsetti[44b,44a], J. Faltova[136], C. Fan[168], K.Y. Fan[64b], Y. Fan[14], Y. Fang[14,114c], M. Fanti[71a,71b], M. Faraj[69a,69b], Z. Farazpay[99], A. Farbin[8], A. Farilla[77a], K. Farman[154], T. Farooque[109], J.N. Farr[178], S.M. Farrington[137,52], F. Fassi[36e], D. Fassouliotis[9], L. Fayard[66], P. Federic[136], P. Federicova[134], O.L. Fedin[38,a], M. Feickert[176], L. Feligioni[104], D.E. Fellers[18a], C. Feng[143a], Y. Feng[14], Z. Feng[117], M.J. Fenton[165], L. Ferencz[48], B. Fernandez Barbadillo[93], P. Fernandez Martinez[67], M.J.V. Fernoux[104], J. Ferrando[93], A. Ferrari[167], P. Ferrari[117,116], R. Ferrari[73a], D. Ferrere[56], C. Ferretti[108], M.P. Fewell[1], D. Fiacco[75a,75b], F. Fiedler[102], P. Fiedler[135], S. Filimonov[39], M.S. Filip[28b,t], A. Filipčič[95], E.K. Filmer[162a], F. Filthaut[116], M.C.N. Fiolhais[133a,133c,c], L. Fiorini[169], W.C. Fisher[109], T. Fitschen[103], P.M. Fitzhugh[138], I. Fleck[147], P. Fleischmann[108], T. Flick[177], M. Flores[34d,ag], L.R. Flores Castillo[64a], L. Flores Sanz De Acedo[37], F.M. Follega[78a,78b], N. Fomin[33], J.H. Foo[161], A. Formica[138], A.C. Forti[103], E. Fortin[37], A.W. Fortman[18a], L. Foster[18a], L. Fountas[9,i], D. Fournier[66], H. Fox[93], P. Francavilla[74a,74b], S. Francescato[61], S. Franchellucci[56], M. Franchini[24b,24a], S. Franchino[63a], D. Francis[37], L. Franco[116], L. Franconi[48], M. Franklin[61], G. Frattari[27], Y.Y. Frid[157], J. Friend[59], N. Fritzsche[37], A. Froch[56], D. Froidevaux[37], J.A. Frost[129], Y. Fu[109], S. Fuenzalida Garrido[140g], M. Fujimoto[104], K.Y. Fung[64a], E. Furtado De Simas Filho[83e], M. Furukawa[159], J. Fuster[169], A. Gaa[55], A. Gabrielli[24b,24a], A. Gabrielli[161], P. Gadow[37], G. Gagliardi[57b,57a], L.G. Gagnon[18a], S. Gaid[88b], S. Galantzan[157], J. Gallagher[1], E.J. Gallas[129], A.L. Gallen[167], B.J. Gallop[137], K.K. Gan[122], S. Ganguly[159], Y. Gao[52], A. Garabaglu[142], F.M. Garay Walls[140a,140b], C. García[169], A. Garcia Alonso[117], A.G. Garcia Caffaro[178], J.E. García Navarro[169], M.A. Garcia Ruiz[23b], M. Garcia-Sciveres[18a], G.L. Gardner[131], R.W. Gardner[40], N. Garelli[164], R.B. Garg[149], J.M. Gargan[52], C.A. Garner[161], C.M. Garvey[34a], V.K. Gassmann[164], G. Gaudio[73a], V. Gautam[13], P. Gauzzi[75a,75b], J. Gavranovic[95], I.L. Gavrilenko[133a], A. Gavrilyuk[38], C. Gay[170], G. Gaycken[126], E.N. Gazis[10], A. Gekow[122], C. Gemme[57b], M.H. Genest[60], A.D. Gentry[115], S. George[97], T. Geralis[46], A.A. Gerwin[123], P. Gessinger-Befurt[37], M.E. Geyik[177], M. Ghani[173], K. Ghorbanian[96], A. Ghosal[147], A. Ghosh[165], A. Ghosh[7], B. Giacobbe[24b], S. Giagu[75a,75b], T. Giani[117], A. Giannini[62], S.M. Gibson[97], M. Gignac[139], D.T. Gil[86b], A.K. Gilbert[86a], B.J. Gilbert[42], D. Gillberg[35], G. Gilles[117], D.M. Gingrich[2,ai], M.P. Giordani[69a,69c], P.F. Giraud[138], G. Giugliarelli[69a,69c], D. Giugni[71a], F. Giuli[76a,76b], I. Gkialas[9,i], L.K. Gladilin[38], C. Glasman[101], M. Glazewska[20], R.M. Gleason[165], G. Glemža[48], M. Glisic[126], I. Gnesi[44b], Y. Go[30], M. Goblirsch-Kolb[37], B. Gocke[49], D. Godin[110], B. Gokturk[22a], S. Goldfarb[107], T. Golling[56], M.G.D. Gololo[34c], D. Golubkov[38], J.P. Gombas[109], A. Gomes[133a,133b], G. Gomes Da Silva[147], A.J. Gomez Delegido[37], R. Gonçalo[133a], L. Gonella[21], A. Gongadze[155c], F. Gonnella[21], J.L. Gonski[149], R.Y. González Andana[52], S. González de la Hoz[169], M.V. Gonzalez Rodrigues[48], R. Gonzalez Suarez[167], S. Gonzalez-Sevilla[56], L. Goossens[37], B. Gorini[37], E. Gorini[70a,70b], A. Gorišek[95], T.C. Gosart[131], A.T. Goshaw[51], M.I. Gostkin[39], S. Goswami[124], C.A. Gottardo[37], S.A. Gotz[111], M. Gouighri[36b], A.G. Goussiou[142], N. Govender[34c], R.P. Grabarczyk[129], I. Grabowska-Bold[86a], K. Graham[35], E. Gramstad[128], S. Grancagnolo[70a,70b], C.M. Grant[1], P.M. Gravila[28f], F.G. Gravili[70a,70b], H.M. Gray[18a], M. Greco[112], M.J. Green[1], C. Grefe[25], A.S. Grefsrud[17], I.M. Gregor[48], K.T. Greif[165], P. Grenier[149], S.G. Grewe[112], A.A. Grillo[139], K. Grimm[32], S. Grinstein[13,x], J.-F. Grivaz[66], E. Gross[175], J. Grosse-Knetter[55], L. Guan[108], G. Guerrieri[37], R. Guevara[128], R. Gugel[102],

J.A.M. Guhit[108], A. Guida[19], E. Guilloton[173], S. Guindon[37], F. Guo[14,114c], J. Guo[144a], L. Guo[48], L. Guo[114b,v], Y. Guo[108], A. Gupta[49], R. Gupta[132], S. Gupta[27], S. Gurbuz[25], S.S. Gurdasani[48], G. Gustavino[75a,75b], P. Gutierrez[123], L.F. Gutierrez Zagazeta[131], M. Gutsche[50], C. Gutschow[98], C. Gwenlan[129], C.B. Gwilliam[94], E.S. Haaland[128], A. Haas[120], M. Habedank[59], C. Haber[18a], H.K. Hadavand[8], A. Haddad[41], A. Hadef[50], A.I. Hagan[93], J.J. Hahn[147], E.H. Haines[98], M. Haleem[172], J. Haley[124], G.D. Hallewell[104], K. Hamano[171], H. Hamdaoui[167], M. Hamer[25], S.E.D. Hammoud[66], E.J. Hampshire[97], J. Han[143a], L. Han[114a], L. Han[62], S. Han[14], K. Hanagaki[84], M. Hance[139], D.A. Hangal[42], H. Hanif[148], M.D. Hank[131], J.B. Hansen[43], P.H. Hansen[43], D. Harada[56], T. Harenberg[177], S. Harkusha[179], M.L. Harris[105], Y.T. Harris[25], J. Harrison[13], N.M. Harrison[122], P.F. Harrison[173], M.L.E. Hart[98], N.M. Hartman[112], N.M. Hartmann[111], R.Z. Hasan[97,137], Y. Hasegawa[146], F. Haslbeck[129], S. Hassan[17], R. Hauser[109], M. Haviernik[136], C.M. Hawkes[21], R.J. Hawkings[37], Y. Hayashi[159], D. Hayden[109], C. Hayes[108], R.L. Hayes[117], C.P. Hays[129], J.M. Hays[96], H.S. Hayward[94], M. He[14,114c], Y. He[48], Y. He[98], N.B. Heatley[96], V. Hedberg[100], C. Heidegger[54], K.K. Heidegger[54], J. Heilman[35], S. Heim[48], T. Heim[18a], J.G. Heinlein[131], J.J. Heinrich[126], L. Heinrich[112], J. Hejbal[134], M. Helbig[50], A. Held[176], S. Hellesund[17], C.M. Helling[170], S. Hellman[47a,47b], A.M. Henriques Correia[37], H. Herde[100], Y. Hernández Jiménez[151], L.M. Herrmann[25], T. Herrmann[50], G. Herten[54], R. Hertenberger[111], L. Hervas[37], M.E. Hesping[102], N.P. Hessey[162a], J. Hessler[112], M. Hidaoui[36b], N. Hidic[136], E. Hill[161], T.S. Hillersoy[17], S.J. Hillier[21], J.R. Hinds[109], F. Hinterkeuser[25], M. Hirose[127], S. Hirose[163], D. Hirschbuehl[177], T.G. Hitchings[103], B. Hiti[95], J. Hobbs[151], R. Hobincu[28e], N. Hod[175], A.M. Hodges[168], M.C. Hodgkinson[145], B.H. Hodkinson[129], A. Hoecker[37], D.D. Hofer[108], J. Hofer[169], M. Holzbock[37], L.B.A.H. Hommels[33], V. Homsak[129], B.P. Honan[103], J.J. Hong[68], T.M. Hong[132], B.H. Hooberman[168], W.H. Hopkins[6], M.C. Hoppesch[168], Y. Horii[113], M.E. Horstmann[112], S. Hou[154], M.R. Housenga[168], J. Howarth[59], J. Hoya[6], M. Hrabovsky[125], T. Hryn'ova[4], P.J. Hsu[65], S.-C. Hsu[142], T. Hsu[66], M. Hu[18a], Q. Hu[62], S. Huang[33], X. Huang[14,114c], Y. Huang[136], Y. Huang[114b], Y. Huang[14], Z. Huang[66], Z. Hubacek[135], F. Huegging[25], T.B. Huffman[129], M. Hufnagel Maranha De Faria[83a], C.A. Hugli[48], M. Huhtinen[37], S.K. Huiberts[17], R. Hulsken[106], C.E. Hultquist[18a], D.L. Humphreys[105], N. Huseynov[12], J. Huston[109], J. Huth[61], L. Huth[48], R. Hyneman[7], G. Iacobucci[56], G. Iakovidis[30], L. Iconomidou-Fayard[66], J.P. Iddon[37], P. Iengo[72a,72b], R. Iguchi[159], Y. Iiyama[159], T. Iizawa[159], Y. Ikegami[84], D. Iliadis[158], N. Ilic[161], H. Imam[36a], G. Inacio Goncalves[83d], S.A. Infante Cabanas[140c], T. Ingebretsen Carlson[47a,47b], J.M. Inglis[96], G. Introzzi[73a,73b], M. Iodice[77a], V. Ippolito[75a,75b], R.K. Irwin[94], M. Ishino[159], W. Islam[176], C. Issever[19], S. Istin[22a,ao], K. Itabashi[84], H. Ito[174], R. Iuppa[78a,78b], A. Ivina[175], V. Izzo[72a], P. Jacka[135], P. Jackson[1], P. Jain[48], K. Jakobs[54], T. Jakoubek[175], J. Jamieson[59], W. Jang[159], S. Jankovych[136], M. Javurkova[105], P. Jawahar[103], L. Jeanty[126], J. Jejelava[155a,ae], P. Jenni[54,f], C.E. Jessiman[35], C. Jia[143a], H. Jia[170], J. Jia[151], X. Jia[112,114c], Z. Jia[114a], C. Jiang[52], Q. Jiang[64b], S. Jiggins[48], M. Jimenez Ortega[169], J. Jimenez Pena[13], S. Jin[114a], A. Jinaru[28b], O. Jinnouchi[141], P. Johansson[145], K.A. Johns[7], J.W. Johnson[139], F.A. Jolly[48], D.M. Jones[152], E. Jones[48], K.S. Jones[8], P. Jones[33], R.W.L. Jones[93], T.J. Jones[94], H.L. Joos[55], R. Joshi[122], J. Jovicevic[16], X. Ju[18a], J.J. Junggeburth[37], T. Junkermann[63a], A. Juste Rozas[13,x], M.K. Juzek[87], S. Kabana[140f], A. Kaczmarska[87], S.A. Kadir[149], M. Kado[112], H. Kagan[122], M. Kagan[149], A. Kahn[131], C. Kahra[102], T. Kaji[159], E. Kajomovitz[156], N. Kakati[175], N. Kakoty[13], I. Kalaitzidou[54], S. Kandel[8], N.J. Kang[139], D. Kar[34h], E. Karentzos[25], K. Karki[8], O. Karkout[117],

S.N. Karpov [39], Z.M. Karpova [39], V. Kartvelishvili [93], A.N. Karyukhin [38], E. Kasimi [158], J. Katzy [48], S. Kaur [35], K. Kawade [146], M.P. Kawale [123], C. Kawamoto [89], T. Kawamoto [62], E.F. Kay [37], F.I. Kaya [164], S. Kazakos [109], V.F. Kazanin [38], J.M. Keaveney [34a], R. Keeler [171], G.V. Kehris [61], J.S. Keller [35], J.M. Kelly [171], J.J. Kempster [152], O. Kepka [134], J. Kerr [162b], B.P. Kerridge [137], B.P. Kerševan [95], L. Keszeghova [29a], R.A. Khan [132], A. Khanov [124], A.G. Kharlamov [38], T. Kharlamova [38], E.E. Khoda [142], M. Kholodenko [133a], T.J. Khoo [19], G. Khoriauli [172], Y. Khoulaki [36a], J. Khubua [155b,*], Y.A.R. Khwaira [130], B. Kibirige [34h], D. Kim [6], D.W. Kim [47a,47b], Y.K. Kim [40], N. Kimura [98], M.K. Kingston [55], A. Kirchhoff [55], C. Kirfel [25], F. Kirfel [25], J. Kirk [137], A.E. Kiryunin [112], S. Kita [163], O. Kivernyk [25], M. Klassen [164], C. Klein [35], L. Klein [172], M.H. Klein [45], S.B. Klein [56], U. Klein [94], A. Klimentov [30], T. Klioutchnikova [37], P. Kluit [117], S. Kluth [112], E. Kneringer [79], T.M. Knight [161], A. Knue [49], M. Kobel [50], D. Kobylianskii [175], S.F. Koch [129], M. Kocian [149], P. Kodyš [136], D.M. Koeck [126], T. Koffas [35], O. Kolay [50], I. Koletsou [4], T. Komarek [87], K. Köneke [55], A.X.Y. Kong [1], T. Kono [121], N. Konstantinidis [98], P. Kontaxakis [56], B. Konya [100], R. Kopeliansky [42], S. Koperny [86a], K. Korcyl [87], K. Kordas [158,d], A. Korn [98], S. Korn [55], I. Korolkov [13], N. Korotkova [38], B. Kortman [117], O. Kortner [112], S. Kortner [112], W.H. Kostecka [118], M. Kostov [29a], V.V. Kostyukhin [147], A. Kotsokechagia [37], A. Kotwal [51], A. Koulouris [37], A. Kourkoumeli-Charalampidi [73a,73b], C. Kourkoumelis [9], E. Kourlitis [112], O. Kovanda [126], R. Kowalewski [171], W. Kozanecki [126], A.S. Kozhin [38], V.A. Kramarenko [38], G. Kramberger [95], P. Kramer [25], M.W. Krasny [130], A. Krasznahorkay [105], A.C. Kraus [118], J.W. Kraus [177], M. Kraus [181], J.A. Kremer [48] N.B. Krengel [147], T. Kresse [50], L. Kretschmann [177], J. Kretzschmar [94], P. Krieger [161], K. Krizka [21], K. Kroeninger [49], H. Kroha [112], J. Kroll [134], J. Kroll [131], K.S. Krowpman [109], U. Kruchonak [39], H. Krüger [25], N. Krumnack [81], M.C. Kruse [51], O. Kuchinskaia [39], S. Kuday [3a], S. Kuehn [37], R. Kuesters [54], T. Kuhl [48], V. Kukhtin [39], Y. Kulchitsky [39], S. Kuleshov [140d,140b], J. Kull [1], E.V. Kumar [111], M. Kumar [34h], N. Kumari [48], P. Kumari [162b], A. Kupco [134], A. Kupich [38], O. Kuprash [54], H. Kurashige [85], L.L. Kurchaninov [162a], O. Kurdysh [4], Y.A. Kurochkin [38], A. Kurova [38], M. Kuze [141], A.K. Kvam [105], J. Kvita [125], N.G. Kyriacou [142], C. Lacasta [169], F. Lacava [75a,75b], H. Lacker [19], D. Lacour [130], N.N. Lad [98], E. Ladygin [39], A. Lafarge [41], B. Laforge [130], T. Lagouri [178], F.Z. Lahbabi [36a], S. Lai [55,37], W.S. Lai [98], J.E. Lambert [171], S. Lammers [68], W. Lampl [7], C. Lampoudis [158,d], G. Lamprinoudis [102], A.N. Lancaster [118], E. Lançon [30], U. Landgraf [54], M.P.J. Landon [96], V.S. Lang [54], O.K.B. Langrekken [128], A.J. Lankford [165], F. Lanni [37], K. Lantzsch [25], A. Lanza [73a], M. Lanzac Berrocal [169], J.F. Laporte [138], T. Lari [71a], D. Larsen [17], L. Larson [11], F. Lasagni Manghi [24b], M. Lassnig [37], S.D. Lawlor [145], R. Lazaridou [165], M. Lazzaroni [71a,71b], H.D.M. Le [109], E.M. Le Boulicaut [178], L.T. Le Pottier [18a], B. Leban [24b,24a], F. Ledroit-Guillon [60], T.F. Lee [162b], L.L. Leeuw [34c], M. Lefebvre [171], C. Leggett [18a], G. Lehmann Miotto [37], M. Leigh [56], W.A. Leight [105], W. Leinonen [116], A. Leisos [158,u], M.A.L. Leite [83c], C.E. Leitgeb [19], R. Leitner [136], K.J.C. Leney [45], T. Lenz [25], S. Leone [74a], C. Leonidopoulos [52], A. Leopold [150], J.H. Lepage Bourbonnais [35], R. Les [109], C.G. Lester [33], M. Levchenko [38], J. Levêque [4], L.J. Levinson [175], G. Levrini [24b,24a], M.P. Lewicki [87], C. Lewis [142], D.J. Lewis [4], L. Lewitt [145], A. Li [30], B. Li [143a], C. Li [108], C-Q. Li [112], H. Li [143a], H. Li [103], H. Li [15], H. Li [62], H. Li [143a], J. Li [144a], K. Li [14], L. Li [144a], R. Li [178], S. Li [14,114c], S. Li [144b,144a], T. Li [5], X. Li [106], Y. Li [14], Z. Li [159], Z. Li [14,114c], Z. Li [62], S. Liang [14,114c], Z. Liang [14], M. Liberatore [138], B. Liberti [76a], G.B. Libotte [83d], K. Lie [64c], J. Lieber Marin [83e], H. Lien [68], H. Lin [108], S.F. Lin [151], L. Linden [111], R.E. Lindley [7], J.H. Lindon [37], J. Ling [61], E. Lipeles [131], A. Lipniacka [17], A. Lister [170], J.D. Little [68], B. Liu [14], B.X. Liu [114b], D. Liu [144b,144a], D. Liu [139], E.H.L. Liu [21], J.K.K. Liu [120], K. Liu [144b], K. Liu [144b,144a],

M. Liu [62], M.Y. Liu [62], P. Liu [14], Q. Liu [144b,142,144a], S. Liu [151], X. Liu [62], X. Liu [143a], Y. Liu [114b,114c], Y.L. Liu [143a], Y.W. Liu [62], Z. Liu [66,k], S.L. Lloyd [96], E.M. Lobodzinska [48], P. Loch [7], E. Lodhi [161], K. Lohwasser [145], E. Loiacono [48], J.D. Lomas [21], J.D. Long [42], I. Longarini [165], R. Longo [168], A. Lopez Solis [13], N.A. Lopez-canelas [7], N. Lorenzo Martinez [4], A.M. Lory [111], M. Losada [119a], G. Löschcke Centeno [4], X. Lou [47a,47b], X. Lou [14,114c], A. Lounis [66], P.A. Love [93], M. Lu [66], S. Lu [131], Y.J. Lu [154], H.J. Lubatti [142], C. Luci [75a,75b], F.L. Lucio Alves [114a], F. Luehring [68], B.S. Lunday [131], O. Lundberg [150], J. Lunde [37], N.A. Luongo [6], M. Lupattelli [180, 182], M.S. Lutz [37], A.B. Lux [26], D. Lynn [30], R. Lysak [134], V. Lysenko [135], E. Lytken [100], V. Lyubushkin [39], T. Lyubushkina [39], M.M. Lyukova [151], M.Firdaus M. Soberi [52], H. Ma [30], K. Ma [62], L.L. Ma [143a], W. Ma [62], Y. Ma [124], J.C. MacDonald [102], P.C. Machado De Abreu Farias [83e], D. Macina [37], R. Madar [41], T. Madula [98], J. Maeda [85], T. Maeno [30], P.T. Mafa [34c,j], H. Maguire [145], M. Maheshwari [33], V. Maiboroda [66], A. Maio [133a,133b,133d], K. Maj [86a], O. Majersky [48], S. Majewski [126], R. Makhmanazarov [38], N. Makovec [66], V. Maksimovic [16], B. Malaescu [130], J. Malamant [128], Pa. Malecki [87], V.P. Maleev [38], F. Malek [60,o], M. Mali [95], D. Malito [97], U. Mallik [80,*], A. Maloizel [5], S. Maltezos [10], A. Malvezzi Lopes [83d], S. Malyukov [39], J. Mamuzic [95], G. Mancini [53], M.N. Mancini [27], G. Manco [73a,73b], J.P. Mandalia [96], S.S. Mandarry [152], I. Mandić [95], L. Manhaes de Andrade Filho [83a], I.M. Maniatis [175], J. Manjarres Ramos [91], D.C. Mankad [175], A. Mann [111], T. Manoussos [37], M.N. Mantinan [40], S. Manzoni [37], L. Mao [144a], X. Mapekula [34c], A. Marantis [158], R.R. Marcelo Gregorio [96], G. Marchiori [5], C. Marcon [71a], E. Maricic [16], M. Marinescu [48], S. Marium [48], M. Marjanovic [123], A. Markhoos [54], M. Markovitch [66], M.K. Maroun [105], M.C. Marr [148], G.T. Marsden [103], E.J. Marshall [93], Z. Marshall [18a], S. Marti-Garcia [169], J. Martin [98], T.A. Martin [137], V.J. Martin [52], B. Martin dit Latour [17], L. Martinelli [75a,75b], M. Martinez [13,x], P. Martinez Agullo [169], V.I. Martinez Outschoorn [105], P. Martinez Suarez [37], S. Martin-Haugh [137], G. Martinovicova [136], V.S. Martoiu [28b], A.C. Martyniuk [98], A. Marzin [37], D. Mascione [78a,78b], L. Masetti [102], J. Masik [103], A.L. Maslennikov [39], S.L. Mason [42], P. Massarotti [72a,72b], P. Mastrandrea [74a,74b], A. Mastroberardino [44b,44a], T. Masubuchi [127], T.T. Mathew [126], J. Matousek [136], D.M. Mattern [49], J. Maurer [28b], T. Maurin [59], A.J. Maury [66], B. Maček [95], C. Mavungu Tsava [104], D.A. Maximov [38], A.E. May [103], E. Mayer [41], R. Mazini [34h], I. Maznas [118], S.M. Mazza [139], E. Mazzeo [37], J.P. Mc Gowan [171], S.P. Mc Kee [108], C.A. Mc Lean [6], C.C. McCracken [170], E.F. McDonald [107], A.E. McDougall [117], L.F. Mcelhinney [93], J.A. Mcfayden [152], R.P. McGovern [131], R.P. Mckenzie [34h], T.C. Mclachlan [48], D.J. Mclaughlin [98], S.J. McMahon [137], C.M. Mcpartland [94], R.A. McPherson [171,ab], S. Mehlhase [111], A. Mehta [94], D. Melini [169], B.R. Mellado Garcia [34h], A.H. Melo [55], F. Meloni [48], A.M. Mendes Jacques Da Costa [103], L. Meng [93], S. Menke [112], M. Mentink [37], E. Meoni [44b,44a], G. Mercado [118], S. Merianos [158], C. Merlassino [69a,69c], C. Meroni [71a,71b], J. Metcalfe [6], A.S. Mete [6], E. Meuser [102], C. Meyer [68], J-P. Meyer [138], Y. Miao [114a], R.P. Middleton [137], M. Mihovilovic [66], L. Mijović [52], G. Mikenberg [175], M. Mikestikova [134], M. Mikuž [95], H. Mildner [102], A. Milic [37], D.W. Miller [40], E.H. Miller [149], A. Milov [175], D.A. Milstead [47a,47b], T. Min [114a], A.A. Minaenko [38], I.A. Minashvili [155b], A.I. Mincer [120], B. Mindur [86a], M. Mineev [39], Y. Mino [89], L.M. Mir [13], M. Miralles Lopez [59], M. Mironova [18a], M.C. Missio [116], A. Mitra [173], V.A. Mitsou [169], Y. Mitsumori [113], O. Miu [161], P.S. Miyagawa [96], T. Mkrtchyan [63a], M. Mlinarevic [98], T. Mlinarevic [98], M. Mlynarikova [136], L. Mlynarska [86a], C. Mo [144a], S. Mobius [20], M.H. Mohamed Farook [115], S. Mohapatra [42], S. Mohiuddin [124], G. Mokgatitswane [34h], L. Moleri [175], U. Molinatti [129], L.G. Mollier [20], B. Mondal [134], S. Mondal [135], K. Mönig [48], E. Monnier [104], L. Monsonis Romero [169], J. Montejo Berlingen [13], A. Montella [47a,47b],

M. Montella[122], F. Montereali[77a,77b], F. Monticelli[92], S. Monzani[69a,69c], A. Morancho Tarda[43], N. Morange[66], A.L. Moreira De Carvalho[48], M. Moreno Llácer[169], C. Moreno Martinez[56], J.M. Moreno Perez[23b], P. Morettini[57b], S. Morgenstern[37], M. Morii[61], M. Morinaga[159], M. Moritsu[90], F. Morodei[75a,75b], P. Moschovakos[37], B. Moser[54], M. Mosidze[155b], T. Moskalets[45], P. Moskvitina[116], J. Moss[32], P. Moszkowicz[86a], A. Moussa[36d], Y. Moyal[175], H. Moyano Gomez[13], E.J.W. Moyse[105], T.G. Mroz[87], O. Mtintsilana[34h], S. Muanza[104], M. Mucha[25], J. Mueller[132], R. Müller[37], G.A. Mullier[167], A.J. Mullin[33], J.J. Mullin[51], A.C. Mullins[45], A.E. Mulski[61], D.P. Mungo[161], D. Munoz Perez[169], F.J. Munoz Sanchez[103], W.J. Murray[173,137], M. Muškinja[95], C. Mwewa[48], A.G. Myagkov[38,a], A.J. Myers[8], G. Myers[108], M. Myska[135], B.P. Nachman[149], K. Nagai[129], K. Nagano[84], R. Nagasaka[159], J.L. Nagle[30,al], E. Nagy[104], A.M. Nairz[37], Y. Nakahama[84], K. Nakamura[84], K. Nakkalil[5], A. Nandi[63b], H. Nanjo[127], E.A. Narayanan[45], Y. Narukawa[159], I. Naryshkin[38], L. Nasella[71a,71b], S. Nasri[119b], C. Nass[25], G. Navarro[23a], A. Nayaz[19], P.Y. Nechaeva[38], S. Nechaeva[24b,24a], F. Nechansky[134], L. Nedic[129], T.J. Neep[21], A. Negri[73a,73b], M. Negrini[24b], C. Nellist[117], C. Nelson[106], K. Nelson[108], S. Nemecek[134], M. Nessi[37,g], M.S. Neubauer[168], J. Newell[94], P.R. Newman[21], Y.W.Y. Ng[168], B. Ngair[119a], H.D.N. Nguyen[110], J.D. Nichols[123], R.B. Nickerson[129], R. Nicolaidou[138], J. Nielsen[139], M. Niemeyer[55], J. Niermann[37], N. Nikiforou[37], V. Nikolaenko[38,a], I. Nikolic-Audit[130], P. Nilsson[30], I. Ninca[48], G. Ninio[157], A. Nisati[75a], R. Nisius[112], N. Nitika[69a,69c], J-E. Nitschke[50], E.K. Nkadimeng[34b], T. Nobe[159], D. Noll[18a], T. Nommensen[153], M.B. Norfolk[145], B.J. Norman[35], M. Noury[36a], J. Novak[95], T. Novak[95], R. Novotny[135], L. Nozka[125], K. Ntekas[165], N.M.J. Nunes De Moura Junior[83b], J. Ocariz[130], I. Ochoa[133a], S. Oerdek[48,y], J.T. Offermann[40], A. Ogrodnik[136], A. Oh[103], C.C. Ohm[150], H. Oide[84], M.L. Ojeda[37], Y. Okumura[159], L.F. Oleiro Seabra[133a], I. Oleksiyuk[56], G. Oliveira Correa[13], D. Oliveira Damazio[30], J.L. Oliver[165], R. Omar[68], Ö.O. Öncel[54], A.P. O'Neill[20], A. Onofre[133a,133e,e], P.U.E. Onyisi[11], M.J. Oreglia[40], D. Orestano[77a,77b], R. Orlandini[77a,77b], R.S. Orr[161], L.M. Osojnak[42], Y. Osumi[113], G. Otero y Garzon[31], H. Otono[90], M. Ouchrif[36d], F. Ould-Saada[128], T. Ovsiannikova[142], M. Owen[59], R.E. Owen[137], V.E. Ozcan[22a], F. Ozturk[87], N. Ozturk[8], S. Ozturk[82], H.A. Pacey[129], K. Pachal[162a], A. Pacheco Pages[13], C. Padilla Aranda[13], G. Padovano[75a,75b], S. Pagan Griso[18a], G. Palacino[68], A. Palazzo[70a,70b], J. Pampel[25], J. Pan[178], T. Pan[64a], D.K. Panchal[11], C.E. Pandini[60], J.G. Panduro Vazquez[137], H.D. Pandya[1], H. Pang[138], P. Pani[48], G. Panizzo[69a,69c], L. Panwar[130], L. Paolozzi[56], S. Parajuli[168], A. Paramonov[6], C. Paraskevopoulos[53], D. Paredes Hernandez[64b], A. Pareti[73a,73b], K.R. Park[42], T.H. Park[112], F. Parodi[57b,57a], J.A. Parsons[42], U. Parzefall[54], B. Pascual Dias[41], L. Pascual Dominguez[101], E. Pasqualucci[75a], S. Passaggio[57b], F. Pastore[97], P. Patel[87], U.M. Patel[51], J.R. Pater[103], T. Pauly[37], F. Pauwels[136], C.I. Pazos[164], M. Pedersen[128], R. Pedro[133a], S.V. Peleganchuk[38], O. Penc[134], E.A. Pender[52], S. Peng[15], G.D. Penn[178], K.E. Penski[111], M. Penzin[38], B.S. Peralva[83d], A.P. Pereira Peixoto[142], L. Pereira Sanchez[149], D.V. Perepelitsa[30,al], G. Perera[105], E. Perez Codina[37], M. Perganti[10], H. Pernegger[37], S. Perrella[75a,75b], K. Peters[48], R.F.Y. Peters[103], B.A. Petersen[37], T.C. Petersen[43], E. Petit[104], V. Petousis[135], A.R. Petri[71a,71b], C. Petridou[158,d], T. Petru[136], A. Petrukhin[147], M. Pettee[18a], A. Petukhov[82], K. Petukhova[37], R. Pezoa[140g], L. Pezzotti[24b,24a], G. Pezzullo[178], L. Pfaffenbichler[37], A.J. Pfleger[79], T.M. Pham[176], T. Pham[107], P.W. Phillips[137], G. Piacquadio[151], E. Pianori[18a], F. Piazza[126], R. Piegaia[31], D. Pietreanu[28b], A.D. Pilkington[103], M. Pinamonti[69a,69c], J.L. Pinfold[2], B.C. Pinheiro Pereira[133a], J. Pinol Bel[13], A.E. Pinto Pinoargote[130], L. Pintucci[69a,69c], K.M. Piper[152], A. Pirttikoski[56], D.A. Pizzi[35], L. Pizzimento[64b], A. Plebani[33],

M.-A. Pleier[30], V. Pleskot[136], E. Plotnikova[39], G. Poddar[96], R. Poettgen[100], L. Poggioli[130], S. Polacek[136], G. Polesello[73a], A. Poley[148], A. Polini[24b], C.S. Pollard[173], Z.B. Pollock[122], E. Pompa Pacchi[123], N.I. Pond[98], D. Ponomarenko[68], L. Pontecorvo[37], S. Popa[28a], G.A. Popeneciu[28d], A. Poreba[37], D.M. Portillo Quintero[162a], S. Pospisil[135], M.A. Postill[145], P. Postolache[28c], K. Potamianos[173], P.A. Potepa[86a], I.N. Potrap[39], C.J. Potter[33], H. Potti[153], J. Poveda[169], M.E. Pozo Astigarraga[37], R. Pozzi[37], A. Prades Ibanez[76a,76b], S.R. Pradhan[145], J. Pretel[171], D. Price[103], M. Primavera[70a], L. Primomo[69a,69c], M.A. Principe Martin[101], R. Privara[125], T. Procter[86b], M.L. Proffitt[142], N. Proklova[131], K. Prokofiev[64c], G. Proto[112], J. Proudfoot[6], M. Przybycien[86a], W.W. Przygoda[86b], A. Psallidas[46], J.E. Puddefoot[145], D. Pudzha[53], H.I. Purnell[1], D. Pyatiizbyantseva[116], J. Qian[108], R. Qian[109], D. Qichen[129], Y. Qin[13], T. Qiu[52], A. Quadt[55], M. Queitsch-Maitland[103], G. Quetant[56], R.P. Quinn[170], G. Rabanal Bolanos[61], D. Rafanoharana[112], F. Raffaeli[76a,76b], F. Ragusa[71a,71b], J.L. Rainbolt[40], S. Rajagopalan[30], E. Ramakoti[39], L. Rambelli[57b,57a], I.A. Ramirez-Berend[35], K. Ran[48,114c], D.S. Rankin[131], N.P. Rapheeha[34h], H. Rasheed[28b], D.F. Rassloff[63a], A. Rastogi[18a], S. Rave[102], S. Ravera[57b,57a], B. Ravina[37], I. Ravinovich[175], M. Raymond[37], A.L. Read[128], N.P. Readioff[145], D.M. Rebuzzi[73a,73b], A.S. Reed[59], K. Reeves[27], J.A. Reidelsturz[177], D. Reikher[37], M.Reinartz[180], A. Rej[49], C. Rembser[37], H. Ren[62], M. Renda[28b], F. Renner[48], A.G. Rennie[59], A.L. Rescia[57b,57a], S. Resconi[71a], M. Ressegotti[57b,57a], S. Rettie[117], W.F. Rettie[35], M.M. Revering[33], E. Reynolds[18a], O.L. Rezanova[39], P. Reznicek[136], H. Riani[36d], N. Ribaric[51], B. Ricci[69a,69c], E. Ricci[78a,78b], R. Richter[112], S. Richter[47a,47b], E. Richter-Was[86b], M. Ridel[130], S. Ridouani[36d], P. Rieck[120], P. Riedler[37], E.M. Riefel[47a,47b], J.O. Rieger[117], M. Rijssenbeek[151], M. Rimoldi[37], L. Rinaldi[24b,24a], P. Rincke[167,55], G. Ripellino[167], I. Riu[13], J.C. Rivera Vergara[171], F. Rizatdinova[124], E. Rizvi[96], B.R. Roberts[18a], S.S. Roberts[139], D. Robinson[33], M. Robles Manzano[102], A. Robson[59], A. Rocchi[76a,76b], C. Roda[74a,74b], S. Rodriguez Bosca[37], Y. Rodriguez Garcia[23a], A.M. Rodríguez Vera[118], S. Roe[37], J.T. Roemer[37], O. Røhne[128], R.A. Rojas[37], C.P.A. Roland[130], A. Romaniouk[79], E. Romano[73a,73b], M. Romano[24b], A.C. Romero Hernandez[168], N. Rompotis[94], L. Roos[130], S. Rosati[75a], B.J. Rosser[40], E. Rossi[129], E. Rossi[72a,72b], L.P. Rossi[61], L. Rossini[54], R. Rosten[122], M. Rotaru[28b], B. Rottler[54], D. Rousseau[66], D. Rousso[48], S. Roy-Garand[161], A. Rozanov[104], Z.M.A. Rozario[59], Y. Rozen[156], A. Rubio Jimenez[169], V.H. Ruelas Rivera[19], T.A. Ruggeri[1], A. Ruggiero[129], A. Ruiz-Martinez[169], A. Rummler[37], Z. Rurikova[54], N.A. Rusakovich[39], S. Ruscelli[49], H.L. Russell[171], G. Russo[75a,75b], J.P. Rutherfoord[7], S. Rutherford Colmenares[33], M. Rybar[136], P. Rybczynski[86a], A. Ryzhov[45], J.A. Sabater Iglesias[56], H.F-W. Sadrozinski[139], F. Safai Tehrani[75a], S. Saha[1], M. Sahinsoy[82], B. Sahoo[175], A. Saibel[169], B.T. Saifuddin[123], M. Saimpert[138], G.T. Saito[83c], M. Saito[159], T. Saito[159], A. Sala[71a,71b], A. Salnikov[149], J. Salt[169], A. Salvador Salas[157], F. Salvatore[152], A. Salzburger[37], D. Sammel[54], E. Sampson[93], D. Sampsonidis[158,d], D. Sampsonidou[126], J. Sánchez[169], V. Sanchez Sebastian[169], H. Sandaker[128], C.O. Sander[48], J.A. Sandesara[176], M. Sandhoff[177], C. Sandoval[23b], L. Sanfilippo[63a], D.P.C. Sankey[137], T. Sano[89], A. Sansoni[53], M. Santana Queiroz[18b], L. Santi[37], C. Santoni[41], H. Santos[133a,133b], A. Santra[175], E. Sanzani[24b,24a], K.A. Saoucha[88b], J.G. Saraiva[133a,133d], J. Sardain[7], O. Sasaki[84], K. Sato[163], C. Sauer[37], E. Sauvan[4], P. Savard[161,ai], R. Sawada[159], C. Sawyer[137], L. Sawyer[99], C. Sbarra[24b], A. Sbrizzi[24b,24a], T. Scanlon[98], J. Schaarschmidt[142], U. Schäfer[102], A.C. Schaffer[66,45], D. Schaile[111], R.D. Schamberger[151], C. Scharf[19], M.M. Schefer[20], V.A. Schegelsky[38], D. Scheirich[136], M. Schernau[140f], C. Scheulen[56], C. Schiavi[57b,57a], M. Schioppa[44b,44a], B. Schlag[149], S. Schlenker[37], J. Schmeing[177],

E. Schmidt[112], M.A. Schmidt[177], K. Schmieden[102], C. Schmitt[102], N. Schmitt[102], S. Schmitt[48], N.A. Schneider[111], L. Schoeffel[138], A. Schoening[63b], P.G. Scholer[35], E. Schopf[147], M. Schott[25], S. Schramm[56], T. Schroer[56], H-C. Schultz-Coulon[63a], M. Schumacher[54], B.A. Schumm[139], Ph. Schune[138], H.R. Schwartz[7], A. Schwartzman[149], T.A. Schwarz[108], Ph. Schwemling[138], R. Schwienhorst[109], F.G. Sciacca[20], A. Sciandra[30], G. Sciolla[27], F. Scuri[74a], C.D. Sebastiani[37], K. Sedlaczek[118], S.C. Seidel[115], A. Seiden[139], B.D. Seidlitz[42], C. Seitz[48], J.M. Seixas[83b], G. Sekhniaidze[72a], L. Selem[60], N. Semprini-Cesari[24b,24a], A. Semushin[179], D. Sengupta[56], V. Senthilkumar[169], L. Serin[66], M. Sessa[72a,72b], H. Severini[123], F. Sforza[57b,57a], A. Sfyrla[56], Q. Sha[14], E. Shabalina[55], H. Shaddix[118], A.H. Shah[33], R. Shaheen[150], J.D. Shahinian[131], M. Shamim[37], L.Y. Shan[14], M. Shapiro[18a], A. Sharma[37], A.S. Sharma[170], P. Sharma[30], P.B. Shatalov[38], K. Shaw[152], S.M. Shaw[103], Q. Shen[144a], D.J. Sheppard[148], P. Sherwood[98], L. Shi[98], X. Shi[14], S. Shimizu[84], C.O. Shimmin[178], I.P.J. Shipsey[129,*], S. Shirabe[90], M. Shiyakova[39,z], M.J. Shochet[40], D.R. Shope[128], B. Shrestha[123], S. Shrestha[122,an], I. Shreyber[39], M.J. Shroff[171], P. Sicho[134], A.M. Sickles[168], E. Sideras Haddad[34h,166], A.C. Sidley[117], A. Sidoti[24b], F. Siegert[50], Dj. Sijacki[16], F. Sili[92], J.M. Silva[52], I. Silva Ferreira[83b], M.V. Silva Oliveira[30], S.B. Silverstein[47a], S. Simion[66], R. Simoniello[37], E.L. Simpson[103], H. Simpson[152], L.R. Simpson[6], S. Simsek[82], S. Sindhu[55], P. Sinervo[161], S.N. Singh[27], S. Singh[30], S. Sinha[48], S. Sinha[103], M. Sioli[24b,24a], K. Sioulas[9], I. Siral[37], E. Sitnikova[48], J. Sjölin[47a,47b], A. Skaf[55], E. Skorda[21], P. Skubic[123], M. Slawinska[87], I. Slazyk[17], I. Sliusar[128], V. Smakhtin[175], B.H. Smart[137], S.Yu. Smirnov[140b], Y. Smirnov[82], L.N. Smirnova[38,a], O. Smirnova[100], A.C. Smith[42], D.R. Smith[165], J.L. Smith[103], M.B. Smith[35], R. Smith[149], H. Smitmanns[102], M. Smizanska[93], K. Smolek[135], P. Smolyanskiy[135], A.A. Snesarev[39], H.L. Snoek[117], S. Snyder[30], R. Sobie[171,ab], A. Soffer[157], C.A. Solans Sanchez[37], E.Yu. Soldatov[39], U. Soldevila[169], A.A. Solodkov[34h], S. Solomon[27], A. Soloshenko[39], K. Solovieva[54], O.V. Solovyanov[41], P. Sommer[50], A. Sonay[13], A. Sopczak[135], A.L. Sopio[52], F. Sopkova[29b], J.D. Sorenson[115], I.R. Sotarriva Alvarez[141], V. Sothilingam[63a], O.J. Soto Sandoval[140c,140b], S. Sottocornola[68], R. Soualah[88a], Z. Soumaimi[36e], D. South[48], N. Soybelman[175], S. Spagnolo[70a,70b], M. Spalla[112], D. Sperlich[54], B. Spisso[72a,72b], D.P. Spiteri[59], L. Splendori[104], M. Spousta[136], E.J. Staats[35], R. Stamen[63a], E. Stanecka[87], W. Stanek-Maslouska[48], M.V. Stange[50], B. Stanislaus[18a], M.M. Stanitzki[48], B. Stapf[48], E.A. Starchenko[38], G.H. Stark[139], J. Stark[91], P. Staroba[134], P. Starovoitov[88b], R. Staszewski[87], C. Stauch[111], G. Stavropoulos[46], A. Stefl[37], A. Stein[102], P. Steinberg[30], B. Stelzer[148,162a], H.J. Stelzer[132], O. Stelzer-Chilton[162a], H. Stenzel[58], T.J. Stevenson[152], G.A. Stewart[37], J.R. Stewart[124], G. Stoicea[28b], M. Stolarski[133a], S. Stonjek[112], A. Straessner[50], J. Strandberg[150], S. Strandberg[47a,47b], M. Stratmann[177], M. Strauss[123], T. Strebler[104], P. Strizenec[29b], R. Ströhmer[172], D.M. Strom[126], R. Stroynowski[45], A. Strubig[47a,47b], S.A. Stucci[30], B. Stugu[17], J. Stupak[123], N.A. Styles[48], D. Su[149], S. Su[62], X. Su[62], D. Suchy[29a], A.D. Sudhakar Ponnu[55], K. Sugizaki[131], V.V. Sulin[38], D.M.S. Sultan[129], L. Sultanaliyeva[25], S. Sultansoy[3b], S. Sun[176], W. Sun[14], O. Sunneborn Gudnadottir[167], N. Sur[100], M.R. Sutton[152], M. Svatos[134], P.N. Swallow[33], M. Swiatlowski[162a], T. Swirski[172], A. Swoboda[37], I. Sykora[29a], M. Sykora[136], T. Sykora[136], D. Ta[102], K. Tackmann[48,y], A. Taffard[165], R. Tafirout[162a], Y. Takubo[84], M. Talby[104], A.A. Talyshev[38], K.C. Tam[64b], N.M. Tamir[157], A. Tanaka[159], J. Tanaka[159], R. Tanaka[66], M. Tanasini[151], Z. Tao[170], S. Tapia Araya[140g], S. Tapprogge[102], A. Tarek Abouelfadl Mohamed[37], S. Tarem[156], K. Tariq[14], G. Tarna[37], G.F. Tartarelli[71a], M.J. Tartarin[91], P. Tas[136], M. Tasevsky[134], E. Tassi[44b,44a], A.C. Tate[168], Y. Tayalati[36e,aa],

G.N. Taylor[107], W. Taylor[162b], R.J. Taylor Vara[169], A.S. Tegetmeier[91], P. Teixeira-Dias[97], J.J. Teoh[161], K. Terashi[159], J. Terron[101], S. Terzo[13], M. Testa[53], R.J. Teuscher[161,ab], A. Thaler[79], O. Theiner[56], T. Theveneaux-Pelzer[104], D.W. Thomas[97], J.P. Thomas[21], E.A. Thompson[18a], P.D. Thompson[21], E. Thomson[131], R.E. Thornberry[45], C. Tian[62], Y. Tian[56], V. Tikhomirov[82], Yu.A. Tikhonov[39], S. Timoshenko[38], D. Timoshyn[136], E.X.L. Ting[1], P. Tipton[178], A. Tishelman-Charny[30], K. Todome[141], S. Todorova-Nova[136], L. Toffolin[69a,69c], M. Togawa[84], J. Tojo[90], S. Tokár[29a], O. Toldaiev[68], G. Tolkachev[104], M. Tomoto[84], L. Tompkins[149,n], E. Torrence[126], H. Torres[91], E. Torró Pastor[169], M. Toscani[31], C. Tosciri[40], M. Tost[11], D.R. Tovey[145], T. Trefzger[172], P.M. Tricarico[13], A. Tricoli[30], I.M. Trigger[162a], S. Trincaz-Duvoid[130], D.A. Trischuk[27], A. Tropina[39], L. Truong[34c], M. Trzebinski[87], A. Trzupek[87], F. Tsai[151], M. Tsai[108], A. Tsiamis[158], P.V. Tsiareshka[39], S. Tsigaridas[162a], A. Tsirigotis[158,u], V. Tsiskaridze[155a], E.G. Tskhadadze[155a], Y. Tsujikawa[89], I.I. Tsukerman[38], V. Tsulaia[18a], S. Tsuno[84], K. Tsuri[121], D. Tsybychev[151], Y. Tu[64b], A. Tudorache[28b], V. Tudorache[28b], S.B. Tuncay[129], S. Turchikhin[57b,57a], I. Turk Cakir[3a], R. Turra[71a], T. Turtuvshin[39,ac], P.M. Tuts[42], S. Tzamarias[158,d], Y. Uematsu[84], F. Ukegawa[163], P.A. Ulloa Poblete[140c,140b], E.N. Umaka[30], G. Unal[37], A. Undrus[30], G. Unel[165], J. Urban[29b], P. Urrejola[140e], G. Usai[8], R. Ushioda[160], M. Usman[110], F. Ustuner[52], Z. Uysal[82], V. Vacek[135], B. Vachon[106], T. Vafeiadis[37], A. Vaitkus[98], C. Valderanis[111], E. Valdes Santurio[47a,47b], M. Valente[37], S. Valentinetti[24b,24a], A. Valero[169], E. Valiente Moreno[169], A. Vallier[91], J.A. Valls Ferrer[169], D.R. Van Arneman[117], A. Van Der Graaf[49], H.Z. Van Der Schyf[34h], P. Van Gemmeren[6], M. Van Rijnbach[37], S. Van Stroud[98], I. Van Vulpen[117], P. Vana[136], M. Vanadia[76a,76b], U.M. Vande Voorde[150], W. Vandelli[37], E.R. Vandewall[124], D. Vannicola[157], L. Vannoli[53], R. Vari[75a], M. Varma[178], E.W. Varnes[7], C. Varni[118], D. Varouchas[66], L. Varriale[169], K.E. Varvell[153], M.E. Vasile[28b], L. Vaslin[84], M.D. Vassilev[149], A. Vasyukov[39], L.M. Vaughan[124], R. Vavricka[136], T. Vazquez Schroeder[13], J. Veatch[32], V. Vecchio[103], M.J. Veen[105], I. Veliscek[30], I. Velkovska[95], L.M. Veloce[161], F. Veloso[133a,133c], S. Veneziano[75a], A. Ventura[70a,70b], A. Verbytskyi[112], M. Verducci[74a,74b], C. Vergis[96], M. Verissimo De Araujo[83b], W. Verkerke[117], J.C. Vermeulen[117], C. Vernieri[149], M. Vessella[165], M.C. Vetterli[148,ai], A. Vgenopoulos[102], N. Viaux Maira[140g,af], T. Vickey[145], O.E. Vickey Boeriu[145], G.H.A. Viehhauser[129], L. Vigani[63b], M. Vigl[112], M. Villa[24b,24a], M. Villaplana Perez[169], E.M. Villhauer[40], E. Vilucchi[53], M. Vincent[169], M.G. Vincter[35], A. Visibile[117], A. Visive[117], C. Vittori[37], I. Vivarelli[24b,24a], M.I. Vivas Albornoz[48], E. Voevodina[112], F. Vogel[111], J.C. Voigt[50], P. Vokac[135], Yu. Volkotrub[86b], L. Vomberg[25], E. Von Toerne[25], B. Vormwald[37], K. Vorobev[51], M. Vos[169], K. Voss[147], M. Vozak[37], L. Vozdecky[123], N. Vranjes[16], M. Vranjes Milosavljevic[16], M. Vreeswijk[117], N.K. Vu[144b,144a], R. Vuillermet[37], O. Vujinovic[102], I. Vukotic[40], I.K. Vyas[35], J.F. Wack[33], S. Wada[163], C. Wagner[149], J.M. Wagner[18a], W. Wagner[177], S. Wahdan[177], H. Wahlberg[92], C.H. Waits[123], J. Walder[137], R. Walker[111], K. Walkingshaw Pass[59], W. Walkowiak[147], A. Wall[131], E.J. Wallin[100], T. Wamorkar[18a], K. Wandall-Christensen[169], A. Wang[62], A.Z. Wang[139], C. Wang[102], C. Wang[11], H. Wang[18a], J. Wang[64c], P. Wang[103], P. Wang[98], R. Wang[61], R. Wang[6], S.M. Wang[154], S. Wang[14], T. Wang[116], T. Wang[62], W.T. Wang[129], W. Wang[14], X. Wang[168], X. Wang[144a], X. Wang[48], Y. Wang[114a], Y. Wang[62], Z. Wang[108], Z. Wang[144b], Z. Wang[108], C. Wanotayaroj[84], A. Warburton[106], A.L. Warnerbring[147], S. Waterhouse[97], A.T. Watson[21], H. Watson[52], M.F. Watson[21], E. Watton[59], G. Watts[142], B.M. Waugh[98], J.M. Webb[54], C. Weber[30], H.A. Weber[19], M.S. Weber[20], S.M. Weber[63a], C. Wei[62], Y. Wei[54], A.R. Weidberg[129], E.J. Weik[120], J. Weingarten[49], C. Weiser[54],

C.J. Wells[48], T. Wenaus[30], T. Wengler[37], N.S. Wenke[112], N. Wermes[25], M. Wessels[63a], A.M. Wharton[93], A.S. White[61], A. White[8], M.J. White[1], D. Whiteson[165], L. Wickremasinghe[127], W. Wiedenmann[176], M. Wielers[137], R. Wierda[150], C. Wiglesworth[43], H.G. Wilkens[37], J.J.H. Wilkinson[33], D.M. Williams[42], H.H. Williams[131], S. Williams[33], S. Willocq[105], B.J. Wilson[103], D.J. Wilson[103], P.J. Windischhofer[40], F.I. Winkel[31], F. Winklmeier[126], B.T. Winter[54], M. Wittgen[149], M. Wobisch[99], T. Wojtkowski[60], Z. Wolffs[117], J. Wollrath[37], M.W. Wolter[87], H. Wolters[133a,133c], M.C. Wong[139], E.L. Woodward[42], M. Worek[180], S.D. Worm[48], B.K. Wosiek[87], K.W. Woźniak[87], S. Wozniewski[55], K. Wraight[59], C. Wu[161], C. Wu[21], J. Wu[159], M. Wu[114b], M. Wu[116], S.L. Wu[176], S. Wu[14,ak], X. Wu[62], Y.Q. Wu[161], Y. Wu[62], Z. Wu[4], Z. Wu[114a], J. Wuerzinger[112], T.R. Wyatt[103], B.M. Wynne[52], S. Xella[43], L. Xia[114a], M. Xia[15], M. Xie[62], A. Xiong[126], J. Xiong[18a], D. Xu[14], H. Xu[62], L. Xu[62], R. Xu[131], T. Xu[108], Y. Xu[142], Z. Xu[52], R. Xue[132], B. Yabsley[153], S. Yacoob[34a], Y. Yamaguchi[84], E. Yamashita[159], H. Yamauchi[163], T. Yamazaki[18a], Y. Yamazaki[85], S. Yan[59], Z. Yan[105], H.J. Yang[144a,144b], H.T. Yang[62], S. Yang[62], T. Yang[64c], X. Yang[37], X. Yang[14], Y. Yang[159], Y. Yang[62], W-M. Yao[18a], C.L. Yardley[152], J. Ye[14], S. Ye[30], X. Ye[62], Y. Yeh[98], I. Yeletskikh[39], B. Yeo[18b], M.R. Yexley[98], T.P. Yildirim[129], K. Yorita[174], C.J.S. Young[37], C. Young[149], N.D. Young[126], Y. Yu[62], J. Yuan[14,114c], M. Yuan[108], R. Yuan[144b,144a], L. Yue[98], M. Zaazoua[62], B. Zabinski[87], I. Zahir[36a], A. Zaio[57b,57a], Z.K. Zak[87], T. Zakareishvili[169], S. Zambito[56], J.A. Zamora Saa[140d], J. Zang[159], R. Zanzottera[71a,71b], O. Zaplatilek[135], C. Zeitnitz[177], H. Zeng[14], J.C. Zeng[168], D.T. Zenger Jr[27], O. Zenin[38], T. Ženiš[29a], S. Zenz[96], D. Zerwas[66], M. Zhai[14,114c], D.F. Zhang[145], G. Zhang[14,ak], J. Zhang[143a], J. Zhang[6], K. Zhang[14,114c], L. Zhang[62], L. Zhang[114a], P. Zhang[14,114c], R. Zhang[114a], S. Zhang[91], T. Zhang[159], Y. Zhang[142], Y. Zhang[98], Y. Zhang[62], Y. Zhang[114a], Z. Zhang[18a], Z. Zhang[143a], Z. Zhang[66], H. Zhao[142], T. Zhao[143a], Y. Zhao[35], Z. Zhao[62], Z. Zhao[62], A. Zhemchugov[39], J. Zheng[114a], K. Zheng[168], X. Zheng[62], Z. Zheng[149], D. Zhong[168], B. Zhou[108], H. Zhou[7], N. Zhou[144a], Y. Zhou[15], Y. Zhou[114a], Y. Zhou[7], C.G. Zhu[143a], J. Zhu[108], X. Zhu[144b], Y. Zhu[144a], Y. Zhu[62], X. Zhuang[14], K. Zhukov[68], N.I. Zimine[39], J. Zinsser[63b], M. Ziolkowski[147], L. Živković[16], A. Zoccoli[24b,24a], K. Zoch[61], A. Zografos[37], T.G. Zorbas[145], O. Zormpa[46], L. Zwalinski[37].

[1]Department of Physics, University of Adelaide, Adelaide; Australia.
[2]Department of Physics, University of Alberta, Edmonton AB; Canada.
[3(a)]Department of Physics, Ankara University, Ankara;[(b)]Division of Physics, TOBB University of Economics and Technology, Ankara; Türkiye.
[4]LAPP, Université Savoie Mont Blanc, CNRS/IN2P3, Annecy; France.
[5]APC, Université Paris Cité, CNRS/IN2P3, Paris; France.
[6]High Energy Physics Division, Argonne National Laboratory, Argonne IL; United States of America.
[7]Department of Physics, University of Arizona, Tucson AZ; United States of America.
[8]Department of Physics, University of Texas at Arlington, Arlington TX; United States of America.
[9]Physics Department, National and Kapodistrian University of Athens, Athens; Greece.
[10]Physics Department, National Technical University of Athens, Zografou; Greece.
[11]Department of Physics, University of Texas at Austin, Austin TX; United States of America.
[12]Institute of Physics, Azerbaijan Academy of Sciences, Baku; Azerbaijan.
[13]Institut de Física d'Altes Energies (IFAE), Barcelona Institute of Science and Technology, Barcelona; Spain.
[14]Institute of High Energy Physics, Chinese Academy of Sciences, Beijing; China.

[15]Physics Department, Tsinghua University, Beijing; China.
[16]Institute of Physics, University of Belgrade, Belgrade; Serbia.
[17]Department for Physics and Technology, University of Bergen, Bergen; Norway.
[18(a)]Physics Division, Lawrence Berkeley National Laboratory, Berkeley CA;[(b)]University of California, Berkeley CA; United States of America.
[19]Institut für Physik, Humboldt Universität zu Berlin, Berlin; Germany.
[20]Albert Einstein Center for Fundamental Physics and Laboratory for High Energy Physics, University of Bern, Bern; Switzerland.
[21]School of Physics and Astronomy, University of Birmingham, Birmingham; United Kingdom.
[22(a)]Department of Physics, Bogazici University, Istanbul;[(b)]Department of Physics Engineering, Gaziantep University, Gaziantep;[(c)]Department of Physics, Istanbul University, Istanbul; Türkiye.
[23(a)]Facultad de Ciencias y Centro de Investigaciónes, Universidad Antonio Nariño, Bogotá;[(b)]Departamento de Física, Universidad Nacional de Colombia, Bogotá; Colombia.
[24(a)]Dipartimento di Fisica e Astronomia A. Righi, Università di Bologna, Bologna;[(b)]INFN Sezione di Bologna; Italy.
[25]Physikalisches Institut, Universität Bonn, Bonn; Germany.
[26]Department of Physics, Boston University, Boston MA; United States of America.
[27]Department of Physics, Brandeis University, Waltham MA; United States of America.
[28(a)]Transilvania University of Brasov, Brasov;[(b)]Horia Hulubei National Institute of Physics and Nuclear Engineering, Bucharest;[(c)]Department of Physics, Alexandru Ioan Cuza University of Iasi, Iasi;[(d)]National Institute for Research and Development of Isotopic and Molecular Technologies, Physics Department, Cluj-Napoca;[(e)]National University of Science and Technology Politechnica, Bucharest;[(f)]West University in Timisoara, Timisoara;[(g)]Faculty of Physics, University of Bucharest, Bucharest; Romania.
[29(a)]Faculty of Mathematics, Physics and Informatics, Comenius University, Bratislava;[(b)]Department of Subnuclear Physics, Institute of Experimental Physics of the Slovak Academy of Sciences, Kosice; Slovak Republic.
[30]Physics Department, Brookhaven National Laboratory, Upton NY; United States of America.
[31]Universidad de Buenos Aires, Facultad de Ciencias Exactas y Naturales, Departamento de Física, y CONICET, Instituto de Física de Buenos Aires (IFIBA), Buenos Aires; Argentina.
[32]California State University, CA; United States of America.
[33]Cavendish Laboratory, University of Cambridge, Cambridge; United Kingdom.
[34(a)]Department of Physics, University of Cape Town, Cape Town;[(b)]iThemba Labs, Western Cape;[(c)]Department of Mechanical Engineering Science, University of Johannesburg, Johannesburg;[(d)]National Institute of Physics, University of the Philippines Diliman (Philippines);[(e)]Department of Physics, Stellenbosch University, Matieland;[(f)]University of South Africa, Department of Physics, Pretoria;[(g)]University of Zululand, KwaDlangezwa;[(h)]School of Physics, University of the Witwatersrand, Johannesburg; South Africa.
[35]Department of Physics, Carleton University, Ottawa ON; Canada.
[36(a)]Faculté des Sciences Ain Chock, Université Hassan II de Casablanca;[(b)]Faculté des Sciences, Université Ibn-Tofail, Kénitra;[(c)]Faculté des Sciences Semlalia, Université Cadi Ayyad, LPHEA-Marrakech;[(d)]LPMR, Faculté des Sciences, Université Mohamed Premier, Oujda;[(e)]Faculté des sciences, Université Mohammed V, Rabat;[(f)]Institute of Applied Physics, Mohammed VI Polytechnic University, Ben Guerir; Morocco.
[37]CERN, Geneva; Switzerland.
[38]Affiliated with an institute formerly covered by a cooperation agreement with CERN.
[39]Affiliated with an international laboratory covered by a cooperation agreement with CERN.
[40]Enrico Fermi Institute, University of Chicago, Chicago IL; United States of America.

[41]LPC, Université Clermont Auvergne, CNRS/IN2P3, Clermont-Ferrand; France.
[42]Nevis Laboratory, Columbia University, Irvington NY; United States of America.
[43]Niels Bohr Institute, University of Copenhagen, Copenhagen; Denmark.
[44(a)]Dipartimento di Fisica, Università della Calabria, Rende;[(b)]INFN Gruppo Collegato di Cosenza, Laboratori Nazionali di Frascati; Italy.
[45]Physics Department, Southern Methodist University, Dallas TX; United States of America.
[46]National Centre for Scientific Research "Demokritos", Agia Paraskevi; Greece.
[47(a)]Department of Physics, Stockholm University;[(b)]Oskar Klein Centre, Stockholm; Sweden.
[48]Deutsches Elektronen-Synchrotron DESY, Hamburg and Zeuthen; Germany.
[49]Fakultät Physik , Technische Universität Dortmund, Dortmund; Germany.
[50]Institut für Kern- und Teilchenphysik, Technische Universität Dresden, Dresden; Germany.
[51]Department of Physics, Duke University, Durham NC; United States of America.
[52]SUPA - School of Physics and Astronomy, University of Edinburgh, Edinburgh; United Kingdom.
[53]INFN e Laboratori Nazionali di Frascati, Frascati; Italy.
[54]Physikalisches Institut, Albert-Ludwigs-Universität Freiburg, Freiburg; Germany.
[55]II. Physikalisches Institut, Georg-August-Universität Göttingen, Göttingen; Germany.
[56]Département de Physique Nucléaire et Corpusculaire, Université de Genève, Genève; Switzerland.
[57(a)]Dipartimento di Fisica, Università di Genova, Genova;[(b)]INFN Sezione di Genova; Italy.
[58]II. Physikalisches Institut, Justus-Liebig-Universität Giessen, Giessen; Germany.
[59]SUPA - School of Physics and Astronomy, University of Glasgow, Glasgow; United Kingdom.
[60]LPSC, Université Grenoble Alpes, CNRS/IN2P3, Grenoble INP, Grenoble; France.
[61]Laboratory for Particle Physics and Cosmology, Harvard University, Cambridge MA; United States of America.
[62]Department of Modern Physics and State Key Laboratory of Particle Detection and Electronics, University of Science and Technology of China, Hefei; China.
[63(a)]Kirchhoff-Institut für Physik, Ruprecht-Karls-Universität Heidelberg, Heidelberg;[(b)]Physikalisches Institut, Ruprecht-Karls-Universität Heidelberg, Heidelberg; Germany.
[64(a)]Department of Physics, Chinese University of Hong Kong, Shatin, N.T., Hong Kong;[(b)]Department of Physics, University of Hong Kong, Hong Kong;[(c)]Department of Physics and Institute for Advanced Study, Hong Kong University of Science and Technology, Clear Water Bay, Kowloon, Hong Kong; China.
[65]Department of Physics, National Tsing Hua University, Hsinchu; Taiwan.
[66]IJCLab, Université Paris-Saclay, CNRS/IN2P3, 91405, Orsay; France.
[67]Centro Nacional de Microelectrónica (IMB-CNM-CSIC), Barcelona; Spain.
[68]Department of Physics, Indiana University, Bloomington IN; United States of America.
[69(a)]INFN Gruppo Collegato di Udine, Sezione di Trieste, Udine;[(b)]ICTP, Trieste;[(c)]Dipartimento Politecnico di Ingegneria e Architettura, Università di Udine, Udine; Italy.
[70(a)]INFN Sezione di Lecce;[(b)]Dipartimento di Matematica e Fisica, Università del Salento, Lecce; Italy.
[71(a)]INFN Sezione di Milano;[(b)]Dipartimento di Fisica, Università di Milano, Milano; Italy.
[72(a)]INFN Sezione di Napoli;[(b)]Dipartimento di Fisica, Università di Napoli, Napoli; Italy.
[73(a)]INFN Sezione di Pavia;[(b)]Dipartimento di Fisica, Università di Pavia, Pavia; Italy.
[74(a)]INFN Sezione di Pisa;[(b)]Dipartimento di Fisica E. Fermi, Università di Pisa, Pisa; Italy.
[75(a)]INFN Sezione di Roma;[(b)]Dipartimento di Fisica, Sapienza Università di Roma, Roma; Italy.
[76(a)]INFN Sezione di Roma Tor Vergata;[(b)]Dipartimento di Fisica, Università di Roma Tor Vergata, Roma; Italy.
[77(a)]INFN Sezione di Roma Tre;[(b)]Dipartimento di Matematica e Fisica, Università Roma Tre, Roma; Italy.
[78(a)]INFN-TIFPA;[(b)]Università degli Studi di Trento, Trento; Italy.

[79]Universität Innsbruck, Department of Astro and Particle Physics, Innsbruck; Austria.
[80]University of Iowa, Iowa City IA; United States of America.
[81]Department of Physics and Astronomy, Iowa State University, Ames IA; United States of America.
[82]Istinye University, Sariyer, Istanbul; Türkiye.
[83(a)]Departamento de Engenharia Elétrica, Universidade Federal de Juiz de Fora (UFJF), Juiz de Fora;[(b)]Universidade Federal do Rio De Janeiro COPPE/EE/IF, Rio de Janeiro;[(c)]Instituto de Física, Universidade de São Paulo, São Paulo;[(d)]Rio de Janeiro State University, Rio de Janeiro;[(e)]Federal University of Bahia, Bahia; Brazil.
[84]KEK, High Energy Accelerator Research Organization, Tsukuba; Japan.
[85]Graduate School of Science, Kobe University, Kobe; Japan.
[86(a)]AGH University of Krakow, Faculty of Physics and Applied Computer Science, Krakow;[(b)]Marian Smoluchowski Institute of Physics, Jagiellonian University, Krakow; Poland.
[87]Institute of Nuclear Physics Polish Academy of Sciences, Krakow; Poland.
[88(a)]Khalifa University of Science and Technology, Abu Dhabi;[(b)]University of Sharjah, Sharjah; United Arab Emirates.
[89]Faculty of Science, Kyoto University, Kyoto; Japan.
[90]Research Center for Advanced Particle Physics and Department of Physics, Kyushu University, Fukuoka ; Japan.
[91]L2IT, Université de Toulouse, CNRS/IN2P3, UPS, Toulouse; France.
[92]Instituto de Física La Plata, Universidad Nacional de La Plata and CONICET, La Plata; Argentina.
[93]Physics Department, Lancaster University, Lancaster; United Kingdom.
[94]Oliver Lodge Laboratory, University of Liverpool, Liverpool; United Kingdom.
[95]Department of Experimental Particle Physics, Jožef Stefan Institute and Department of Physics, University of Ljubljana, Ljubljana; Slovenia.
[96]Department of Physics and Astronomy, Queen Mary University of London, London; United Kingdom.
[97]Department of Physics, Royal Holloway University of London, Egham; United Kingdom.
[98]Department of Physics and Astronomy, University College London, London; United Kingdom.
[99]Louisiana Tech University, Ruston LA; United States of America.
[100]Fysiska institutionen, Lunds universitet, Lund; Sweden.
[101]Departamento de Física Teorica C-15 and CIAFF, Universidad Autónoma de Madrid, Madrid; Spain.
[102]Institut für Physik, Universität Mainz, Mainz; Germany.
[103]School of Physics and Astronomy, University of Manchester, Manchester; United Kingdom.
[104]CPPM, Aix-Marseille Université, CNRS/IN2P3, Marseille; France.
[105]Department of Physics, University of Massachusetts, Amherst MA; United States of America.
[106]Department of Physics, McGill University, Montreal QC; Canada.
[107]School of Physics, University of Melbourne, Victoria; Australia.
[108]Department of Physics, University of Michigan, Ann Arbor MI; United States of America.
[109]Department of Physics and Astronomy, Michigan State University, East Lansing MI; United States of America.
[110]Group of Particle Physics, University of Montreal, Montreal QC; Canada.
[111]Fakultät für Physik, Ludwig-Maximilians-Universität München, München; Germany.
[112]Max-Planck-Institut für Physik (Werner-Heisenberg-Institut), München; Germany.
[113]Graduate School of Science and Kobayashi-Maskawa Institute, Nagoya University, Nagoya; Japan.
[114(a)]Department of Physics, Nanjing University, Nanjing;[(b)]School of Science, Shenzhen Campus of Sun Yat-sen University;[(c)]University of Chinese Academy of Science (UCAS), Beijing; China.
[115]Department of Physics and Astronomy, University of New Mexico, Albuquerque NM; United States of America.

[116]Institute for Mathematics, Astrophysics and Particle Physics, Radboud University/Nikhef, Nijmegen; Netherlands.
[117]Nikhef National Institute for Subatomic Physics and University of Amsterdam, Amsterdam; Netherlands.
[118]Department of Physics, Northern Illinois University, DeKalb IL; United States of America.
[119(a)]New York University Abu Dhabi, Abu Dhabi;[(b)]United Arab Emirates University, Al Ain; United Arab Emirates.
[120]Department of Physics, New York University, New York NY; United States of America.
[121]Ochanomizu University, Otsuka, Bunkyo-ku, Tokyo; Japan.
[122]Ohio State University, Columbus OH; United States of America.
[123]Homer L. Dodge Department of Physics and Astronomy, University of Oklahoma, Norman OK; United States of America.
[124]Department of Physics, Oklahoma State University, Stillwater OK; United States of America.
[125]Palacký University, Joint Laboratory of Optics, Olomouc; Czech Republic.
[126]Institute for Fundamental Science, University of Oregon, Eugene, OR; United States of America.
[127]Graduate School of Science, University of Osaka, Osaka; Japan.
[128]Department of Physics, University of Oslo, Oslo; Norway.
[129]Department of Physics, Oxford University, Oxford; United Kingdom.
[130]LPNHE, Sorbonne Université, Université Paris Cité, CNRS/IN2P3, Paris; France.
[131]Department of Physics, University of Pennsylvania, Philadelphia PA; United States of America.
[132]Department of Physics and Astronomy, University of Pittsburgh, Pittsburgh PA; United States of America.
[133(a)]Laboratório de Instrumentação e Física Experimental de Partículas - LIP, Lisboa;[(b)]Departamento de Física, Faculdade de Ciências, Universidade de Lisboa, Lisboa;[(c)]Departamento de Física, Universidade de Coimbra, Coimbra;[(d)]Centro de Física Nuclear da Universidade de Lisboa, Lisboa;[(e)]Departamento de Física, Escola de Ciências, Universidade do Minho, Braga;[(f)]Departamento de Física Teórica y del Cosmos, Universidad de Granada, Granada (Spain);[(g)]Departamento de Física, Instituto Superior Técnico, Universidade de Lisboa, Lisboa; Portugal.
[134]Institute of Physics of the Czech Academy of Sciences, Prague; Czech Republic.
[135]Czech Technical University in Prague, Prague; Czech Republic.
[136]Charles University, Faculty of Mathematics and Physics, Prague; Czech Republic.
[137]Particle Physics Department, Rutherford Appleton Laboratory, Didcot; United Kingdom.
[138]IRFU, CEA, Université Paris-Saclay, Gif-sur-Yvette; France.
[139]Santa Cruz Institute for Particle Physics, University of California Santa Cruz, Santa Cruz CA; United States of America.
[140(a)]Departamento de Física, Pontificia Universidad Católica de Chile, Santiago;[(b)]Millennium Institute for Subatomic physics at high energy frontier (SAPHIR), Santiago;[(c)]Instituto de Investigación Multidisciplinario en Ciencia y Tecnología, y Departamento de Física, Universidad de La Serena;[(d)]Universidad Andres Bello, Department of Physics, Santiago;[(e)]Universidad San Sebastian, Recoleta;[(f)]Instituto de Alta Investigación, Universidad de Tarapacá, Arica;[(g)]Departamento de Física, Universidad Técnica Federico Santa María, Valparaíso; Chile.
[141]Department of Physics, Institute of Science, Tokyo; Japan.
[142]Department of Physics, University of Washington, Seattle WA; United States of America.
[143(a)]Institute of Frontier and Interdisciplinary Science and Key Laboratory of Particle Physics and Particle Irradiation (MOE), Shandong University, Qingdao;[(b)]School of Physics, Zhengzhou University; China.
[144(a)]State Key Laboratory of Dark Matter Physics, School of Physics and Astronomy, Shanghai Jiao Tong University, Key Laboratory for Particle Astrophysics and Cosmology (MOE), SKLPPC, Shanghai;[(b)]State

Key Laboratory of Dark Matter Physics, Tsung-Dao Lee Institute, Shanghai Jiao Tong University, Shanghai; China.
[145]Department of Physics and Astronomy, University of Sheffield, Sheffield; United Kingdom.
[146]Department of Physics, Shinshu University, Nagano; Japan.
[147]Department Physik, Universität Siegen, Siegen; Germany.
[148]Department of Physics, Simon Fraser University, Burnaby BC; Canada.
[149]SLAC National Accelerator Laboratory, Stanford CA; United States of America.
[150]Department of Physics, Royal Institute of Technology, Stockholm; Sweden.
[151]Departments of Physics and Astronomy, Stony Brook University, Stony Brook NY; United States of America.
[152]Department of Physics and Astronomy, University of Sussex, Brighton; United Kingdom.
[153]School of Physics, University of Sydney, Sydney; Australia.
[154]Institute of Physics, Academia Sinica, Taipei; Taiwan.
[155(a)]E. Andronikashvili Institute of Physics, Iv. Javakhishvili Tbilisi State University, Tbilisi;[(b)]High Energy Physics Institute, Tbilisi State University, Tbilisi;[(c)]University of Georgia, Tbilisi; Georgia.
[156]Department of Physics, Technion, Israel Institute of Technology, Haifa; Israel.
[157]Raymond and Beverly Sackler School of Physics and Astronomy, Tel Aviv University, Tel Aviv; Israel.
[158]Department of Physics, Aristotle University of Thessaloniki, Thessaloniki; Greece.
[159]International Center for Elementary Particle Physics and Department of Physics, University of Tokyo, Tokyo; Japan.
[160]Graduate School of Science and Technology, Tokyo Metropolitan University, Tokyo; Japan.
[161]Department of Physics, University of Toronto, Toronto ON; Canada.
[162(a)]TRIUMF, Vancouver BC;[(b)]Department of Physics and Astronomy, York University, Toronto ON; Canada.
[163]Division of Physics and Tomonaga Center for the History of the Universe, Faculty of Pure and Applied Sciences, University of Tsukuba, Tsukuba; Japan.
[164]Department of Physics and Astronomy, Tufts University, Medford MA; United States of America.
[165]Department of Physics and Astronomy, University of California Irvine, Irvine CA; United States of America.
[166]University of West Attica, Athens; Greece.
[167]Department of Physics and Astronomy, University of Uppsala, Uppsala; Sweden.
[168]Department of Physics, University of Illinois, Urbana IL; United States of America.
[169]Instituto de Física Corpuscular (IFIC), Centro Mixto Universidad de Valencia - CSIC, Valencia; Spain.
[170]Department of Physics, University of British Columbia, Vancouver BC; Canada.
[171]Department of Physics and Astronomy, University of Victoria, Victoria BC; Canada.
[172]Fakultät für Physik und Astronomie, Julius-Maximilians-Universität Würzburg, Würzburg; Germany.
[173]Department of Physics, University of Warwick, Coventry; United Kingdom.
[174]Waseda University, Tokyo; Japan.
[175]Department of Particle Physics and Astrophysics, Weizmann Institute of Science, Rehovot; Israel.
[176]Department of Physics, University of Wisconsin, Madison WI; United States of America.
[177]Fakultät für Mathematik und Naturwissenschaften, Fachgruppe Physik, Bergische Universität Wuppertal, Wuppertal; Germany.
[178]Department of Physics, Yale University, New Haven CT; United States of America.
[179]Yerevan Physics Institute, Yerevan; Armenia.
[180]Institute for Theoretical Particle Physics and Cosmology, RWTH Aachen University; Germany.
[181]Departamento de Física Teórica, Instituto de Física, Universidad Nacional Autónoma de México, Cd. de México; México.

[182]Institute for Theoretical Physics, University of Münster, Münster; Germany.
[a] Also at Affiliated with an institute formerly covered by a cooperation agreement with CERN.
[b] Also at An-Najah National University, Nablus; Palestine.
[c] Also at Borough of Manhattan Community College, City University of New York, New York NY; United States of America.
[d] Also at Center for Interdisciplinary Research and Innovation (CIRI-AUTH), Thessaloniki; Greece.
[e] Also at Centre of Physics of the Universities of Minho and Porto (CF-UM-UP); Portugal.
[f] Also at CERN, Geneva; Switzerland.
[g] Also at Département de Physique Nucléaire et Corpusculaire, Université de Genève, Genève; Switzerland.
[h] Also at Departament de Fisica de la Universitat Autonoma de Barcelona, Barcelona; Spain.
[i] Also at Department of Financial and Management Engineering, University of the Aegean, Chios; Greece.
[j] Also at Department of Mathematical Sciences, University of South Africa, Johannesburg; South Africa.
[k] Also at Department of Modern Physics and State Key Laboratory of Particle Detection and Electronics, University of Science and Technology of China, Hefei; China.
[l] Also at Department of Physics, Bolu Abant Izzet Baysal University, Bolu; Türkiye.
[m] Also at Department of Physics, King's College London, London; United Kingdom.
[n] Also at Department of Physics, Stanford University, Stanford CA; United States of America.
[o] Also at Department of Physics, Stellenbosch University; South Africa.
[p] Also at Department of Physics, University of Fribourg, Fribourg; Switzerland.
[q] Also at Department of Physics, University of Thessaly; Greece.
[r] Also at Department of Physics, Westmont College, Santa Barbara; United States of America.
[s] Also at Faculty of Physics, Sofia University, 'St. Kliment Ohridski', Sofia; Bulgaria.
[t] Also at Faculty of Physics, University of Bucharest ; Romania.
[u] Also at Hellenic Open University, Patras; Greece.
[v] Also at Henan University; China.
[w] Also at Imam Mohammad Ibn Saud Islamic University; Saudi Arabia.
[x] Also at Institucio Catalana de Recerca i Estudis Avancats, ICREA, Barcelona; Spain.
[y] Also at Institut für Experimentalphysik, Universität Hamburg, Hamburg; Germany.
[z] Also at Institute for Nuclear Research and Nuclear Energy (INRNE) of the Bulgarian Academy of Sciences, Sofia; Bulgaria.
[aa] Also at Institute of Applied Physics, Mohammed VI Polytechnic University, Ben Guerir; Morocco.
[ab] Also at Institute of Particle Physics (IPP); Canada.
[ac] Also at Institute of Physics and Technology, Mongolian Academy of Sciences, Ulaanbaatar; Mongolia.
[ad] Also at Institute of Physics, Azerbaijan Academy of Sciences, Baku; Azerbaijan.
[ae] Also at Institute of Theoretical Physics, Ilia State University, Tbilisi; Georgia.
[af] Also at Millennium Institute for Subatomic physics at high energy frontier (SAPHIR), Santiago; Chile.
[ag] Also at National Institute of Physics, University of the Philippines Diliman (Philippines); Philippines.
[ah] Also at The Collaborative Innovation Center of Quantum Matter (CICQM), Beijing; China.
[ai] Also at TRIUMF, Vancouver BC; Canada.
[aj] Also at Università di Napoli Parthenope, Napoli; Italy.
[ak] Also at University of Chinese Academy of Sciences (UCAS), Beijing; China.
[al] Also at University of Colorado Boulder, Department of Physics, Colorado; United States of America.
[am] Also at University of Sienna; Italy.
[an] Also at Washington College, Chestertown, MD; United States of America.
[ao] Also at Yeditepe University, Physics Department, Istanbul; Türkiye.
[*] Deceased